## *Trace element geochemistry of Belizean and Bermudan stalagmites: new tools, proxies and applications.*

JAMIESON, ROBERT,ANDREW


# Trace element geochemistry of Belizean and Bermudan stalagmites: new tools, proxies and applications.

*Robert Andrew Jamieson*

**This thesis is submitted in partial fulfilment of the requirements for the degree of**

**Doctor of Philosophy**

**Durham University**

**Department of Earth Sciences, Durham University**

**2016**

I declare that this thesis, which I submit for the degree of Doctor of Philosophy at Durham University, is my own work and not substantially the same as any which has previously been submitted at this or any other university.

Robert A. Jamieson

Durham University

*This thesis is dedicated to my mum, Alison Jamieson. Without her tireless support I'd never have made it this far. Thanks mum!*

*Personally, I liked the university. They gave us money and facilities, we didn't have to produce anything! You've never been out of college! You don't know what it's like out there! I've* ***worked*** *in the private sector. They expect* ***results****.*

-Dr. Raymond Stantz

## Abstract

Speleothem trace elements are an important and effective tool for palaeoenvironmental reconstruction. They can be used to reconstruct a plethora of climate variables, and are a vital tool for improving our understanding of the climate system. This is particularly important given the on-going challenges of comprehending and tackling anthropogenic climate change. Only by thoroughly understanding controls on climate variability can we attempt to predict future change. This thesis presents a broad study of current speleothem trace element proxies. In addition to reviewing the current state of knowledge, this thesis presents several additions and developments to the speleothem trace element toolkit.

The 22 year ATM-7 trace element record from Belize has a greater than seasonal resolution, and a highly precise chronology. As a result of this exceptional chronology, combined with extremely high resolution LA-ICP-MS analysis, it is possible to detect the geochemical indicators of volcanic ash deposition. Principal Component Analysis identifies a clear signal of a multi-elemental input of trace elements at the beginning of the wet season following volcanic eruptions with ash reaching the cave site.

U/Ca variability in aragonitic speleothems is strongly influenced by the occurrence of Prior Aragonite Precipitation. The U/Ca record in Belizean stalagmite YOK-G strongly suggests that modern drying has occurred in Belize, primarily caused by a reduction in wet season rainfall. This is consistent with published stable isotope data from YOK-G, previously interpreted as the result of southward ITCZ displacement. These results strongly suggest that U/Ca values in aragonitic speleothems are excellent proxies for rainfall variability. This new tool, combined with the exceptional chronological control characteristic of aragonitic stalagmites and the high spatial resolution afforded by modern microanalytical techniques, should facilitate the construction of new exquisitely resolved rainfall records, providing rare insights into seasonality changes as well as long-term changes in local recharge conditions.

In the Bermudan stalagmite BER-SWI-13, magnesium concentrations record, via varying prior calcite precipitation, changes in local rainfall which appear to correspond to variation in the North Atlantic Oscillation (NAO). Through a different mechanism, phosphorous also correlates with changes in the NAO. We infer that local effective rainfall changes, influenced by NAO state, influence bioproductivity above the cave and thus the amount of phosphorous in dripwaters. Surprisingly, for a location such as Bermuda, we see no evidence of clear direct anthropogenic influence on speleothem chemistry. These results

suggest that Bermudan speleothems are well situated to record basin scale climate changes in the North Atlantic.

Together, these three separate studies demonstrate the strength and versatility of high-resolution trace element analysis of speleothems. They establish new techniques of data analysis, new proxies, and the applications of existing proxies in new contexts to reconstruct palaeoenvironmental variables. Looking forward, these discoveries demonstrate that speleothem trace elements continue to have a great deal to offer to the field of palaeoclimate reconstruction, and that there are still new techniques and applications to be developed.

## Table of Contents

## List of Figures

## Acknowledgements

Without the tireless support and apparently endless patience of James Baldini this thesis would not exist. Thank you James for everything you've done in support of my PhD; whether it be your excellent advice, encyclopaedic knowledge of speleothem science, or simply hiring me in the first place. It can't have been easy, and I'm sorry about how frequently I use the passive voice in my writing!

Thank you to every member of the HURRICANE project, both official and unofficial. I couldn't have done it without all of you. Thank you Alex, James, Lisa, Marianne, Zoë, Franzi, Harriet, Jess and Iza. Every single one of you contributed to this project, whether with discussion in group meetings, assistance in the lab, or as excellent companions during field work.

Thank you again Marianne and Jess for choosing to do your fourth year projects in our lab. Your work on samples from YOK-G, making a sizeable dent in that collection of 3600 powders, probably saved my sanity.

Research can't be done alone, so I'd like to thank all of the collaborators with whom I've had the pleasure of working. Thank you to Chris Ottley, Amy Frappier, David Richards, Chris Standish, Geoff Nowell, Wolfgang Müller, David Evans, Viola Warter, Damiano Della Lunga, Sebastian Breitenbach, Keith Prufer, Jasper Wassenburg, and Denis Scholz.

Thank you to the many additional people without whom this research would not be possible but who are too many to name here, the collaborators, supervisors and students of those named above, as well as the hundreds of excellent scientists who have contributed

to speleothem science. Newton wasn't wrong when he said that we achieve by standing on the shoulders of giants. Never has that been clearer than when I attended the European Workshop on Laser Ablation at Royal Holloway, Karst Record 7 in Melbourne, or Speleothem Summer School in Oxford - there are a lot of fantastic people doing great work in the field. Thanks too to the members of our "Chemistry of Caves, Karst & Speleothems" Facebook group, and particularly to the members of our on-going "stalgossip" roundtable group chat. You're a never-ending source of helpful knowledge and interesting conversation.

I would also like to thank all of the staff and students from Durham University Earth Science Department who I've known in my time here. Every one of you deserves my thanks, though I can't possibly list each one of you who added in some way to my time here. In particular though, I'd like to thank everyone who ever went for a bike ride, climbed, lived with me, or even just had a beer at happy hour. You're all great. In particular I'd like to thank Charlotte. Thanks for keeping me sane these last few months.

The ladies of the admin and finance offices also have my thanks, you were always the ones to go to when I needed help. Each of you goes above and beyond the call of duty every single day as you keep that crazy department stumbling along. I'm especially grateful to Janice for listening to all of my helpful suggestions.

*Addendum*: I would also like to thank my reviewers, Pablo Cubillas and Sophie Verheyden for their excellent discussion during my viva and for their contributions towards improving this thesis.

*Specific acknowledgements of funding sources and resource providers are included before each relevant chapter. This project as a whole was funded by a European Research Council grant (240167) to James Baldini. Thank you James for allocating some of those precious resources to this PhD project, and thank you to the taxpayers of the European Union for paying for it.*

# Chapter 1 Introduction and Background

# Chapter 1: Introduction and Background

## Thesis Rationale

Climate change may be the greatest threat which humanity has ever faced. Climate change has the potential to disrupt human society at an unprecedented scale, with risks to food and water resources, human habitation, health, and the geopolitical consequences of those risks (Potsdam Institute for Climate Impact Research and Climate Analytics, 2012). Additionally, potential changes in weather patterns and sea levels place new areas at risk from destructive climate events including floods, droughts and hurricanes – areas which may not have the infrastructure or resources to cope with these changes. Although human influence on the climate system is now widely recognised and quantified (IPCC, 2013a, b), the impacts of this change on specific climate phenomena remain in many respects uncertain.

Comprehensive understanding of processes, feedbacks and tipping points in the climate system requires high quality datasets of past interactions between climate variables. In climate science the common geological axiom that "the present is the key to past" is somewhat reversed. Only by understanding past climate variations and the processes which drive them can we attempt to predict future changes in the climate system (IPCC, 2013a).

Archives of past climate are diverse and widespread, present in both marine and terrestrial systems. However, there are gaps in our records. Marine records are plentiful, with sediment cores drilled across the planet and many excellent long-term records produced therefrom (Zachos et al., 2001). High latitudes too are well covered, with ice cores used to reconstruct global climate for almost the last million years (Jouzel et al., 2007). In shorter supply however, are terrestrial and low-latitude archives of palaeoenvironmental change. Speleothems are terrestrial archives of multi-proxy data which can be precisely dated down to sub-annual resolutions and which extend over thousands of years (Baker et al., 2008; Fairchild and Baker, 2012; Fairchild et al., 2006a). Such high quality archives allow reconstruction of multiple climate signals over time periods and at resolutions which are of great interest to modern climate science. These records have the potential to greatly add to the understanding of decadal scale climate variability.

Although speleothem science is a rapidly maturing branch of climate science it is still relatively young compared to studies of ice and sediment cores. Rapid advances in dating

techniques and analytical methods have allowed increasing amounts of information to be extracted from speleothems (Fairchild and Baker, 2012). Stable isotope proxies in stalagmites are now routinely measured and the mechanisms controlling their variability are fairly well understood (Genty et al., 2014; McDermott, 2004; Spötl and Mattey, 2006). However, stalagmites contain many other potential proxies which are often overlooked and have great potential for further development. Trace elements are one such set of proxies.

This thesis focuses on applying existing techniques to construct trace element records of palaeoenvironmental variables. Additionally, it examines novel methods of interpreting trace element variability in a multivariate context, as well as developing new trace element proxies in aragonitic stalagmites. Several different elements are measured including the well-understood systems of magnesium and strontium as well as several elements which have not previously been extensively measured in speleothems such as uranium.

## Speleothems as archives of environmental proxies

Speleothems are invaluable archives for palaeoclimate information. They record multi-proxy information, in high resolutions over (generally) unbroken time periods and are precisely datable using isotopic decay systems (principally U-Th, but also U-Pb to ~600ka and several hundred million years, respectively). Additionally, they are capable of recording palaeoclimate information in continental or low latitude regions which are often unrepresented by other archives such as sediment and ice cores respectively.

A variety of proxies have been measured using speleothem archives, with the most used and well understood being the stable isotope systems of oxygen (e.g. Lachniet (2009)) and carbon (e.g. Lambert and Aharon (2011)). Growth rate measurements (e.g. Tan et al. (2013)), optical properties (e.g. Crowell and White (2012)), a variety of trace element systems (e.g. Fairchild and Treble (2009)), and biomarkers (e.g. Blyth et al. (2008)) have also been used as proxies from speleothem archives for a number of climatic and environmental variables. Of these proxies trace elements are a rapidly developing technique, with on-going research into a variety of different elemental systems (e.g., Bourdin et al. (2011); Wynn et al. (2008)) as well as the development of analytical techniques providing higher resolution measurements (Buckles and Rowe, 2016; Frisia et al., 2005; Müller et al., 2009).

## Caves and Karst

### Locations

Approximately 64% of the Earth's land surface is covered by sediments, and of that roughly a third of those rocks are carbonates (Hartmann and Moosdorf, 2012). As a result karst environments outcrop on every continent (Hollingsworth, 2009), with the probable exception of Antarctica where any karst that may be present is covered by snow and ice (and is in any case inactive due to a lack of flowing water). Caves develop in karst in any location where chemically aggressive waters flow through carbonate lithologies. In most cases this results from meteoric waters passing through organic-rich soils and becoming enriched in dissolved $CO_2$, producing carbonic acid and then dissolving their way into and through carbonate lithologies (Brasier, 2011). The precipitation of secondary carbonates subsequently results when these waters reach a lower $pCO_2$ environment and degas, resulting in supersaturation and hence precipitation of carbonate minerals.

Due to the fact that speleothems can therefore precipitate in almost any surface environment with flowing water they are a climate archive with global terrestrial coverage, recording information in almost all latitudes and climates. Even the periodic absence of speleothem growth can be used as a climate reconstruction tool in cold (Vaks et al., 2013) or hot (Webb et al., 2014) environments.

### Identifying caves and deposits useful for palaeoenvironmental research

Although cave environments are found throughout the world, not all caves are suitable for palaeoenvironmental research. The research question of interest dictates exactly which caves can provide useful information. First and foremost, the cave must be located somewhere which is sensitive to the climate variable of interest. Ocean basin scale climate variables for example, will not generally exert a strong influence on the climate of high altitude inland caves. Similarly, a cave in a marginal environment where a single variable completely controls deposition (e.g., the presence or lack of overlying ice) will not be suitable to reconstruct a long term regional signal.

Conditions in the cave itself will also influence its suitability for palaeoenvironmental research. Generally caves that are well ventilated are preferred, as build up of $CO_2$ can result in dissolution or non-growth of speleothems. However, equally a cave that is too

accessible may be disrupted by human or animal action. In general, ideal caves sit in the cave version of a "goldilocks zone" – where they are sufficiently protected from external disruption, but still influenced by external climate or environment.

For this reason, cave monitoring and characterisation are essential prior to commencing any study of a cave site. Generally, this takes the form of long term monitoring of temperature, humidity, $pCO_2$, and stalagmite drip rates. Additionally, other parameters such as atmospheric pressure or radon content are sometimes also measured (Fairchild and Baker, 2012).

Individual stalagmites themselves also vary in usefulness depending on the research question. Generally, stalagmites that grow straight and relatively narrow are preferred. Growth axis shifts, splash cups and other morphological variations should generally be avoided as they can complicate or obfuscate extraction of information from the stalagmite. There are exceptions to these general guidelines, as specific research questions may require unusual stalagmites. Stalagmites with growth axis shifts for example, may be of interest for researchers investigating palaeoseismicity.

Other stalagmite parameters such as growth rates influence the resolution and length of the record produced, and are therefore of vital consideration when selecting a stalagmite. Drip rate of the particular drip precipitating the stalagmite is vitally important to the information recorded within a speleothem. A slow drip which does not change in response to rainfall is likely averaging water input over a longer period, resulting in a signal which may record long term changes but not short term variability. Conversely, a "flashy" drip that rapidly responds to rainfall events will record information at a high-resolution, but may result in non-growth or very slow growth rates during drier periods. In practice, a stalagmite which lies somewhere between the two is preferable (Baker et al., 2014; Frappier, 2008; Riechelmann et al., 2014; Treble et al., 2015).

## Dating

One of the primary advantages that speleothems offer as paleoclimatic archives is the precision with which they can be dated. Several different dating techniques can be applied to speleothems, each with their own advantages and disadvantages as well as ideal time frames (Table 1.1).

| Dating System | Time Frame | Advantages | Disadvantages |
|---|---|---|---|
| **Radiogenic Isotopes** | Modern, last ~60 years | Very high precision | Low concentrations, only work in the most modern speleothems |
| **Lamina/Cycle Counting** | Any, but chronological resolution must be annual | Potential sub-annual precision, absolute chronology in terms of relative dates | Only relative to each other – require an anchor point to be useful, subjective – can introduce errors from over or undercounting, not always consistently present |
| **Radiocarbon** | Last ~50,000 years (Reimer et al., 2013) | Absolute date of 'bomb spike', potentially very high resolution dating | Dates modified by a variable reservoir effect of dead carbon from karst which is difficult to correct for |
| **U-Th** | Last ~600,000 years | Generally good precision on the order of 0.1-1%, especially in aragonite | Complicated by the presence of detrital thorium introducing large age errors, analytically challenging/expensive |
| **U-Pb** | Up to approximately 300Ma (Woodhead and Pickering, 2012) | Only method for dating very old stalagmites | Challenging, requires variable U content for isochrons, needs low detrital Pb |

Table 1.1: A summary of dating techniques commonly used in speleothems

The precision in a stalagmite age model can therefore vary from, in exceptional cases, as high as seasonal, to, in older stalagmites, several million years. The research question of interest must therefore account for this, by ensuring that the order of precision obtained by dating is suitable for the environmental variable of interest. The research in this thesis exclusively looks at modern speleothems that grew within the last millennium. As such,

they use a mixture of lamina counting, radiocarbon and U-Th dating to produce chronologies varying in precision from seasonal to approximately decadal. These are then used to reconstruct events ranging from seasonal cycles to multi-decadal basin scale variation as appropriate.

## Speleothem derived proxies

Speleothem archives are multi-proxy by their very nature, containing proxies for a range of environmental, hydrological and meteorological variables. Speleothems record some variables (e.g. rainfall) via several independent mechanisms allowing cross-comparison and validation between proxies. As a result, speleothems make excellent paleoclimate archives for studying complex climatic systems such as large-scale circulatory changes.

Speleothems record proxy information in both the way they grow as well as in the geochemistry of their calcium carbonate. Proxies derived from speleothems include growth characteristics such as lamina thickness (Baker et al., 2008) and calcite density (Walczak et al., 2015), stable isotopic records including $\delta^{13}C$ and $\delta^{18}O$ (McDermott, 2004), variations in concentrations of dozens of trace elements (Fairchild and Treble, 2009), and even more exotic proxies such as clumped isotopes (Eiler, 2011) and biomarkers (Blyth et al., 2008). A single speleothem can yield records derived from a dozen or more proxies in a suitable sample. The majority of proxies in speleothems modify and preserve palaeoenvironmental signals in different ways, many of which are completely independent of each other. As such they can be used as independent cross-checks to separate different environmental signals from each other. This, alongside high precision dating, is the greatest strength of stalagmites as a palaeoclimate archive.

This thesis focuses principally on the trace element proxies in speleothems (reviewed in Chapter 3), and as such does not go into detail on the systematics of those others. For a comprehensive review of speleothem science see Fairchild and Baker (2012) and references therein.

## Overview of Thesis

This thesis is made up of seven chapters, the contents of which are summarised below:

Chapter 1 explains the thesis rationale and gives a broad overview of speleothem science.

Chapter 2 provides a brief overview of each of the cave sites studied in the subsequent chapters. This chapter summarises and cites all previous research conducted at these cave sites, as well as providing a brief description of the caves themselves and their surrounding environments.

Chapter 3 summarises trace element proxies in speleothems. It provides a brief overview of the main processes which influence trace element variability in speleothems. This is followed by a discussion of some of the methods used for processing and interpreting speleothem trace element data. Finally, it summarises some of the most commonly used trace element proxies, as well as discussing recent developments in the field and the current state of trace element proxy research.

Chapter 4 presents results of LA-ICP-MS analysis of a modern stalagmite from Actun Tunichil Muknal cave in Belize. The chapter describes the use of Principal Component Analysis to identify a multi-elemental signal resulting from the addition of allochthonous material to the cave site. Analysis of the timings and trajectory modelling using HYSPLIT are used to determine that the source of this material is volcanic ash, which is flushed seasonally into the speleothem at the onset of the Belizean rainy season.

Chapter 5 discusses the chemistry of uranium incorporation into aragonitic stalagmites. Using published speleothem data, a distribution co-efficient for uranium in aragonite is derived. Then, using a stalagmite trace element dataset from Yok Balum cave in Belize this distribution coefficient is used to demonstrate that varying amounts of Prior Aragonite Precipitation in the overlying karst can control U/Ca ratios in aragonitic speleothems.

Chapter 6 presents a new stalagmite trace element dataset from Leamington Cave, Bermuda. This dataset is used to examine variation in effective rainfall at this cave site, the larger climatic variables influencing that rainfall, as well as assessing the impact of any anthropogenic influence on the cave.

Chapter 7 concludes this thesis with a summary of the results, and a brief discussion of future possibilities for research leading on from the studies presented herein.

# Chapter 2 Site Descriptions

# Chapter 2: Site Descriptions

## A Note On Site Selection

Three different cave sites were used for this project: two from central and southern Belize, as well as one from Bermuda. The original selection of these sites, alongside a fourth in Turks and Caicos, was to study a transect across the predominant range of tropical storm trajectories in the North Atlantic. The larger HURRICANE project, of which this PhD thesis is a small part, was aimed at extending the work of Frappier et al. (2007b) to produce a record of tropical storm activity in the Caribbean. This project examines the trace elements of samples from these sites, the climate of which is influenced by Atlantic storm tracks.

## Actun Tunichil Muknal, Belize

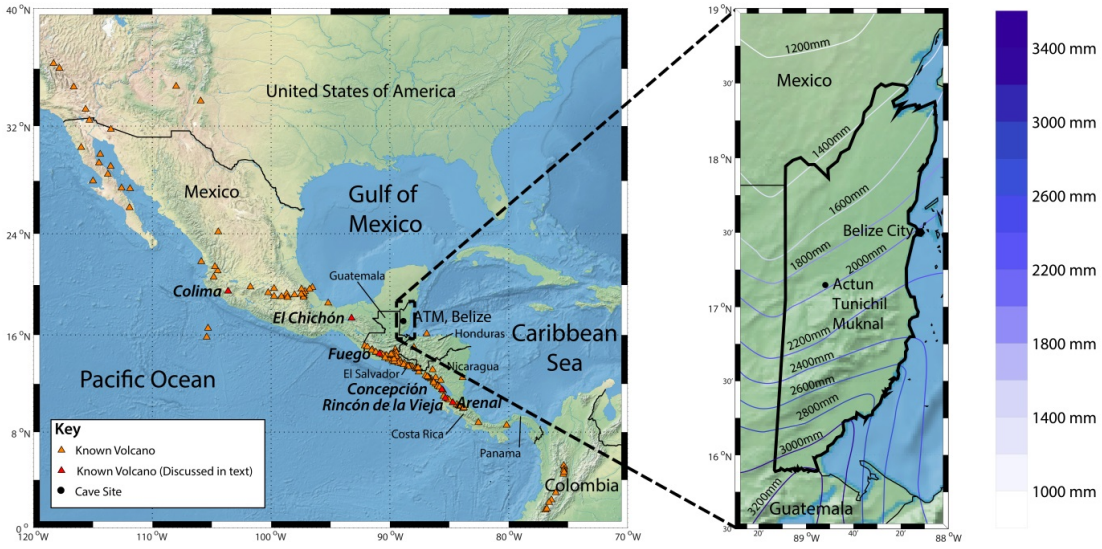


Figure 2.1: Left: Location of Actun Tunichil Muknal and all volcanoes in Central America. Right: Location of ATM in Belize, with contoured mean annual rainfall (Medina-Elizalde and Rohling, 2012).

Actun Tunichil Muknal (ATM) cave is located in central Belize (Figure 2.1) (17° 7' 4.8" N, 88° 51' 57.6" W) in a group of limestones and dolomites of late Cretaceous and Paleozoic age (Miller, 1996). ATM itself occurs in a massive pink limestone Breccia that is located in a rock unit in Central Belize known as the Albion formation or "Teakettle Diamictite," which has been identified as the approximate position of the K-T boundary in central Belize. ATM is an active, phreatic cave with a river flowing through it (Figure 2.2). Passages are heavily decorated with actively growing speleothems.

The location of ATM is optimal for recording a great deal of palaeoenvironmental information. Its position in Belize suggests sensitivity to basin scale variability in both the Atlantic and Pacific. Furthermore, it is located in the path of southerly tropical storm tracks which periodically strike Belize. Similarly, it is near a number of active volcanoes which may influence climate and local geochemistry.

Several papers have already been published based on research from this cave. Frappier et al. (2002) reported a correlation between $\delta^{13}C$ in stalagmite ATM-7 (the same sample used in Chapter 4 of this thesis) and El Niño events, suggesting that ENSO-driven changes in terrestrial ecosystem carbon cycle dynamics were responsible. Frappier et al. (2007b)

followed up on this research by identifying negative $\delta^{18}O$ excursions in ATM7 which resulted from tropical cyclone rainfall at the study site. They suggest that tropical cyclones can produce short-lived negative excursions in $\delta^{18}O$ in fast growing speleothems. This result has subsequently been used to suggest criteria for sample selection for studies aimed at examining tropical cyclone occurrence (Frappier et al., 2007a; Frappier, 2008). The subtleties of $\delta^{18}O$ behavior due to these tropical cyclone strikes, as well as the interaction with ENSO driven changes in $\delta^{18}O$ have subsequently been further discussed in Frappier (2013).

In addition to the climate records produced from ATM7, Frappier (2006) also examined trace element variability and suggested that ATM7 may record a signal of the El Chichón eruption. These findings prompted the higher-resolution study undertaken in Chapter 4, which includes further details and images of this stalagmite.

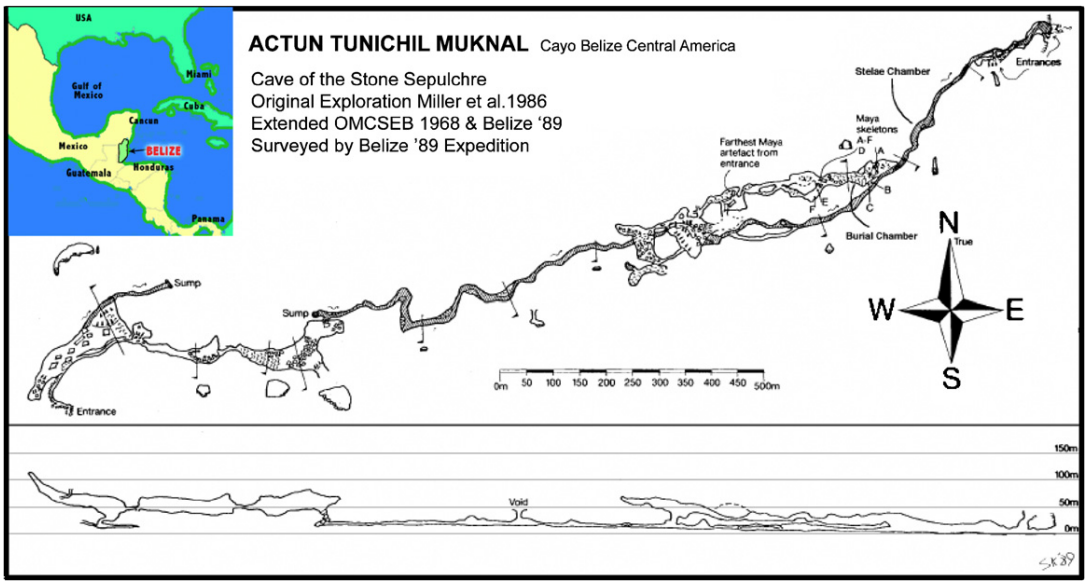


Figure 2.2: Cave map of Actun Tunichil Muknal from Frappier (2008).

## Yok Balum, Belize

Yok Balum cave in southern Belize (16° 12' 30.78" N, 89° 40' 24.42"W; 366m above sea level; Figure 2.3) is a well monitored tropical cave developed in a SW-to-NE trending karst ridge composed of Campur Formation limestone in the Toledo district of southern Belize. The cave is well studied, with cave monitoring records (Ridley et al., 2015b) as well as stable isotope records from two stalagmites already published (Kennett et al., 2012; Ridley et al., 2015a).

The cave consists of a single main trunk passage approximately 540m in length with two entrances (see Figure 2.4). These entrances are a small eastern opening and a larger, higher opening to the southwest formed by a cave roof collapse. The cave ventilates daily through these two entrances, ensuring that $CO_2$ concentrations in the cave never rise to a level where dissolution of carbonate speleothems would occur. The cave is developed in a tectonically active area, and field observations suggest that it may have formed along a local fault. The stalagmite YOK-G was collected in 2006 from an actively dripping area of the cave approximately 80m from the smaller eastern entrance.

Southern Belize has a tropical climate, with seasonal temperatures only ranging approximately 4°C about the annual mean of 22.8°C. Latitude and elevation control rainfall distribution in Belize, with total annual rainfall ranging from 1300mm in the north to 4500mm in the south (Figure 2.1). Rainfall in the region exhibits a strong seasonality with >80% of the annual rainfall occurring between June and September in the peak of the May-January wet season. February to April receives significantly less rainfall, with evaporation greatly reducing soil and karst infiltration (Kennett et al., 2012).

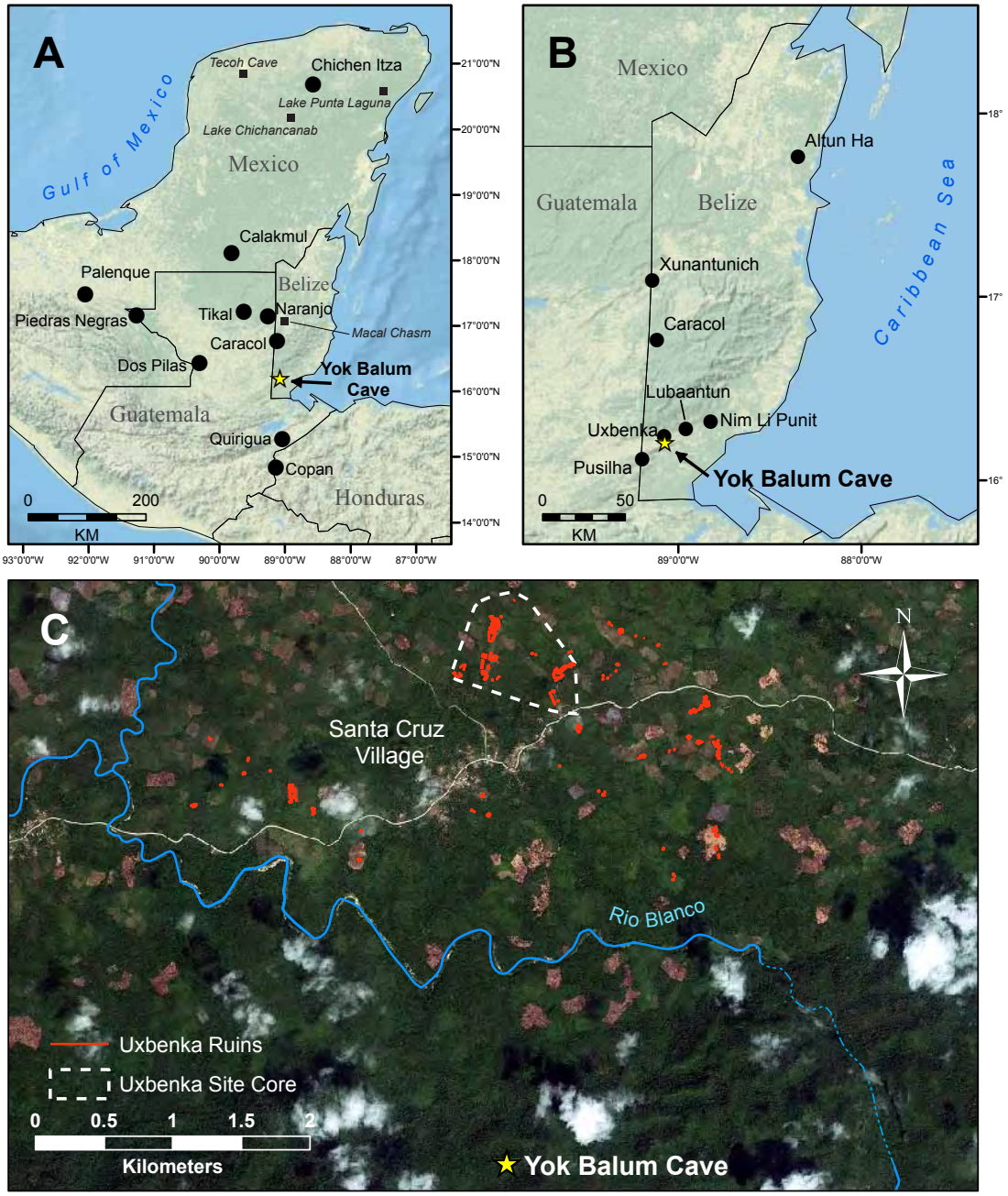


Figure 2.3: Maps showing the location of Yok Balum Cave in Belize (A and B), relative to nearby Mayan archaeological sites (dots) and published climate archives (squares). Map C shows the position of Yok Balum relative to nearby settlements. Figure taken from Kennett et al. (2012) (Supplementary Material).

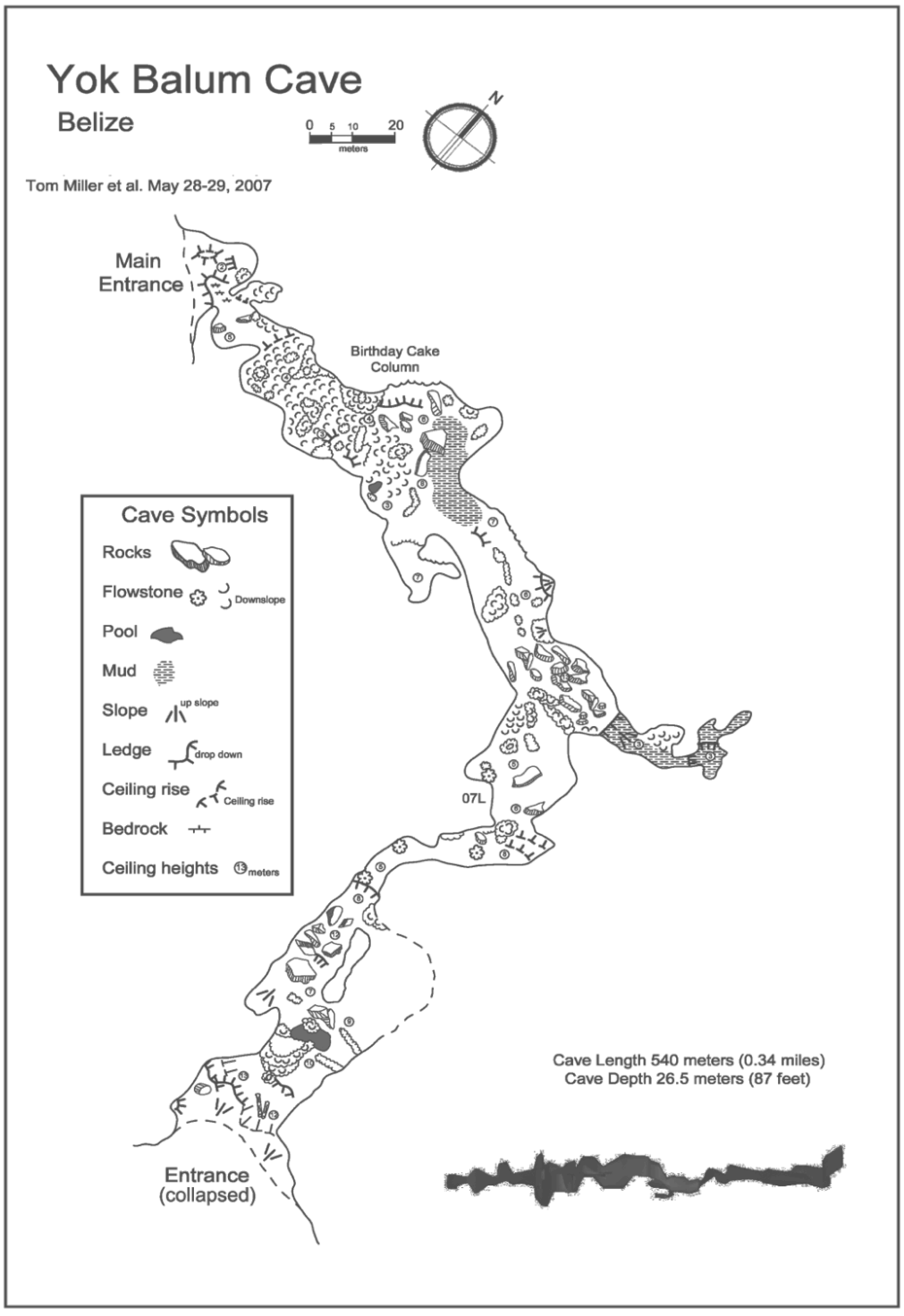


Figure 2.4: Yok Balum cave map (Mapped by Miller et al., 2007)

Stable isotope records from two Yok Balum speleothems (YOK-G and YOK-I) have been produced and published. YOK-G yielded a 453-year long record of aerosol forced ITCZ positioning recorded via effective rainfall control of $\delta^{13}C$ variation (Ridley et al., 2015a). $\delta^{18}O$ isotopes in YOK-G are similarly influenced by climatic controls, but instead correlate with Northern Hemisphere Temperature, suggesting that temperature and evapotranspiration influence $\delta^{18}O$ values in this region, modifying the signal and complicating its use as a palaeo-rainfall record.

A longer $\delta^{18}O$ record from YOK-I was used by Kennett et al. (2012) to examine rainfall variability over the last 2000 years, identifying periods of historical droughts. YOK-I $\delta^{13}C$ is also thought to reflect rainfall variability, with notable responses to NAO state, solar activity and volcanic forcing (Ridley, 2014).

Both stalagmites were sampled from the “Birthday Cake” formation (see Figure 2.4 and Ridley (2014)) and are aragonitic in mineralogy.

The first trace element results from Yok Balum, derived from stalagmite YOK-G, are presented in Chapter 5 of this thesis.


Figure 2.5: YOK-G Top Slab

## Leamington Cave, Bermuda

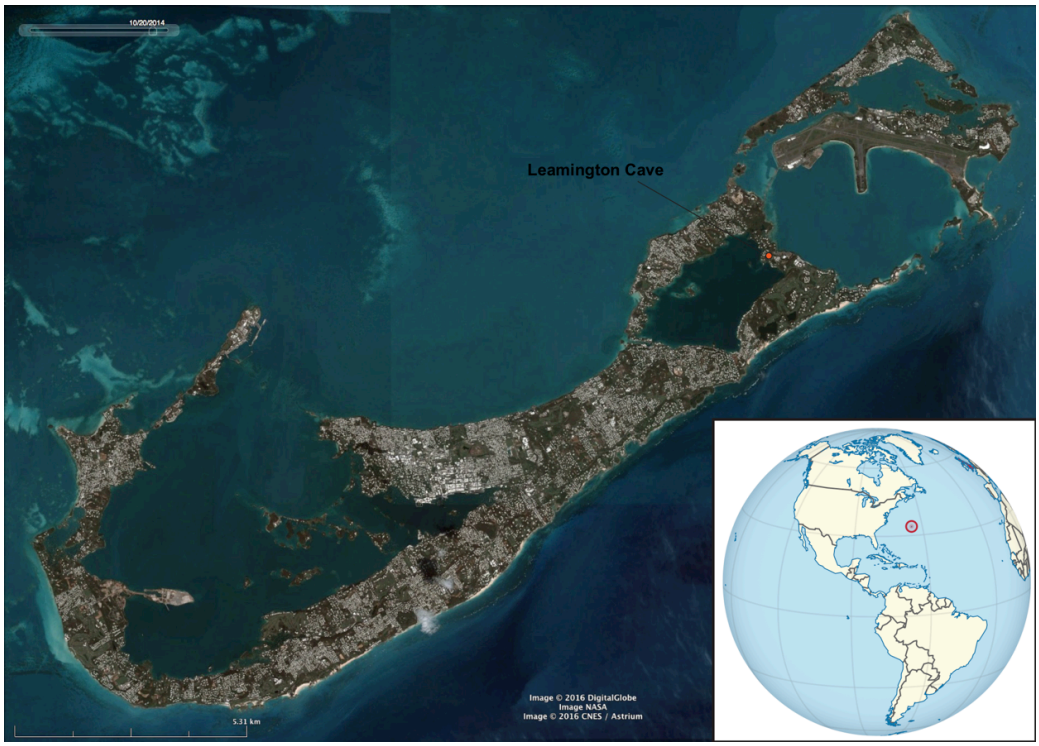


Figure 2.6: Aerial view of Bermuda with the location of Leamington Cave marked (orange circle) (image source: Google Earth). Inset: Bermuda's position in the North Atlantic (image source: Wikicommons, licensed under a Creative Commons Attribution-Share Alike 3.0 Unported license).

The Bermuda islands are a carbonate platform developed atop a volcanic seamount in the North Atlantic. The modern subaerial exposure in Bermuda consists almost entirely of carbonate rocks, the majority of which are either aeolianites with clear dune structures, or more massive limestones. Facies changes in Bermudan geology generally result from eustatic sea level changes during the Pleistocene. Caves in Bermuda develop almost exclusively in the highly weathered and karstified Walsingham Formation (Swinnerton, 1929), some of the oldest rocks on the island (deposited approximately 1.1-0.8Ma (Hearty and Vacher, 1994)), which outcrop in a narrow band along the North-East coast of the main island between Harrington Sound and Castle Harbour.

Leamington Cave (32°20'31.64"N, 64°42'30.93"W) is one such cave, a privately owned former show cave that is richly decorated with actively growing speleothems and which has been continuously monitored for $CO_2$ fluctuations, temperature, and drip rate changes for

a year (Walczak, 2016). The cave pool, which dominates the main cave chamber, connects to the ocean and causes the cave to ventilate daily thanks to a tidal flushing mechanism. This suggests that speleothems in Leamington Cave are unlikely to undergo dissolution due to build-up of $CO_2$. Stalagmite BER-SWI-13 (or 'Swizzle') was selected based on its hydrology (e.g., active but moderate response to rainfall) and a favourable internal structure as revealed by CT scans (Walczak, 2016). It is a solid stalagmite with no evidence of voids or diagenetic alteration, and reasonably clear growth laminae (see discussion of age models in Chapter 6).

Bermuda is located at 32°N in the North Atlantic, and has a humid subtropical climate. The island group's position on the eastern edge of the Gulf Stream results in warmer temperatures and slightly wetter conditions than latitude alone accounts for. This position also puts Bermuda on the south-eastern side of the Atlantic hurricane belt which often influences Bermudan weather. Seasonally, temperatures vary by approximately 10°C with a clear seasonal contrast between summer and winter. Rainfall is more uniform throughout the year with no pronounced dry season, however rainfall does increase somewhat in autumn.

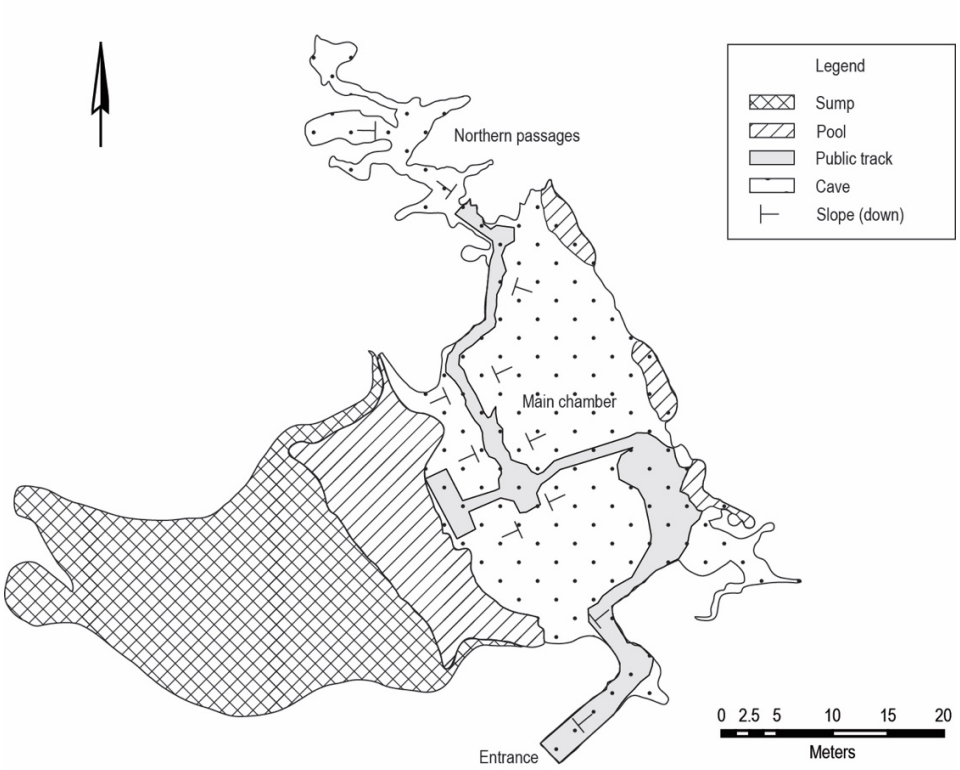


Figure 2.7: Leamington Cave plan. Surveyed by members of the Bermuda Cave Diving Association

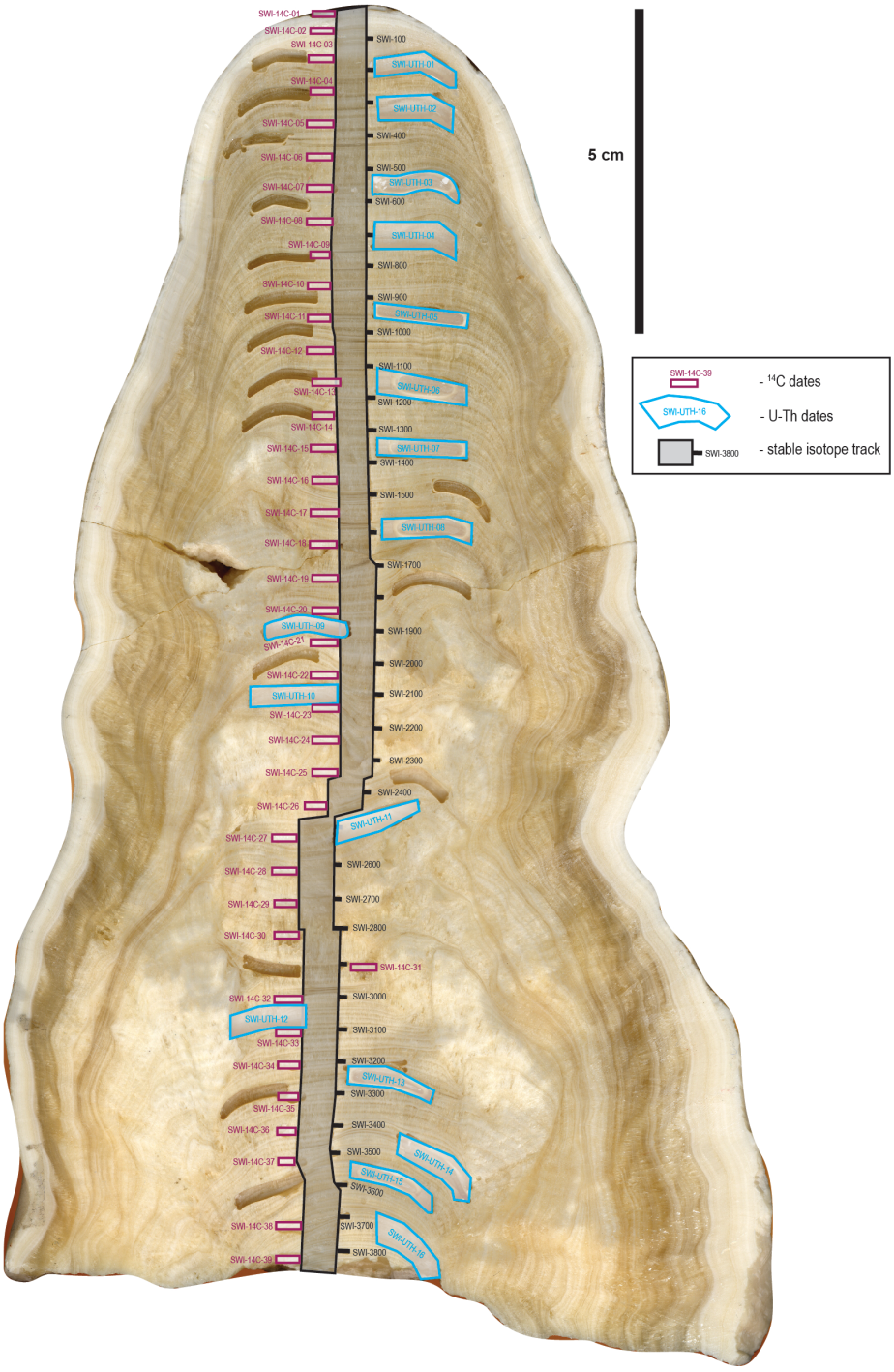


Figure 2.8: Scan of stalagmite BER-SWI-13 with positions of dating powders and isotope milling track annotated (Walczak, 2016), laser ablation transects were performed on the facing half (not shown).

# Chapter 3 Trace element proxies in speleothems: controls, analysis, uses and next steps

# Chapter 3: Trace element proxies in speleothems: controls, analysis, uses and next steps

## 3.1 Introduction

Speleothems are used extensively as archives of palaeoenvironmental proxy data. Speleothems record climatic (and other) information via a variety of proxies ranging from their fundamental growth characteristics to the chemistry they inherit from their formation dripwaters. Additionally, they are amenable to precise and absolute dating through several methods including radiocarbon, uranium decay series and layer counting. In exceptional cases absolute chronologies can be constructed down to seasonal resolutions in records that can extend for many thousands of years.

The proxies used from speleothem archives are diverse, both in their nature and in what syn-depositional information they record. Whilst stable isotopes remain the most commonly utilised proxy in speleothems, other proxies are the subjects of increasing research interest as they reveal additional palaeoenvironmental information. Trace element proxies in speleothems record a broad range of environmental factors, and are increasingly used both individually and in conjunction with other proxies to reconstruct past climate, as well as records of other processes. However, in the case of many proxies, our understanding of the processes controlling trace element concentrations in speleothems is still limited. This chapter discusses the current state of understanding of speleothem trace element proxies, citing examples from this thesis and the larger literature, as well as discussing some of the challenges in analysing and interpreting trace element proxies.

“Trace Element” in speleothem science is a definition which is commonly used somewhat differently than in the broader field of geochemistry. Typically “trace elements” in geochemistry refers to elements with a concentration less than 1000ppm or 0.1% of the whole rock. In speleothem science the term is more broadly applied to any elements occurring in carbonates which are not Ca, C, or O. This is true even in cases where an element may have a greater concentration which would otherwise be considered minor elements (e.g. magnesium in high-Mg calcites).

## 3.2 Processes Controlling Speleothem Trace Element Concentrations

Concentrations of trace elements in speleothems are the result of a complex interplay of processes ranging from supply to the site through to incorporation into the crystal lattice. Each trace element can behave differently due to each of these processes and the relative importance of each can vary on a site-to-site basis. Any use of trace element proxies in speleothems must include a thorough consideration of each of these processes, both to understand exactly what information is being recorded, as well as any modification of that signal. This section summarises the processes controlling speleothem trace element proxies from "source to sink", discussing sources of, and changes to, various elements as a result of these processes.

### 3.2.1 External Supply to Site

External supply of trace elements to a cave site can be a significant control on concentrations in speleothems. Many elements which are not abundant in soils or local host rock, or which have been successively leached out over time will only appear in significant concentrations when an increased external supply is delivered to the cave site. This can be in the form of volcanic products (Badertscher et al., 2014; Borsato et al., 2015; Jamieson et al., 2015), sea spray (Baldini et al., 2015; Tremaine et al., 2016), aerosols (Dredge et al., 2013) or anthropogenic sources (Pons-Branchu et al., 2015). Chapter 4 of this thesis discusses an example of this process, where the coincident increase in several elements is interpreted as the result of addition of volcanic ash into the cave system. Subsequent processes in the soil, karst and cave influence this signal's timing and magnitude in speleothems. For example, as detailed in Chapter 4, the timing of any trace element signal resulting from external inputs to the cave site may be controlled by climatic variables. Elements may not appear in the stalagmite at the time of their arrival, but may instead require conditions at the site to favour their transport (e.g., during a rainy season or autumnal flushing event where mobilised organic material can facilitate transport (see section 3.2.3), a change in redox conditions, etc.). As a result, variability of trace elements that are sourced largely from external supply can result from more than one environmental signal. They record both the supply to the cave site, and thus information about wind direction and source of material, as well as recording information about any environmental variables which control their supply to the cave itself, such as seasonality or rainfall.

Disentangling these factors can be complex, but must be considered when reconstructing palaeoenvironmental information using these proxies.

At Actun Tunichil Muknal (ATM) cave in Belize (Chapter 4) the presence of volcanic signals in the ATM7 stalagmite is dependent on wind direction; when the site is downwind of an eruption volcanic ash reached the cave (as reconstructed using HYSPLIT modelling using reanalysis data). Additionally, volcanic signals are not recorded in the speleothem at the time of eruption but are instead recorded at the start of the next rainy season in Belize, when the volcanic material is washed into the speleothem. Understanding the processes involved in this transport of material, both aerially and hydrologically, is essential to the interpretation of such speleothem records.

### 3.2.2 Biosphere and soil processes

Elements that are biologically active can be influenced by the presence (or absence) of biology (principally plants and soil processes) above the cave site. This has been documented in at least one cave site, where biogeochemical processes result in a variable lag in the delivery of sulphur into the cave. Borsato et al. (2015) documented variations in sulphate concentration in dripwaters and speleothems in Grotta di Ernesto in northern Italy. Long term monitoring of dripwaters, combined with an approximately 200 year long modern record of stalagmite sulphur content are used to reconstruct geochemical processing of sulphur compounds prior to stalagmite incorporation. They report that at fast drip sites $SO_4^{2-}$ concentration lags peak atmospheric values by approximately 15 years, and at slow drip sites by a further ~4.5 years. A similar result is found in the stalagmite at the slow drip site, which displays an approximately 20 year lag relative to peak atmospheric sulphate values. Borsato et al. (2015) attribute these lags to a combination of biogeochemical cycling and aquifer storage. Importantly however, they note that this lag is not constant throughout time. In older parts of the record, prior to major anthropogenic emissions they find much shorter lag times of 4-8 years. This suggests that lag times in records which result from biogeochemical processes in the biosphere, soil and karst are not simply constant throughout time but can instead vary with environmental conditions and elemental concentrations. At the same site, peaks in trace elements including Br and Y, are the result of disruption to the biosphere above the cave as a result of tree-felling, demonstrating that substantial changes to ecosystems above caves can be directly

recorded in speleothems by disruption to the soil and subsequent elemental fluxes (Borsato et al., 2007).

Soil processes may also be significant in determining which elements are stored and transported, with different types of organic matter mobilising different elements. Transport of elements with low solubility in water has been widely attributed to complexation by organic colloids (Fairchild and Treble, 2009). Several elements such as Pb and Zn, which are not commonly transported in solution and tend to be bound in soils, have been correlated in speleothems to bands rich in organic material (Borsato et al., 2007). However, it has only been comparatively recently that studies have confirmed that colloid- and particle-facilitated transport is behind these commonly observed patterns e.g. (Hartland et al., 2012). Hartland et al. (2012) have linked particular element ratios in dripwaters to their binding strength and the types of organic matter present. Different flow conditions favour varying sizes of organic matter, and thus may have an influence on trace element transport and resultant incorporation in speleothems. Trace element concentrations in speleothems may therefore record changes in organic matter composition, reflecting changes in hydrology, soil structure or overlying ecosystems (Hartland et al., 2013). The relationship between organic material and trace elements in speleothems is a rapidly progressing branch of speleothem science and recent studies suggest that a great deal of potential information can be uncovered from examining these relationships (Blyth et al., 2016).

Elements with a strong biological role such as phosphorous have been linked to bioproductivity above cave sites (Baldini et al., 2002; Treble et al., 2003), with their dripwater and speleothem concentrations dependant on their take up and subsequent release by biology. The variability of these elements in speleothems can therefore be used as a proxy for bioproductivity and hence the climate variable which influences that productivity (often, but not necessarily, rainfall). As with most speleothem processes disentangling these can be challenging due to the multiple signals integrated into a single proxy record, however by utilising multiple proxies it may be possible to statistically separate these records (see section 3.3.4.3).

An often-neglected component of speleothem science is the influence of soil and biology on the effective rainfall amount reaching the karst. Canopy interception and soil uptake of moisture are significant modifiers of the amount of moisture passing through the soil above a site (Mathias et al., 2015). To date, rainfall at a site has not been quantitatively linked to these processes, with the majority of numerical models of karst water movement only applying a potential evaporation modification to rainfall data (Baker and Bradley, 2010; Fairchild et al., 2006b). Baldini et al. (2005) did describe the effects of changing vegetation cover altering both soil pCO2 and water budgets, and thus speleothem growth rates and stable isotopes, but this process has not yet been examined in detail with regards to trace element concentrations or in a quantitative manner.

### 3.2.3 Transportation

Elements which are less water soluble, or generally immobile, can also be incorporated into speleothems (Baldini et al., 2012). However, the availability of these elements is limited unless they can be more readily transported through the karst system. Organic material making up the colloidal fraction of particulate organic matter is particularly good at complexing and mobilising a variety of trace elements such as transition metals and rare earth elements (Hartland et al., 2012) (as discussed above). As a result, these elements tend to build up in the soil until conditions are right to enable their transport into the karst system. In many caves around the world this manifests as a trace element concentration maximum synchronous with an autumnal flushing event, where the availability of large amounts of organic matter and water result in a peak in transport of these elements into the speleothem (Borsato et al., 2007). Often this corresponds with the more organic rich layers of a speleothem which can be observed using fluorescence spectrophotometry (Uchida et al., 2013). Fluctuations in these elements have been used as an alternative to visual counting of laminae when producing date models and can be used as a tuning technique (Smith et al., 2009).

### 3.2.4 Host Rock Dissolution

The influence of increased host-rock dissolution on trace element chemistry is generally overlooked as a simple process dependant only on residence time. However, it is also dependent on a host of other variables including lithology, hydrology (and thus climate), and water chemistry.

The lithologies overlying a speleothem drip site are unlikely to change during the lifetime of a speleothem record so any influence they may have on trace element variability should be constant. However, changes in flow path whether by blockage, erosion over time, or by changes in flow volume may sample different overlying lithologies. The nature of these changes means that they are essentially impossible to observe directly. The possibility that a speleothem drip regime has not remained constant through the whole of a record should be considered however, especially when hiatuses or growth axis shifts are present in a speleothem.

Increased residence time allows more fluid-rock interaction, such as dissolution of calcite and/or dolomite (and in some cases other mineral phases) up to saturation, resulting in increased trace element concentrations within dripwater. This process, although complex on a crystal scale with variations in surface area, mineralogy and localised incongruent dissolution, is fairly uniform on a karst scale (Fairchild and Baker, 2012). Residence time in karst decreases with increasing flow rate as additional water is added (effectively following Darcy's Law). As such, it can be directly related to effective rainfall amounts passing through the karst. The majority of intra-karst factors influencing dissolution (e.g. lithology) are constant over time, therefore the link between residence time and effective rainfall should remain fairly constant (assuming no major shifts in hydrology).

In more complex cases increased rainfall can activate different fluid pathways through the karst, resulting in non-linear changes in response to rainfall amount. This process is often difficult to study in detail without extensive monitoring at the cave site itself using local weather data, drip monitoring, and tracer tests where possible. Subsequent numerical modelling can be used to attempt to determine the flow paths feeding a particular drip (Fairchild et al., 2006b). The hydrology of karst systems is complex and spatiotemporally variable with individual drip sites potentially sampling waters with multiple fluid pathways and residence times. Even simple modelling of these processes has to incorporate multiple pathways including both seepage flow and fracture flow, whilst more complex models may include additional "overflow" flow pathways, soil moisture models and accounting for evapotranspiration. Although complex and difficult to disentangle, these factors can

influence dripwater trace element chemistry and thus are important considerations. As a general rule, lower residence times result in less dissolution of the slower to dissolve dolomites and silicate rocks which may be present in the karst and as a result lead to lower trace element concentrations in drip waters. However, trace element concentrations do not necessarily scale linearly with residence time.

In practice, complete characterisation of karst hydrology in a study site is effectively impossible without prohibitively high resource and time investment, however some degree of understanding of drip response to rainfall is essential for trace element record interpretation. The "flashiness" of a drip's response to rainfall dictates to some degree the potential temporal resolution with which a proxy record can be constructed. A seepage flow drip with little or no response to individual rainfall events will average any geochemical signals over a longer time frame (Baker et al., 2014; Baldini et al., 2012; Treble et al., 2015). This will obscure any event scale variability, but may provide a more useful dataset for reconstructing seasonal, annual or inter-annual variability. Conversely, a "flashy" drip response where rainfall is reflected in increased drip rates within minutes or hours will better preserve higher resolution events such as tropical storms (Frappier, 2008). This response however, may be at the expense of clear long-term signals and may result in more variable and difficult to characterise stalagmite growth rates. As such, hydrology should be considered during both interpretation of a stalagmite record and in initial sample selection.

### 3.2.5 Trace Element Incorporation, Distribution Coefficients, and Prior Carbonate Precipitation

The proportion of any given trace element incorporated in a substance precipitating from a solution can be quantified by a value referred to as a distribution coefficient (or sometimes partition coefficient). This can be expressed simply as the ratio of trace element content in the precipitate to that of the precipitating fluid:

$$D_{Tr} = \frac{Tr/_{Ca}\,(calcite)}{Tr/_{Ca}\,(fluid)}$$

Where $D_{Tr}$ is the distribution coefficient for a give trace element (Tr). This simple measure contains a great deal of information about trace element behaviour in a speleothem, because its value indicates how strongly an element is incorporated or excluded from a precipitating speleothem, as well as influencing dripwater evolution prior to speleothem deposition. Extensive research has been done in both the general field of chemistry, as well as specific to speleothem science, with the aim of constraining the value of $D_{Tr}$ for particular elements and precipitating minerals. Much of this research has focused on the behaviour of elements with regard to temperature, leading to the development of the Mg/Ca temperature proxy in foraminifera (Barker et al., 2005). However, the exact values of distribution coefficients are influenced by many factors, including temperature, growth rate, competition effects (i.e., solution composition), pH, biological factors, elemental form (e.g., valence state, complexation, etc.), crystallography, and many others (Gabitov et al., 2008; Gabitov et al., 2014; Huang and Fairchild, 2001; Meece and Benninger, 1993; Mucci and Morse, 1983). Additionally, care must be taken to ensure that the trace element dataset being studied is relevant to interpretation using the distribution coefficient concept. If much of the incorporated (or indeed fluid component) trace element is sourced from detrital or biological components within the crystal or solution then the measured trace element ratio cannot be used as a true distribution coefficient between the solution and solid in a chemical sense. Distribution coefficients are therefore principally used for the interpretation of elements which are primarily transported in aqueous solution, and subsequently incorporated within the carbonate crystal lattice.

Prior Carbonate Precipitation is perhaps the most commonly invoked process controlling trace element concentrations in speleothems and has been recognised as far back as Holland et al. (1964). During drier conditions, more degassing occurs higher in the karst system, resulting in precipitation of calcite (or aragonite) prior to precipitation on the studied speleothem. Often this is in the form of speleothem material higher in the cave on a stalactite or in a higher void, but in particularly arid locations can also include calcrete precipitation within the soil zone. Because the distribution coefficient of magnesium in calcite is less than one the result of this precipitation is an increase in Mg/Ca ratios in the remaining dripwater solution (Huang and Fairchild, 2001) and hence in the subsequently precipitated calcite. The same processes are also known to control variations of Sr/Ca and Ba/Ca within calcite speleothems (Hori et al., 2013), although interpretation of these can

be more complex as other factors such as growth rate and competition effects can also influence these elements (Borsato et al., 2007) (see section 3.2.6.1).

Within environments precipitating aragonite instead of calcite, such as Yok Balum Cave (Chapter 5) or Grotte de Le Chien (Wassenburg et al., 2012), a similar process occurs. However, because the partition coefficients of magnesium and strontium in the formation of aragonite are thought to be greater than one they will behave in the opposite manner, with their ratios decreasing as a result of prior aragonite precipitation. These values have, until recently, been poorly constrained by existing literature, and very little work on aragonite speleothem trace element chemistry has thus far been published. This is starting to change however, as a U/Ca record of Prior Aragonite Precipitation (PAP) (Jamieson et al., 2016) and a multi-sample determination of speleothem aragonite distribution coefficients (Wassenburg et al., 2016) have recently been published.

Greater understanding of not only the values of distribution coefficients, but also the chemical factors which modify them, is essential for furthering our understanding of trace element proxies in speleothems. Their value relative to one allows qualitative interpretation of changes in speleothem concentrations, but for any future quantitative backward modelling of speleothem trace element variability to reconstruct rainfall precise values are essential. Historically, many determinations of these values have been performed in solution chemistries that are markedly different from those occurring in caves, with published values largely being determined from seawater or seawater-like solutions (Jamieson et al., 2016). Both karst analogue (Day and Henderson, 2013) and in-cave determinations (Tremaine and Froelich, 2013) of these values are starting to become more common in the literature. In-cave determinations of these co-efficients are particularly valuable, as the influence of factors as diverse as temperature, growth rate, pH, solution composition, and several others alter distribution co-efficients resulting in cave- and likely even drip-specific values (Jamieson et al., 2016; Wassenburg et al., 2016).

### 3.2.6 Pathways of Trace Element Incorporation into Stalagmites

#### 3.2.6.1 Crystal Incorporation

The importance of incorporation effects on trace element concentrations in stalagmites is often minor, at least relative to other factors controlling speleothem trace element concentrations. Temperature controls on distribution coefficients, for example, are often dismissed as unimportant due to the long-term temperature averaging effect of caves (Fairchild and Baker, 2012). Mg/Ca is not generally used as a temperature proxy in speleothems as it is in biologically precipitated calcium carbonates in oceans because of this factor. Temperatures in caves simply do not vary enough to produce measurable shifts in trace element proxies due to direct influence on elemental incorporation, especially relative to the amplitude of other variations.

However, other influences on elemental incorporation have been demonstrated to influence speleothem trace element concentrations. Growth rate has long been identified as a strong influence on Sr incorporation, with increased growth rates resulting in additional incorporation sites for the $Sr^{2+}$ ion in calcite (Day and Henderson, 2013; Fairchild and Baker, 2012; Lorens, 1981). Additionally, several authors have identified competition effects where the presence of certain elements inhibits the incorporation of others, particularly at the expense of ions with larger atomic radii, which do not easily fit into the calcite lattice (Borsato et al., 2007; Day and Henderson, 2013).

#### 3.2.6.2 Other Incorporation Mechanisms

Not all elements in speleothems are incorporated within the crystal lattice. In some cases elements may be incorporated as part of micro- or macroscopic components trapped within the speleothem such as organic material, sediment particles, and fluid inclusions.

Organic material which has complexed elements (see section 3.2.3) may be incorporated alongside the elements, which it has transported (Hartland et al., 2012). Alternatively elements such as phosphorous may be part of the organic molecule itself (e.g., as organophosphates). These particles may be trapped in the growing speleothem at a variety of size fractions ranging from individual molecules to pollen grains. High levels of this

incorporation can be detected and quantified using optical methods, and often form the basis of seasonal laminae (see section 3.4.7.2). Alternatively, methods generally used for reconstructing organic geochemical proxies can be used to characterise speleothem organic matter (Blyth et al., 2008; Blyth et al., 2016).

Fluid inclusions in stalagmites, if intact and unaltered, theoretically preserve a sample of essentially unmodified dripwater within the stalagmite. Though they are increasingly used to examine the stable isotopes preserved within they are not commonly examined for their trace elemental composition, largely due to the analytical challenges of analysing a sample that small (micron scale, or smaller). They may however be analysed alongside the surrounding sample, contributing to any elemental signal measured (Fairchild and Baker, 2012). Although likely a minor source of error, they should be considered when interpreting records from stalagmites containing large numbers of fluid inclusions. Some authors have suggested that fluid inclusions may be major contributors to any sodium signal, for example (Fairchild et al., 2001).

The analytical method used to examine speleothem trace element chemistry may influence the detection of elements incorporated via non-carbonate material (e.g. sediment particles, fluid inclusions or organic material). In general, beam methods such as SIMS, µXRF and LA-ICPMS will analyse all material struck by the beam used regardless of solubility (Chapters 4 & 6). Solution introduction techniques, such as solution ICP-MS (Chapter 5) may (depending on the protocol and acids used) exclude insoluble sediment particles and any volatile components lost during milling from analysis. The choice of technique depends on the research question and the elements of interest. For example, in Chapter 4 the volcanic ash signal may partially reside in silicate material washed into the stalagmite. This signal may have been lost, if solution ICP-MS were used rather than LA-ICP-MS. Alternatively, in cases where the incorporation of elements into carbonate crystals is the subject of interest (as in Chapter 5), it may be preferable to use solution ICP-MS to exclude those extraneous components.

### 3.3 Analysis and Interpretation of Trace Element Data

Analytical techniques for generating trace element proxy datasets are not discussed in detail here, as they are numerous and well summarised elsewhere. Fairchild and Baker (2012) provide a comprehensive summary of the most commonly used techniques. Techniques relevant to this thesis are discussed in their respective chapters.

#### 3.3.1 Time Series Analysis

At its simplest, analysis of trace element proxies for palaeoenvironmental analysis involves the same forms of time series analysis as any other proxy. Trace element studies generally examine the correlation of elemental concentrations with other time series data using a variety of statistical methods ranging from direct correlations and general trends to more complex tools such as spectral analysis, frequency filtering, and transfer functions (Fairchild and Baker, 2012). An exhaustive list is not presented here, but instead several challenges and methods relevant to speleothem trace elements are examined.

#### 3.3.2 Challenges and Practical Issues in Trace Element Proxy Analyses

A major challenge in all geochemical proxy studies, particularly when operating at high-resolution, is that of age discrepancies. Even a record that faithfully records a climate signal with little noise or modification by other processes may appear to show no statistical relationship with the signal in question if the chronology is inaccurate. This can be tackled in several different ways, each of which has their own strengths and weaknesses. Simple lagging of records, a process that can be automated using autocorrelation tools, can compensate for systematic time offsets in a record. However, it cannot compensate for variable lags that may occur due to either random error in individual stalagmite dates or for real variable lags in the climate system resulting from teleconnections or hydrology.

"Tuning" of records, also sometimes referred to as "wiggle-matching" or "visual matching", involves manually and somewhat subjectively altering the chronology of a record to better match another. This can be done in a variety of ways for a variety of reasons, including using known annual cycles to improve the precision of an age model to seasonal (Ridley et al., 2015a) or to match events in the record to tie-points in another record (Richards and Andersen, 2013). This method is on statistically shaky ground however, as overfitting a record by wiggle matching can result in a dubious correlation which only exists because the record was tuned to create one. As a result, care should be taken to i) only tune within the bounds of dating precision, ii) avoid tuning to a parameter that is the focus of study, and iii)

to clearly state that tuning was undertaken. For example, in the ATM-7 record presented in Chapter 4 it is impossible to link Mg/Ca to El Niño robustly, as the Mg/Ca record was tuned to $\delta^{13}C$ which was previously linked to El Niño. A correlation is therefore an inevitable result of the tuning, even if it is a "true" record of variation due to that climatic variable. A relationship may still be inferred by a subjective visual relationship, however the statistical basis for this is weakened. Additionally, this tuning method can effectively remove important information from a record – such as the occurrence of lags between proxies, variable or otherwise. Blaauw (2012) presents an in depth review of the dangers inherent in tuning proxy records to one another, recommending that researchers should avoid tuning unless essential, re-check for implausible growth/sedimentation rates, ensure that errors and degree of tuning suit the research question, and ensure that any tuning corrections made are explicitly acknowledged.

There is no robust statistical method for correlating records that incorporates flexible time scales commonly in use in speleothem science. Some initial steps have been made in this area, with some age model software (e.g., COPRA) propagating age confidence intervals into the proxy time series outputted from the model (Breitenbach et al., 2012).

### 3.3.3 Other Analysis Methods

Most statistical techniques which are applicable to climate science have also been used to analyse speleothem records, including trace element records.

One technique, which shows great promise for analysis of multivariate trace element datasets, in particular is that of Principal Component Analysis (PCA). PCA is a multivariate statistical analysis technique used to identify the modes of variation within a multivariate dataset which best explain the overall variability (Abdi and Williams, 2010). For example, PCA has been successfully applied to identify distinct signatures of components carried in separate air masses (e.g. atmospheric dust versus sea ice aerosols) from a multivariate dataset of elemental measurements of ice cores, and principal component scores plotted as a time series produced a record of the significance of different components over time (Mayewski et al., 1994). In other cases it has been used to examine groupings of elements that record the same signal, highlighting which groups of elements respond to the same principal component of variation (which likely represents a particular parameter discussed

in section 3.2) (Mischel et al., 2016; Orland et al., 2014). PCA uses an orthogonal transformation to convert a multivariate dataset into a set of principal components orthogonal to each other, which explain the largest possible variance of the dataset, with each successive component explaining the highest remaining variance possible. Thus PCA can be used both as a tool to examine the relative response of elements to a particular controlling factor, as well as for time series analysis to investigate the variation of that factor over the period of the record. Chapter 4 uses this technique to identify a pattern of variation in multiple elements, which corresponds to volcanic ash inputs to the karst environment.

### 3.3.4 Identifying the signature of Prior Carbonate Precipitation

Prior Carbonate Precipitation is one of the most commonly cited mechanisms by which climate information is passed on to speleothem geochemistry. As such it has been the subject of a great deal of study, with various modelling (Stoll et al., 2012), monitoring (Sherwin and Baldini, 2011), and experimental work (Day and Henderson, 2013) devoted to understanding and quantifying the process.

#### 3.3.4.1 Ca vs. Mg/Ca plots

A commonly used method of illustrating the influence of Prior Calcite Precipitation (PCP) on a drip water trace element dataset is to plot calcium concentration against the ratio of magnesium to calcium concentrations. This plot features prominently in many papers, including Fairchild et al. (2000); Fairchild and Treble (2009); Rutlidge et al. (2014); and many others. Indeed, this method of presenting data is not unique to speleothem science and also appears in other fields of geochemistry e.g., igneous petrology (McDermott and Hawkesworth, 1991). This plot invariably shows a "Prior Calcite Precipitation trend" towards higher Mg/Ca values and lower Ca values.

However, this trend is not actually indicative of anything other than falling calcium concentrations in the drip waters. Producing any plot of A against B/A will show the same trend, even when using randomly distributed data. This "trend" will always follow the same hyperbolic trajectory, the position of which is only controlled by the data ranges of B and A, and the initial value of B.

Thus in the case of a Ca vs Mg/Ca plot, the "Prior Calcite Precipitation trend" will always conform to the equation y = n/x where n corresponds to the initial value of the magnesium concentration. This can be demonstrated mathematically as follows:

$$y = \frac{n}{x}$$

$$\text{Where:} \quad y = [Ca] \quad \text{and} \quad x = \frac{[Mg]}{[Ca]}$$

$$[Ca] = \frac{n}{\frac{[Mg]}{[Ca]}}$$

$$n = [Ca].\frac{[Mg]}{[Ca]}$$

$$n = [Mg]$$

This relationship is also apparent when plotted graphically. Figure 3.1 shows a random dataset, with magnesium concentrations between 100-1100ppm and calcium concentrations between 0-1000ppm, which has been generated and plotted in the traditional Ca versus Mg/Ca ratio style. The result is a scatter of data centred on a "Prior Calcite Precipitation trend" where n is the mean magnesium concentration, and bounded by the trends corresponding to the range of data. The position along the trend (i.e. moving from upper left to lower right) is controlled only by falling calcium concentration.

The trend therefore may indeed correspond to increasing amounts of PCP, but could also easily be caused simply by varying amounts of dissolution within the karst, dilution, or any

of a number of other processes operating in karst environments; it is not necessarily diagnostic of PCP.

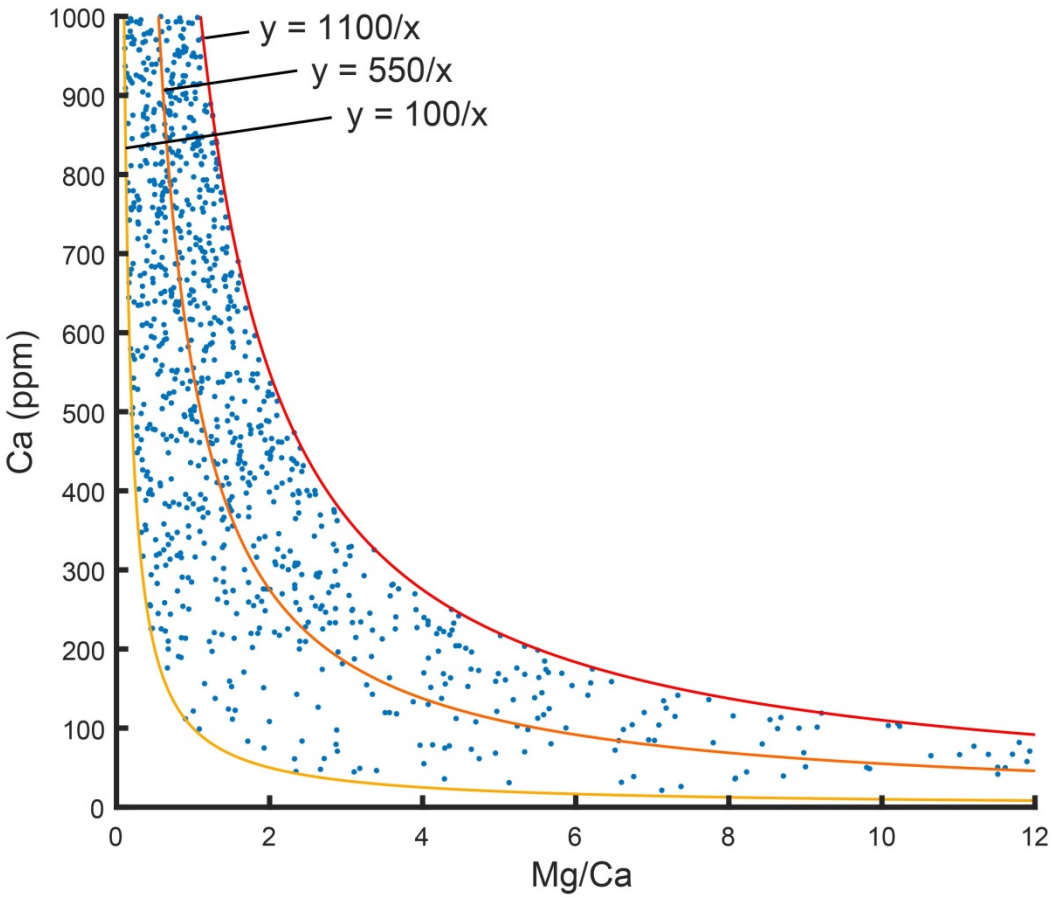


Figure 3.1: Randomly generated dataset of Mg and Ca values (blue), alongside trends defined by y = n/x (n = 100, yellow; n = 550, orange; n = 1100, red)

To further confirm this, a simple calcite precipitation model was used to iteratively calculate fluid composition as calcite progressively precipitates. Initial Ca and Mg concentrations of 1000ppm and 550ppm respectively were altered iteratively using a distribution coefficient based precipitation model to calculate changing Ca concentration and Mg/Ca ratios in a fluid. Plotting this data on the above figure yields an exact match to the predicted y=550/x line as expected from the initial Mg concentration.

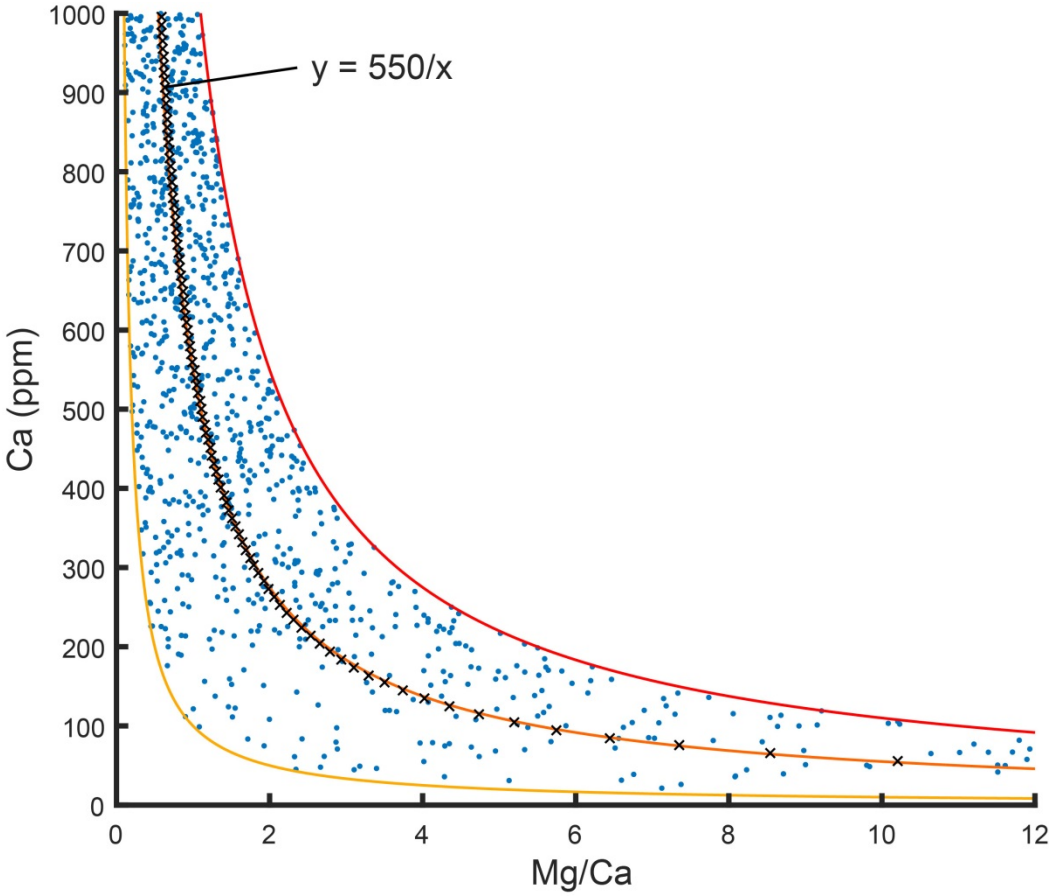


Figure 3.2: Figure 3.1, modified by the addition of a modelled PCP dripwater dataset (black crosses)

Movement down the trend does correspond to increasing amounts of modelled calcite precipitation, but this is solely due to the falling Ca concentration. The same trend can be generated using an array of Ca concentrations between 0 and 1000ppm against their ratio to a fixed Mg concentration of 550ppm. Such an array would not necessarily be produced by a PCP-like effect and in a natural context could represent mixing of high and low ionic strength waters – meaning that this diagrammatic method is not diagnostic of PCP.

Some information can be extracted from this plot, such as the spread of initial Mg values and the variability in Ca concentration within the fluid. However, these do not definitively demonstrate the presence or lack of a PCP mechanism as a control on dripwater/speleothem geochemistry.

Indeed, any two variables can be plotted against each other and produce this same pattern even if completely unrelated. In Figure 3.3 this is demonstrated using daily London temperature data plotted against the opening price of Apple stocks (AAPL), which are unlikely to be directly influenced by either Prior Calcite Precipitation or each other.

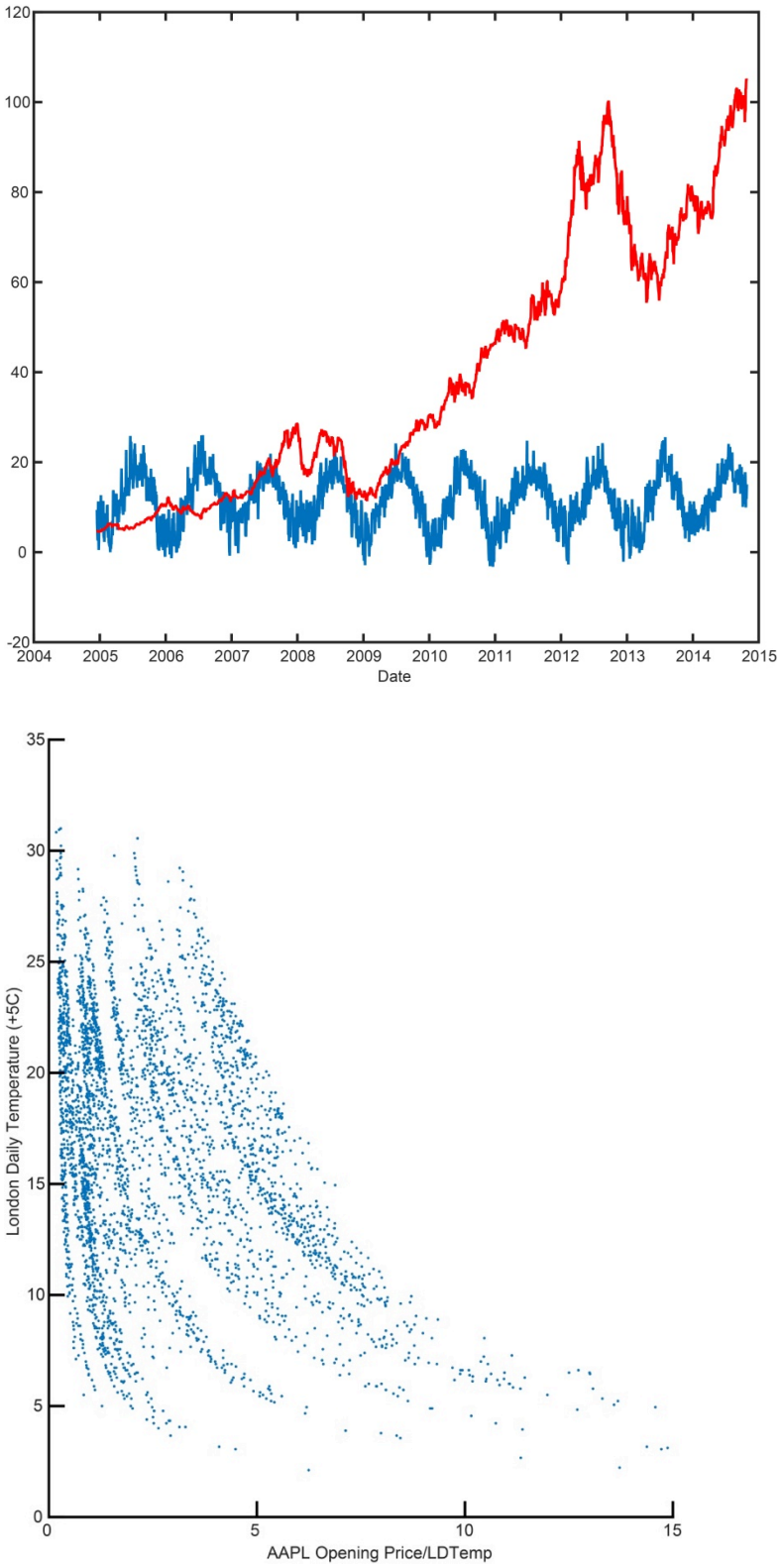


Figure 3.3: Top: London Daily Temperature Data in degrees Celsius (blue) and Apple Stock Price in dollars (red). Bottom: datasets plotted in the style of Figure 3.2.

### 3.3.4.2 Plotting two geochemical variables

The speleothem science community is beginning to explore different methods of plotting geochemical trends to illustrate the influence of PCP. Tremaine and Froelich (2013) also make the point illustrated in section 3.3.4.1, and proposed an alternate method of illustrating the effects of PCP on dripwaters using a "clock diagram" of Mg/Ca plotted against Sr/Ca (Sr/Ca being a second geochemical parameter which is often controlled by PCP, see section 3.2.5). In their method Tremaine and Froelich (2013) plot a series of PCP vectors, defined on the basis of Sr and Mg distribution coefficients in calcite, radiating out from a zone of initial concentrations dependant on initial conditions (as a result of mixing, or variable dissolution). This method has the advantage of allowing calculation of the amount of PCP that has taken place, as well as allowing extrapolation back to initial conditions. This method is also used by Sinclair et al. (2012), who plot ln(Sr/Ca) against ln(Mg/Ca) and define PCP vectors along a distribution coefficient calculated slope. This allows them to diagnose dripwaters as either "Pure PCP" defined, or as more complex mixtures of processes.

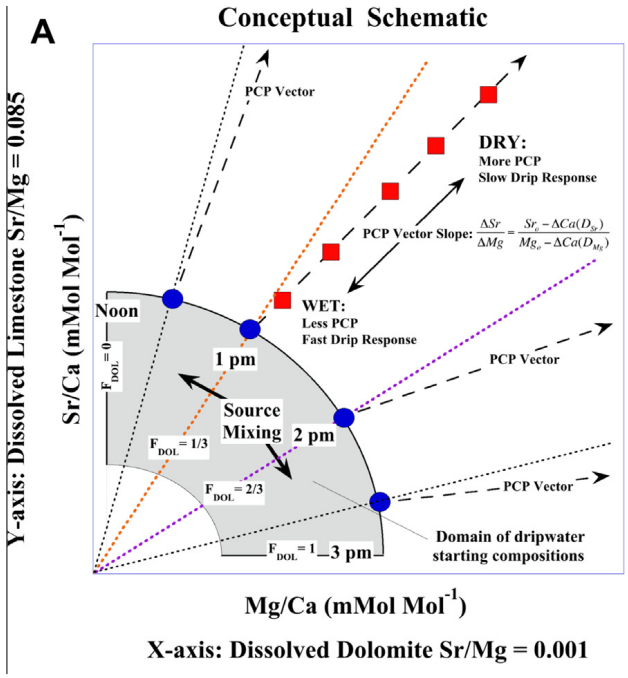


Figure 3.4: Conceptual schematic of the "clock diagram" of Tremaine and Froelich (2013).

This "clock diagram" method is starting to appear with increasing frequency in the literature, and is being applied particularly to dripwater geochemistry (Borsato et al., 2016; Treble et al., 2015). It appears to show promise in eventually leading to quantitative

backwards modelling of PCP (and hence effective rainfall amounts) in caves where drips are geochemically monitored and show strong correlations between drip position on a PCP vector and effective rainfall. However, this methodology may not be universally applicable as many other factors can influence trace element geochemistry. Sr/Ca itself may not always primarily record PCP in caves where growth rates or competition effects are influences on its variability (Gabitov et al., 2014). This may result in trends which do not conform to an expected PCP vector, even in caves where Mg/Ca does record PCP. This once again emphasises the need to consider every process that influences dripwater and speleothem trace element concentrations (Section 3.2).

#### 3.3.4.3 Multivariate Approaches

Ultimately, speleothems are complex natural systems with multiple factors influencing the variability of the data. Generally speaking there is no "one size fits all" solution to plotting the trajectories which PCP/PAP vectors will take due to the variability of distribution coefficients as a result of temperature, competition, biological and crystallographic variations (Day and Henderson, 2013; Wassenburg et al., 2016) as well as potential changes in source inputs or weathering variations in and above the cave site. Indeed, the possible parameter space when including all of the possible variations in inputs, incorporation mechanisms, and distribution coefficients is large enough that a stalagmite dataset can display a very large scatter around any notional PCP vector.

Any method attempting to constrain the different influences on the trace element chemistry of speleothems must be able to flexibly accommodate these (often unknown) variations whilst also retaining information about the climate variable of interest. Fitting a trend to a dataset and attributing that trend to (for example) a PCP trend may be correct, but may very well be the result of overfitting of a model to a noisy dataset due to the flexibility of the model parameters.

### 3.3.5 Modelling Trace Element Behaviour

#### 3.3.5.1 Processes

Simple modelling of the evolution of aqueous solutions is already a fairly mature field, with software such as PHREEQC commonly used to model and examine aspects of solution chemistry relevant to secondary carbonate deposition, particularly when examining

geochemical speciation. On a large scale the chemistry of these processes is reasonably well understood. The reactions involved in carbonate equilibria and their equilibrium constants are well defined for example. Some aspects are less well constrained, such as the previously discussed variability in distribution coefficients as well as some open questions such as the role of biology in carbonate precipitation, but for the most part these can be neglected at all but very small scales.

The I-STAL model of Stoll et al. (2012) specifically models the variation in trace elements which results from water-rock interaction and PCP. It uses a distribution coefficient-based mechanism to evolve dripwater Mg, Sr and Ba concentrations to model the relationship between stalagmite trace element variation and PCP amount. The model effectively simulates these processes and is a useful tool for identifying when cave $pCO_2$ variations or drip rate changes are responsible for trace element cyclicity. As with all models however it is only as good as its inputs, requiring a cave site which is well understood, and free from complicating factors (such as detrital input). Additionally, the model requires reasonably well-constrained distribution coefficients, which (as discussed in Section 3.2.5) are not always available, constant, or applicable to a particular cave site.

#### 3.3.5.2 Mixing

Understanding the chemical evolution of water in the karst is an important process, but when considered alone can produce an incomplete picture of the final composition of dripwaters. Drip sites can contain water sourced from several different flow pathways, each of which has had a distinct geochemical evolution and residence time. It may sample different lithologies (section 3.2.4), have different residence times (section 3.2.4), and may even only be active during high flow periods (periods of high effective rainfall). Modelling this process is a significant challenge. Flow paths in the karst are commonly categorised into two main categories: seepage flow and fracture flow. These flow paths may feed drip sites individually, or may mix in a reservoir prior to reaching the stalagmite. Furthermore, the relative dominance of these flowpaths is not constant over time and relates to both effective rainfall and aquifer conditions. In periods of high flow additional flowpaths may be activated, as “overflow” pathways which can occur when karst stores saturate. Drip monitoring and modelling can, together, help to characterise the flowpaths feeding a particular drip and characterise their responses to rainfall. However, many of the factors

influencing drip rates are complex, non-linear, and difficult to characterise without extensive site characterisation. Any model of fluid movement in the karst will be specific to a particular drip, rendering it difficult to produce a general model for all speleothems.

#### 3.3.5.3 Challenges in modelling trace element behaviour

The challenges in modelling trace elements again come down to the incorporation and characterisation of the plentiful inputs that can influence trace element variability in speleothems. Ultimately no model will be able to perfectly account for every factor influencing stalagmite trace element geochemistry: “Essentially, all models are wrong, but some are useful" (Box and Draper, 1987). However, with sufficient understanding of a cave system gained through monitoring and thorough site characterisation it may be possible to produce models of trace element behaviour in karst that explain the majority of their behaviour, and hence quantitatively reconstruct climate parameters with high confidence.

### 3.4.0 Speleothem Trace Elements as Environmental Proxies

Having established that speleothem trace element concentrations are the result of a variety of spatially, temporally, and chemically variable processes, many of which are complex and challenging to completely characterise, this section can now discuss the interpretation of different trace elements as proxies for these processes. Many trace element proxies discussed here record multiple environmental signals, and understanding the relative dominance of those signals in a record is vital to their interpretation.

### 3.4.1 The Alkali Earth Metals

Water-soluble trace elements, which are readily incorporated into calcite such as magnesium, strontium or barium, are the most studied and well understood trace elements in speleothems. Extensive work has been done, particularly focusing on magnesium, using these elements as proxies for rainfall (Fairchild and Baker, 2012). Numerous studies have linked variations in Mg/Ca ratios in speleothems to changes in rainfall. Under drier conditions less water moves through the karst, resulting in several effects which collectively influence magnesium concentrations (Fairchild et al., 2000). Increased residence time allows more fluid-rock interaction, such as dissolution of dolomite up to saturation, resulting in increased magnesium (and other element) concentrations

within dripwater. Additionally, more degassing occurs higher in the karst system, resulting in precipitation of calcite prior to the speleothem being studied. Often this is in the form of speleothem material higher in the cave, but in particularly arid locations may also include calcrete precipitation within the soil zone. Because the partition coefficient of magnesium in calcite is less than one the result of this precipitation is an increase in Mg/Ca ratios in the dripwater solution (Huang and Fairchild, 2001). The same processes are also known to control variations of strontium and barium concentrations within calcite speleothems (Hori et al., 2013), although interpretation of these can be more complex because other factors (e.g., growth rate) can also influence these elements (Borsato et al., 2007). Indeed, in some cases this can be the principal source of variation in Sr/Ca and Ba/Ca (Tan et al., 2014).

Examples of alkali metals as effective rainfall proxies are plentiful within the speleothem literature over a variety of time scales. Cruz Jr. et al. (2007) linked long-term Sr/Ca and Mg/Ca variability over the last 116 ky in southern Brazil to summer insolation driven changes in the South American monsoon. At much shorter time scales authors have also definitively linked sub-annual variations in trace element concentrations to effective rainfall. Johnson et al. (2006) document clear seasonal variations in multiple elements which they attribute to effective rainfall driven changes in $CO_2$ degassing and PCP. Many other studies have produced similar records using these elements, demonstrating that they are an effective and robust proxy for effective rainfall in many environments and locations (Bernal et al., 2016; Borsato et al., 2016; Garnett et al., 2004; Griffiths et al., 2010; Johnson et al., 2006; McMillan et al., 2005; Sinclair et al., 2012; Treble et al., 2003; Tremaine and Froelich, 2013; Ünal-İmer et al., 2016; Verheyden et al., 2000).

Within aragonite speleothems such as the stalagmite YOK-G from Yok Balum Cave (Chapter 5) a similar process occurs. However, because the partition coefficients of strontium and barium in the formation of aragonite are thought to be greater than one they will behave in the opposite manner, with their ratios decreasing as a result of prior aragonite precipitation. These values are poorly constrained by existing literature however, and very little work on aragonite speleothem trace element chemistry has thus far been published (Wassenburg et al., 2016).

Variations of external supply generally have minimal influence on the variability of alkali metals in speleothems, since the amounts of these elements sourced from overlying lithologies are the majority source. However, in some cases sea spray has been cited as a significant input of these elements (Baldini et al., 2015).

### 3.4.2 Uranium

Uranium is an element which, although easily measured as part of a suite of elements during trace element analysis, is rarely used as a proxy in speleothems. Some studies have linked U/Ca to flushes of organic matter in calcite speleothems (Treble et al., 2003), often alongside phosphorous or other organically transported elements (see section 3.2.3). Alternatively, increases in speleothem U/Ca may result from inputs from anthropogenic sources such as mining pollution (Siklosy et al., 2011).

Wassenburg et al. (2016) determine that the distribution coefficient of uranium in aragonite is greater than one, and thus increased prior aragonite precipitation acts to lower U/Ca values in aragonitic speleothems. In Chapter 5 of this thesis U/Ca is linked to varying occurrence of Prior Aragonite Precipitation in an aragonitic speleothem. This new proxy shows a great deal of potential for reconstructing effective rainfall as it reflects rainfall variation on scales varying from seasonal to multi-decadal.

### 3.4.3 Phosphorous

Phosphorous variability in speleothems has been linked to bioproductivity, and is likely sourced predominantly from decaying organic matter in soils. Treble et al. (2003) described phosphorous variability in an Australian speleothem, and link it to vegetation decay and transport processes that are the result of rainfall changes. They also suggest that phosphate concentrations in dripwaters may exert a strong control on transport of U through the karst. The processes controlling phosphorous incorporation in speleothems are little researched however, although some early work suggests that it is incorporated in several forms including phosphate defects in calcite crystals and separate crystalline phosphate phases within the speleothem (Mason et al., 2007). The possibility also exists that phosphorous is incorporated within organic molecules themselves, as the presence of a variety of organic compounds has been documented in speleothems (Blyth et al., 2016).

### 3.4.4 Lead

Lead is an element that is not particularly abundant in speleothems, but which when it is incorporated in appreciable concentrations can function as a useful tool for extracting information from these archives. It has relatively low background concentrations in most settings, so increases in lead content generally correspond to an external input of material to the cave site. This can be anthropogenic in origin (Tan et al., 2014) or derived from volcanic ash (Jamieson et al., 2015). Yang et al. (2015) suggested that when lead is derived from local sources, including both lead minerals and within carbonates, variations in lead isotopic ratios may be controlled by mixing between two distinct sources, and thus perhaps can serve as a proxy for hydrological variation. Allan et al. (2015) also suggests that lead isotope ratios can be used to discriminate between different anthropogenic sources.

### 3.4.5 Sulphur

Sulphur incorporation in speleothems appears to be primarily in the form of sulphate ions (Frisia et al., 2005), incorporated as a substitution for the carbonate ion in speleothem calcite. Multiple studies have demonstrated that sulphate content in speleothems correlates well with the dripwaters from which they precipitate (Borsato et al., 2015), suggesting that speleothems faithfully record sulphate inputs into the cave system. Sulphate concentrations in speleothems are therefore good recorders of sulphur inputs to cave sites, and thus record anthropogenic and volcanic variation in sulphur supply (Wynn et al., 2008). Interpretation of this signal can be challenging however, as sulphur is a biologically active element, and may be delayed in reaching a cave due to variable biogeochemical cycling in the soil and overlying vegetation. In depth site characterisation using long term dripwater monitoring as well as stalagmite derived sulphate records is essential, but can ultimately produce excellent records of both anthropogenic sulphur pollution as well as volcanic deposition (Borsato et al., 2015).

### 3.4.6 Others

Elements which are less water soluble, or generally immobile, can also be incorporated into speleothems. This category includes a wide suite of elements, ranging from more common metals to rare earth elements. However, the availability of these elements is limited unless

they can be more readily transported through the karst system. Organic material making up the colloidal fraction of particulate organic matter is particularly good at complexing and mobilising a variety of trace elements such as transition metals and rare earth elements (Hartland et al., 2012). As a result, these elements tend to build up in the soil until conditions are right to enable their transport into the karst system. In many caves around the world this manifests as a trace element concentration maximum synchronous with an autumnal flushing event, where the availability of large amounts of organic matter and water result in a peak in transport of these elements into the speleothem (Borsato et al., 2007). Often this matches with the more organic rich layers of a speleothem which can be observed using fluorescence spectrophotometry (Uchida et al., 2013). Fluctuations in these elements have been used as an alternative to visual counting of laminae when producing date models and can be used as a tuning technique (Smith et al., 2009).

Other elements, which are more analytically challenging to measure, such as chlorine or bromine have been mooted as potential proxies. Chloride in dripwaters has been used as a tracer for sea salt contributions to other major elemental concentrations in dripwaters (Tremaine et al., 2016). This is potentially an important tool for site characterisation where sea spray inputs may periodically subsume signals of other sources of trace element variability. Bromine has been measured in speleothems using synchrotron radiation based micro X-ray fluorescence. This technique is limited to small sample sizes, but is highly sensitive to very small fluctuations in extremely low concentration trace elements. Badertscher et al. (2014) used this technique to identify the signal of volcanic eruptions in a stalagmite from Turkey. This is potentially a very reliable way of detecting volcanic eruptions in speleothems, but requires some degree of prior information about where to look.

### 3.4.7 Non-Proxy Applications

#### 3.4.7.1 Direct Dating

Several trace elements in speleothems are used for dating samples. The most well known of these are uranium and its decay products. The U-Th system can be used to date stalagmites from approximately 0-500,000 years in age, albeit with some uncertainties introduced by either low concentrations of the measured elements or contamination from

detrital thorium incorporated into a speleothem. A thorough understanding of the sources of Th is crucial and can affect results (Moseley et al., 2016). For older stalagmites, the U-Pb system can also be used (Woodhead and Pickering, 2012).

Short-lived radioisotopes have also been used in modern stalagmites (Condomines and Rihs, 2006), including those produced by nuclear testing. Caesium-137 found in the natural environment is primarily anthropogenic in origin, and can be used to confirm the modernity of a stalagmite sample (Frappier et al., 2007b).

Additionally, clear trace element events such as those resulting from volcanic eruptions (Badertscher et al., 2014) or peak anthropogenic emissions (Borsato et al., 2015) can be used as tie-points to link chronologies to known historical events. Great care must be taken when interpreting these events however, to ensure that the trace element peak is the result of a given event, as well as accounting for any temporal lags introduced by biogeochemical cycling.

#### 3.4.7.2 Annual/Seasonal Layering

Many trace elements exhibit annual or seasonal cyclicity in response to environmental variables (see section 3.2.3). In addition to recording palaeoenvironmental information these cycles can also be used to produce, confirm or better constrain age models in stalagmites (Smith et al., 2009). This technique is not without limitations however. First, to use this technique these trace element variations must confidently be interpreted as truly annual. This requires at least a preliminary understanding of the processes influencing that element in the study site and ideally a rough estimate of annual growth rate. Cycles must be consistently annual and not disrupted by events such as droughts, periods of reduced seasonality, or changes in growth rate. Secondly, any count of cycles is to some degree subjective based on the criteria selected to define a cycle. Duplication or omission of cycles due to either counting error, or unclear cyclicity leads to the introduction of cumulative errors in any cycle count age model. Chapter 6 discusses an example of a stalagmite which exhibits some degree of annual cyclicity in trace element variability, but for which the inconsistency of cycles leads to a significant undercount relative to the more confident U-Th and radiocarbon chronologies.

In general, annual cycles in speleothem proxies work best when used in conjunction with precise anchor points using more traditional dating techniques. In these cases annual cyclicity can be used to refine an age model to a seasonal resolution. Chapter 5 uses such a chronology, although it was originally generated using seasonal cyclicity in $^{13}C$ rather than trace elements (Ridley et al., 2015a).

### 3.5.0 Next Steps: New Proxies, New Methods and New Contexts

Speleothem trace element proxies are a diverse group of proxies. They are influenced to varying degrees by a large number of processes both inside and outside the cave environment. As summarised in this chapter, speleothem science is beginning to constrain many of these processes for several trace element proxies. The understanding of Mg/Ca behaviour, for example, is now relatively well understood with the main challenge characterising the sources of Mg variability in any given location. For many elemental systems, however, there is still a great deal of work to be done. Distribution coefficients for many elements in both calcite and aragonite, and under the range of conditions and chemistries found within caves, are still quite poorly constrained (only Mg has really been thoroughly studied). This is slowly changing with the use of karst analogue (Day and Henderson, 2013), in cave (Tremaine and Froelich, 2013), and speleothem derived (Wassenburg et al., 2016) studies beginning to better constrain these values.

Analytical techniques for speleothem trace element analysis are now capable of extraordinary spatial resolutions and precision measurement of very low concentrations. Many challenges remain, including issues with quantification and heterogeneity. LA-ICP-MS for example is still generally considered to be semi-quantitative due to the lack of matrix-matched standards for carbonates, although this is slowly beginning to change (Barats et al., 2007). The heterogeneity of samples is also coming into play, because at the resolutions now being measured factors such as inclusions, crystal boundaries and microstratigraphy become significant (Frisia, 2015). Despite this, improved resolution is allowing construction of speleothem records with sub-annual resolution (e.g.,Frappier et al. (2007b)). Additionally, almost any element in the periodic table is now technically measurable in speleothems (where present) and, in many cases, can also be examined for isotopic

variability (Yang et al., 2015). This opens the door to a host of additional proxy reconstructions, which have not previously been viable due to detection limitations. One example currently garnering a great deal of interest is the interaction between organic matter and various trace metals. Hartland et al. (2012) demonstrated clear links between trace metal transportation and the forms of organic matter present in dripwaters, suggesting a link to rainfall volumes. This is a rapidly developing branch of speleothem science, with a great deal of potential to produce new records of different palaeoenvironmental information.

Speleothem reconstructions are also becoming available from previously ignored archives. Aragonitic stalagmites show a great deal of potential for the generation of proxy records with extraordinarily precise chronologies thanks to their higher uranium content (Ridley et al., 2015a), and increasing understanding of their geochemistry (Wassenburg et al., 2016). Furthermore, non-cave speleothem-like deposits are showing promise, particularly for the reconstruction of anthropogenic activity (Pons-Branchu et al., 2015).

### 3.6.0 Conclusions

In summary, speleothem trace elements are a diverse and complex suite of proxies, which integrate a great deal of palaeoenvironmental information. In many ways, the number of processes that can exert their influence on trace element geochemistry makes their use challenging for any particular research question. However, by careful characterisation of study sites, as well as using multiple proxies to compare variability, it is possible to extract extremely high quality information from these records. Whilst their interpretation will likely never be as simple as a straightforward global calibration (as is possible with Mg/Ca in foraminifera, or in several biomarker proxies), they can be used to reconstruct high-resolution, temporally precise information about a host of environmental variables.

The following three data chapters each discuss separate speleothem records, which preserve diverse palaeoenvironmental information using several different trace element systems. They describe a new technique for looking at multivariate trace element data collectively, a new proxy for use in aragonitic speleothems, and a reconstruction of a significant climate variable at a sight highly sensitive to basin scale climate variability. Each

of these chapters demonstrates the continued importance and potential of speleothem trace element proxies for palaeoenvironmental reconstruction.

# Chapter 4 Volcanic ash fall events identified using principal component analysis of a high-resolution speleothem trace element dataset

*A version of this chapter has been published in Earth and Planetary Science Letters authored by Robert A. Jamieson [a,*], James U.L. Baldini [a], Amy B. Frappier [b], and Wolfgang Müller [c].*

[a] *Department of Earth Sciences, Durham University, United Kingdom*

[b] *Department of Geosciences, Skidmore College, NY, United States*

[c] *Department of Earth Sciences, Royal Holloway University, London, United Kingdom*

A version of this chapter has been published in Earth and Planetary Science Letters (Jamieson et al., 2015) with contributions from the following authors:

**Robert A. Jamieson** analysed the sample, processed the data, performed the statistical analyses, interpreted the data, and wrote the manuscript thereby contributing to over 90% of the work presented in this chapter.

**James U.L. Baldini** assisted with interpretation of the data and provided extensive comment on the manuscript.

**Amy B. Frappier** collected the sample and did much of the previous work on this sample (Frappier et al., 2002; Frappier et al., 2007b).

**Wolfgang Müller** assisted with the LA-ICP-MS analysis at Royal Holloway University, London

All authors provided comment and approval on the final manuscript.

## Acknowledgements

TOMS Time Series analyses used in this study were produced with the Giovanni online data system, developed and maintained by the NASA GES DISC. The authors gratefully acknowledge the NOAA Air Resources Laboratory (ARL) for the provision of the HYSPLIT transport and dispersion model and READY website (http://www.arl.noaa.gov/ready.php) used in this publication. Eruption timings and magnitudes sourced from the Smithsonian Institution Global Volcanism Program unless otherwise specified.

The Division of Petrology and Volcanology, Department of Mineral Sciences, Smithsonian Institution kindly provided El Chichón ash sample NMNH 115695 to A.B. Frappier.

The European Research Council (240167) supported this research.

We gratefully thank the three anonymous reviewers and editor Derek Vance for their useful comments and critique of the submitted manuscript.

# Chapter 4: Volcanic ash fall events identified using principal component analysis of a high-resolution speleothem trace element dataset


## Abstract

Large multivariate trace element datasets produced by LA-ICP-MS speleothem analysis can pose difficulties for analysis and interpretation. Processes acting on various timescales and magnitudes affect trace element concentrations, and deconvolving the most important controls is often complex. Here Principal Component Analysis (PCA) is applied to identify the modes and timings of variation which best explain the overall variability in an exceptionally high-resolution (10µm vertical resolution) multivariate trace element record produced by LA-ICP-MS from a modern (1979-2001) Belizean stalagmite with excellent age control.

Principal Component 1 (PC1) in this dataset is defined by a weak correlation between multiple elements, and may reflect non-carbonate material incorporated within the speleothem. Elevated PC1 scores in ATM-7 occur following regional volcanic eruptions with ash clouds extending over the cave site, as demonstrated using NASA remote sensing data from the Total Ozone Mapping Spectrometer and HYSPLIT trajectory modelling. Spikes in PC1 occur at the beginning of the wet season, and this may reflect a seasonal flushing event that transports volcanogenic material through the karst and incorporates it within the speleothem.

Our results suggest that PCA can simplify exploration of large laser ablation datasets, and that PCA is a valuable tool for identifying the dominant controls on stalagmite trace element chemistry. Future studies should evaluate how transferable this technique is to other sites with different environmental conditions where volcanic ashfall has occurred. This research potentially adds tephrochronology to the stalagmite dating toolkit or, conversely, opens the door to using stalagmites to identify previously unknown or uncertainly dated eruptions.


## 4.1.1 Introduction

Speleothems are important terrestrial archives of high-resolution palaeoenvironmental information, particularly for low latitudes. They are precisely dateable using a variety of

techniques and contain a wealth of different proxy information. Stable isotope ratios are the proxies most commonly used in speleothem research to infer regional climatic information (McDermott, 2004). However, other proxies including laminae thickness (Baker et al., 2008), optical properties (Proctor et al., 2000), trace element concentrations (Fairchild and Treble, 2009), and calcite density (Zhang et al., 2010) also record various climatic and hydrological information. Trace elements in particular preserve diverse information including both climate (Cruz Jr. et al., 2007) and non-climatic signals such as volcanism (Frisia et al., 2008), land use changes (Borsato et al., 2007) and anthropogenic emissions (Tan et al., 2014).

Detection of volcanic signals in speleothems has focused on two primary avenues of inquiry: indirect records of the environmental effects of volcanism (e.g., aerosol forced cooling (Ridley et al., 2015a) or increased growth rate (Baker et al., 1995)) or direct evidence of volcanism (e.g., elevated sulphate concentrations in speleothems; (Frisia et al., 2005)). The former is generally inferred based on stable isotope ratios (Ridley et al., 2015a) as hydrological or temperature records, whilst direct detection of volcanogenic material has thus far focused on measuring extremely low trace element concentrations using techniques such as synchrotron radiation based micro X-ray fluorescence (Frisia et al., 2005; Frisia et al., 2008). Higher detection limits and an inability to measure certain elements due to common polyatomic interferences (such as high counts of $^{16}O_2$ swamping any $^{32}S$ signal (Reed et al., 1994)) complicate the detection of volcanogenic material using more widely available techniques such as inductively coupled plasma mass spectrometry (ICP-MS). However, these limitations can be overcome by examining multivariate ICP-MS data using methods that examine the covariation of multiple elements derived from volcanogenic sources.

Here we use Principal Component Analysis (PCA) of high-resolution LA-ICP-MS data to detect the signal of volcanic ash deposition in a Belizean stalagmite. PCA is a multivariate statistical analysis technique used to identify the modes of variation within a multivariate dataset which best explain the overall variability (Abdi and Williams, 2010). For example, PCA has been successfully applied to identify distinct signatures of components carried in separate air masses (e.g. atmospheric dust versus sea ice aerosols) from a multivariate dataset of elemental measurements of ice cores, and principal component scores plotted as a time series produced a record of the significance of different components over time (Mayewski et al., 1994). In a speleothem context, this technique could identify different

modes of trace element variation within a time series. This method allows the deconvolution of signals such as volcanism from the background variation in a multivariate trace element dataset.

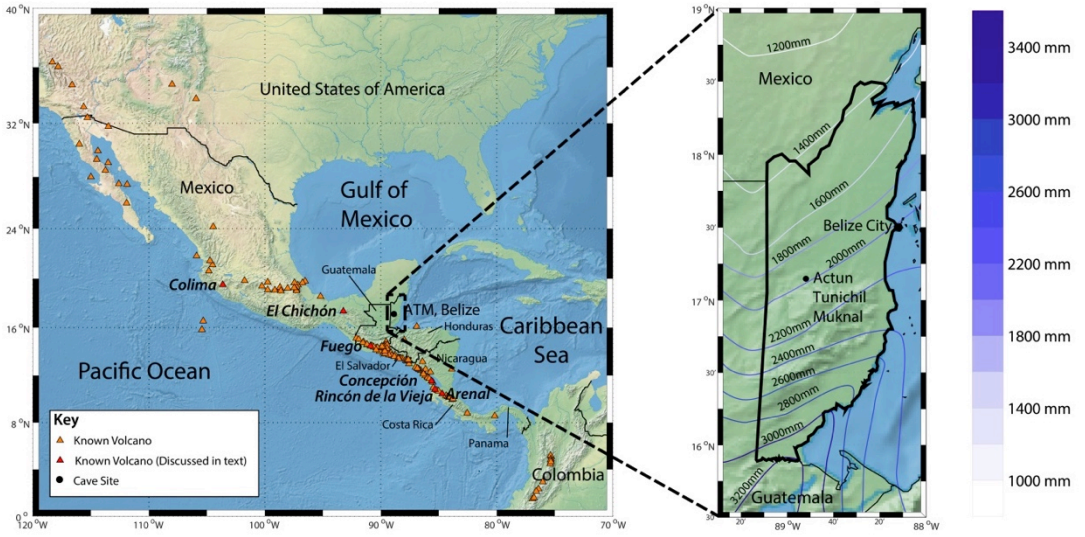


Figure 4.1: Left: Location of Actun Tunichil Muknal and all volcanoes in Central America. Right: Location of ATM in Belize, with contoured mean annual rainfall (Medina-Elizalde and Rohling, 2012).

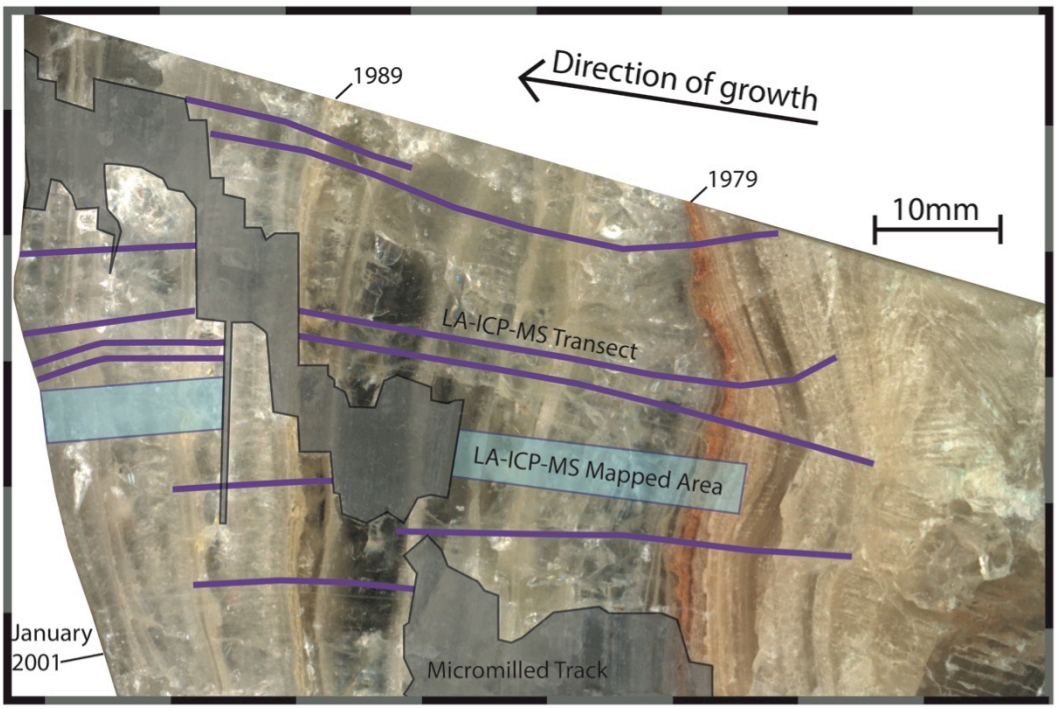


Figure 4.2: Polished section of ATM7 used in this study. Black outlines with grey shading highlight micromilled track used for generating the stable isotope records used in Frappier

et al. (2002) and Frappier et al. (2007). Purple lines show laser ablation tracks. Blue shaded areas show areas of laser ablation mapping.

### 4.2.1 Methods

Stalagmite ATM7 was collected in January 2001 from Actun Tunichil Muknal (ATM) in central Belize (Figure 4.1), dated using radiometric ($^{137}$Cs) and layer-counting methods (Frappier et al., 2002), and $\delta^{13}$C and $\delta^{18}$O records produced and published (Frappier et al., 2002; Frappier et al., 2007b). Frappier et al. (2002) interpreted $\delta^{13}$C variability as a proxy for ENSO driven changes in the soil and local ecosystem carbon cycle. Frappier et al. (2007) interpret $\delta^{18}$O variability as a proxy for rainfall amount, including a record of short-lived negative spikes in $\delta^{18}$O during tropical cyclone events.

Trace element concentrations were measured using a prototype RESOlution M-50 excimer (193 nm) laser-ablation system with two-volume laser-ablation cell coupled to an Agilent 7500ce/cs quadrupole ICPMS at Royal Holloway University, London. Full description of the analytical setup, as well as initial performance metrics can be found in Müller et al. (2009).

Eleven ablation tracks were measured using a 140 by 10µm rectangular laser slit across sections of ATM7 (Figure 2) such that the entire length of the stalagmite was measured by at least three parallel tracks. Prior to measurement, all tracks were pre-ablated to remove any superficial contamination. A 15Hz repetition rate of a 90mJ laser spot and a stage scan speed of 10µm $s^{-1}$ were used during the main track measurement. Two stalagmite areas were ablated for elemental mapping using a circular spot size of 34µm along tracks 50µm apart at a scan speed of 50µm $s^{-1}$. Speleothem analyses were bracketed by analyses of NIST 612, NIST 610 and MACS3 standards for quantification.

Data reduction was performed using the Iolite software package using NIST 610/612 standards for external standardisation (Paton et al., 2011). Calcium-43 was measured throughout the sample runs as an internal standard.

Individual ablation tracks were aligned using a “wiggle-matching” tuning technique to align variation in magnesium concentrations onto a single absolute distance scale shared between all tracks. This method allowed the combination of these datasets whilst also taking into account minor lateral variation in lamina thickness. The lateral consistency in magnesium concentrations in the mapped areas shows this approach to be a viable

method to combine transects (Figure 4.3). All data were then linearly interpolated to allow averaging between the eleven different tracks at the same distance/time intervals. Values at each distance interval outside two standard deviations of the mean were excluded from the final averaged values to remove any outliers, which may have resulted from contamination or heterogeneous areas of the stalagmite. The absolute distance scale was then converted to the age model of Frappier et al. (2007) by matching the final magnesium record to their $\delta^{13}C$ record. Good topological agreement between the Mg and $\delta^{13}C$ time-series data, both proxies for rainfall at this tropical site, strongly supports this approach. Mg and $\delta^{13}C$ both show clear, visible responses to major El Nino events as well as annual to sub-annual fluctuations which we interpret as seasonal rainfall response. $\delta^{13}C$ is used rather than $\delta^{18}O$ due to the fact that although $\delta^{18}O$ in ATM7 is believed to be influenced by the amount effect during tropical cyclone events it does not display sub-annual variability as clearly as $\delta^{13}C$. Additionally, the influence of other factors such as masking effects (Frappier, 2013) or changes in water source region are of concern. Comparison of distance versus age between the stable isotope measurements and the laser ablation tracks shows good similarity, with some slight variations resulting from varying growth rates laterally between the micromilled isotope track and the ablation tracks (Figure 4.4).

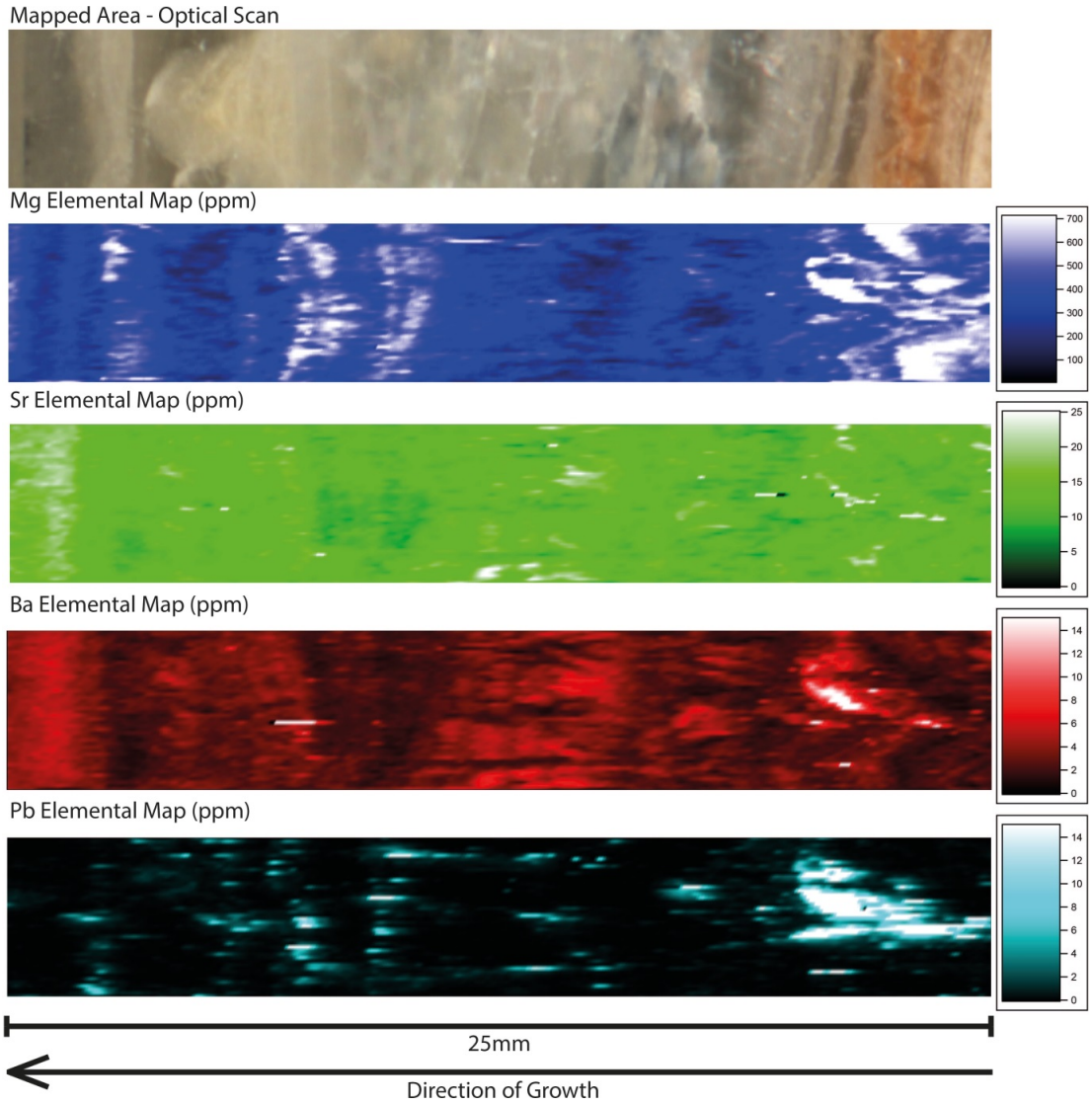


Figure 4.3: Elemental map of magnesium, strontium, barium and lead concentrations in the right hand mapped area of Figure 2. Concentrations show strong lateral consistency along growth layers. Optical scan image is shown for comparison.

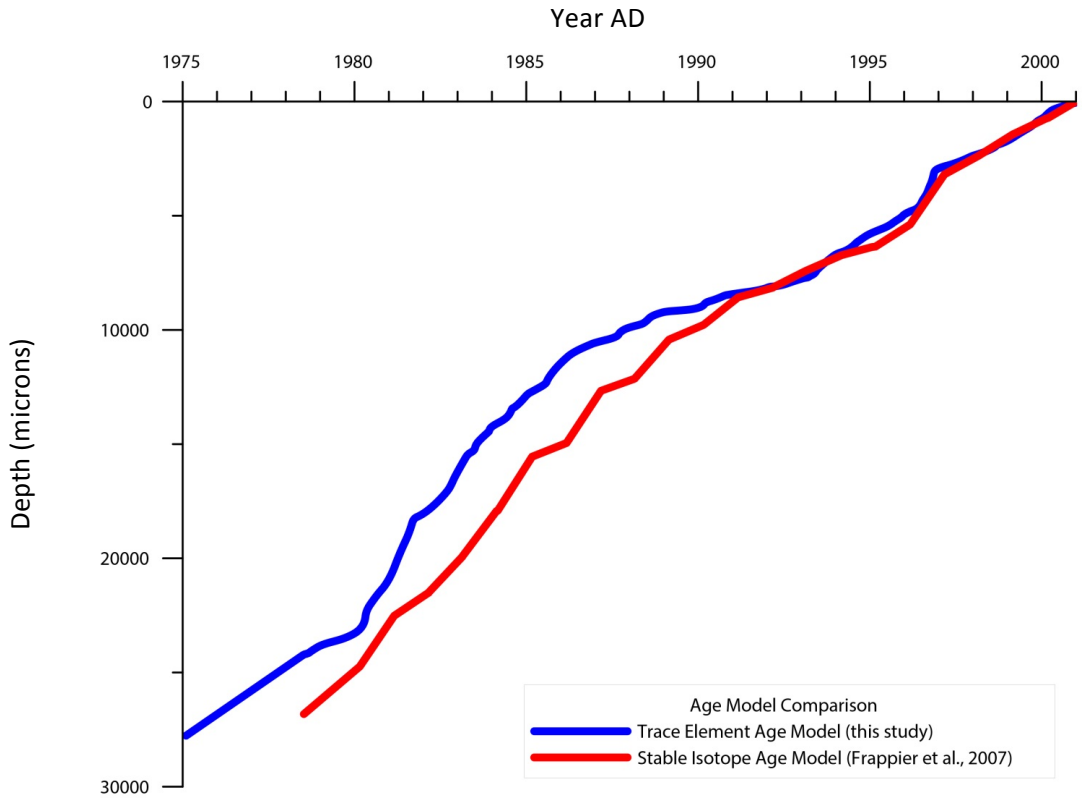


Figure 4.4: Frappier et al. (2007) age vs. depth model compared to age vs. depth model for the trace element transects

To process the trace element dataset prior to performing PCA the data were normalised by calculating the z-scores of each dataset to eliminate PCA's sensitivity to the scaling of the variables. The principal component coefficients, component scores, and percentage variance explained were calculated using the *pca* function in MATLAB (MathWorks, 2013).

Time periods where volcanic ash clouds were present over the cave site were identified using satellite maps of aerosol distributions obtained from the NASA Total Ozone Mapping Spectrometer (TOMS) Volcanic Image Archive for eruptions for which these maps were available. Earth Probe (TOMSEPL3.008) and Nimbus-7 (TOMSN7L3.008) version 8 TOMS daily level 3 global 1.0°x1.25° gridded Aerosol Index data provide a qualitative UV absorbing aerosol record over central and northern Belize (Acker and Leptoukh, 2007; Carn et al., 2003; Krueger et al., 2008).

The NOAA Air Resources Laboratory HYSPLIT Volcanic Ash model was used to compute ash cloud trajectories for eruptions to confirm the aerosol data and increase confidence that the ash cloud had in fact reached the cave site (Draxler and Rolph, 2003; Rolph, 2003). Volcanic Explosivity Index values for known eruptions were used to estimate approximate plume heights (Newhall and Self, 1982).

| | PC1 | Max (ppm) | Median (ppm) | Mean (ppm) | StdDev (ppm) | %RSD |
|---|---|---|---|---|---|---|
| **Mg** | 0.108 | 1137.22 | 317.45 | 348.16 | 162.04 | 46.54 |
| **Sr** | 0.070 | 58.12 | 12.25 | 13.13 | 4.22 | 32.16 |
| **Ba** | 0.217 | 109.06 | 2.68 | 3.60 | 5.09 | 141.84 |
| **Al** | 0.236 | 13655.19 | 2.84 | 138.75 | 730.31 | 526.33 |
| **Si** | 0.207 | 31554.61 | 1475.52 | 1526.03 | 1774.48 | 116.28 |
| **P** | 0.240 | 37413.33 | 12.52 | 181.91 | 1496.98 | 822.93 |
| **V** | 0.238 | 23.69 | 0.08 | 0.26 | 1.20 | 459.88 |
| **Mn** | 0.230 | 58.74 | 0.65 | 1.06 | 3.11 | 292.25 |
| **Fe** | 0.234 | 676.20 | 227.67 | 230.42 | 23.93 | 10.38 |
| **Cu** | 0.243 | 149.63 | 1.01 | 1.95 | 6.49 | 332.51 |
| **Zn** | 0.242 | 466.39 | 0.37 | 4.10 | 21.87 | 534.15 |
| **Rb** | 0.242 | 30.40 | 0.01 | 0.17 | 1.35 | 802.08 |
| **Y** | 0.227 | 7.44 | 0.00 | 0.08 | 0.54 | 666.68 |
| **Zr** | 0.244 | 23.09 | 0.02 | 0.17 | 1.04 | 603.27 |
| **Cd** | 0.231 | 5.39 | 0.00 | 0.04 | 0.24 | 570.04 |
| **La** | 0.233 | 9.25 | 0.00 | 0.08 | 0.57 | 681.99 |
| **Ce** | 0.242 | 12.30 | 0.00 | 0.09 | 0.73 | 787.31 |
| **Pb** | 0.225 | 36.48 | 0.06 | 0.65 | 2.41 | 368.40 |
| **Th** | 0.232 | 1.95 | 0.00 | 0.01 | 0.10 | 802.77 |
| **U** | 0.239 | 2.23 | 0.01 | 0.02 | 0.09 | 425.74 |

Table 4.1: Table of principal component coefficients for Principal Component 1. Also shown are descriptive statistics for the entire dataset population.

### 4.3.1 Results and Discussion

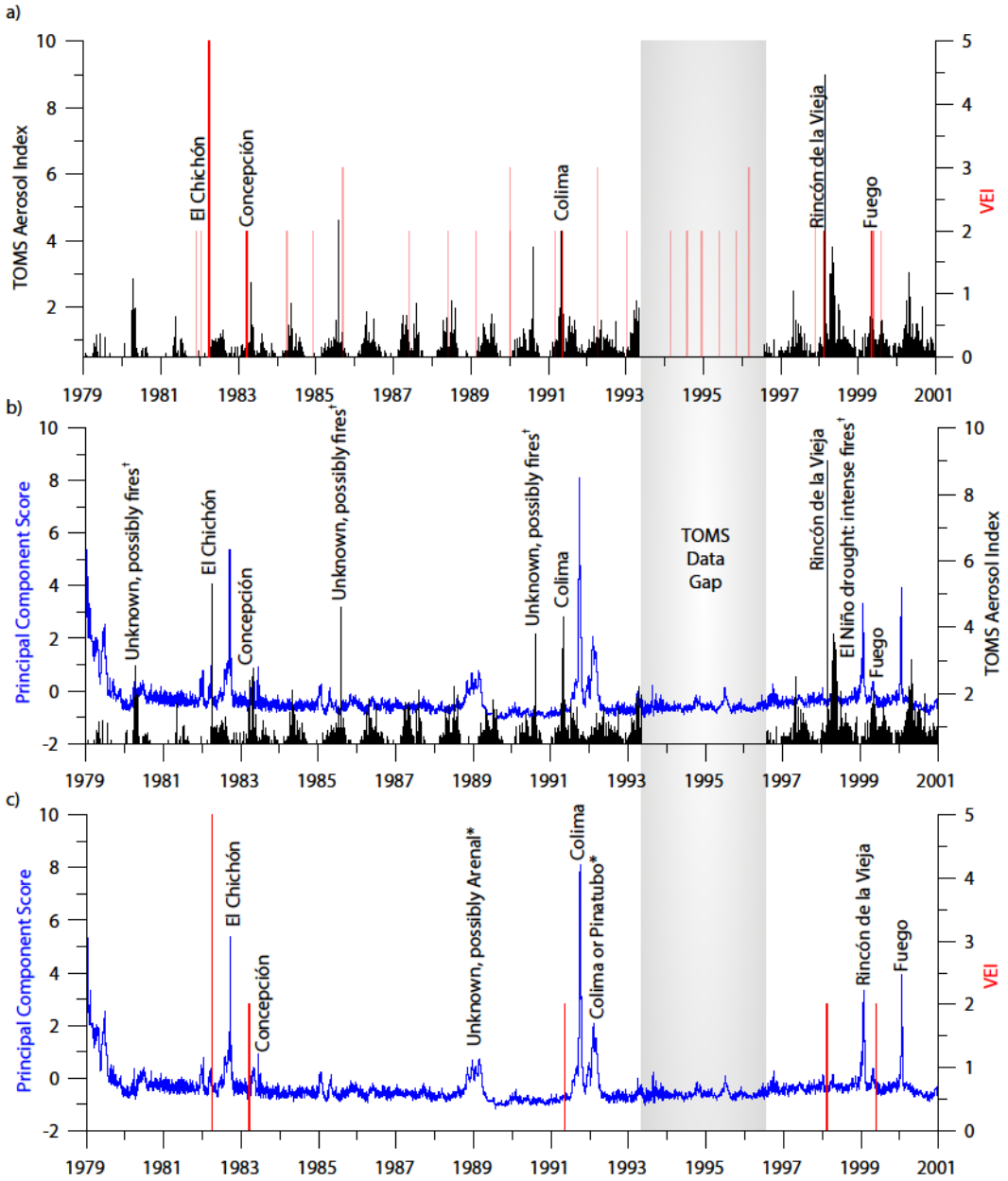


Figure 4.5: Linking remote sensing derived records of volcanic ash clouds to variations in ATM-7 trace element geochemistry. a) Demonstrating synchronicity of Central American volcanic eruptions of VEI 2 or greater (red) with spikes in TOMS Aerosol Index above the ATM cave site (black). This identifies volcanic eruptions with ash clouds which reach the cave site. b) Comparing labelled spikes in TOMS Aerosol Index (black) with PC1 scores over time (blue). c) Volcanic eruptions previously identified as resulting in elevated aerosol levels above the cave plotted against PC1 scores over time. A spike in PC1 follows each of these eruptions within one year. †Elevated Aerosol Index levels in these years, which have no corresponding volcanic eruption, due to a higher prevalence of large wildfires due to droughts in El Niño years. *Uncertain records of eruptions; discussed in text.

#### 4.3.1.1 Principal Component 1

Principal component analysis of the 20-element trace element dataset generated for ATM7 yields a first principal component which explains 81.9% of the variability within the dataset. Principal Component 1 (PC1) consists of a weak correlation between all of the analysed elements, many of which are typically excluded from calcite (Table 4.1) (Day and Henderson, 2013), and probably represents non-calcite material incorporated in the speleothem. The PC1 score time series is characterised by short period high amplitude spikes indicating that, although it explains a substantial portion of the variation within the dataset, PC1 is only a dominant control during infrequent short-lived events (Figure 4.5).

Previous studies have documented peaks in elements such as Zn, Cu, Pb, Y and other metals as a pulse of colloidally transported material driven by a seasonal flushing event (Borsato et al., 2007; Hartland et al., 2012). In this dataset these signals do not occur annually, but instead occur sporadically through the record. Notably however, in years when they do occur, the spikes are synchronous with the wet season onset as inferred from Mg concentrations (Figure 4.7) where a flushing event would typically occur.

We suggest that the observed signal is in fact recording a seasonal flushing event at our site; however, this event is evident only after sufficient raw material has been delivered to the karst to generate detectable levels of these elements. Tropical karst soils are depleted in many micronutrients due to high levels of biological productivity as well as leaching from high rainfall (Vitousek and Sanford, 1986). Substantial additional trace elements delivered to the ATM cave system are limited to particulate material sourced from wind-blown dust or volcanic ash, as the only sources of material above the cave are the karst, thin soil and canopy forest.

The NASA TOMS Aerosol Index dataset identifies intervals when aerosol levels are elevated in the atmosphere over the ATM cave site. Three primary sources of aerosols contribute to elevated Aerosol Index values over central and northern Belize: i) a seasonal signal of wood ash derived from biomass burning (Prins et al., 2003), ii) short-lived spikes in El Niño years corresponding to increased wildfires (Peppler et al., 2000), and iii) volcanic ash plumes over the area (Krueger et al., 2008). Correlation with records of known eruptions in Central America and the Caribbean (Smithsonian, 2014) (Figure 4.5) as well as HYSPLIT trajectory modelling of those eruptions (Figure 4.6) allows identification of intervals of elevated Aerosol Index where volcanic ash is transported over the cave site. Significant spikes in PC1 scores occur at the onset of the wet season following volcanic eruptions that produced an

identifiable increase in the TOMS Aerosol Index over the cave site (Figures 4.5 and 4.8). These spikes record the addition and subsequent flushing of material by volcanic ashfall from these eruptions. Aerosol spikes not corresponding to historical eruptions probably reflect biomass burning which produces aerosols composed primarily of carbon and therefore do not have a subsequent spike in PC1 score.

A comparison of seasonal trace element variability for all years with (Figure 4.8a) and without (Figure 4.8b) eruptions recorded in the stalagmite record clearly demonstrates the difference resulting from the addition of volcanogenic material to the dripwater. In both cases, magnesium concentrations are used to infer seasonality. Mg concentrations gradually rise through the dry season as mean dripwater residence time in the karst increases, then decreases precipitously to a lower baseline level through the wet season. This pattern is consistent through years with and without eruptions. A slight uptick in concentrations occurs in August and September, particularly years with eruptions, which may record the “little dry” midsummer drought which occurs in the region (Magaña et al., 1999).

Lead spikes occur at the onset of the wet season in most years, however in years without eruptions the spikes are barely above the mean background levels at only 1-2ppm. During wet season deposition following volcanic eruptions significant spikes of up to 15ppm of lead occur. This is apparent even in the normalised data, where the post-eruption spike is significantly above the background level of the rest of the year. These spikes coincide with, and indeed are part of, spikes in PC1 scores.

The temporal offset between the eruption date and the recorded spike in the stalagmite record varies from year to year. This reflects eruptions occurring at differing times of the year, rather than the timing of the spike changing. The eruption is always recorded at the start of the wet season following the eruption; this can lead to lags of from between two months up to one year (Figure 4.9). This is true of eruptions occurring in either the dry and wet seasons, as volcanogenic material appears to remain in the soil or karst until flushed through at the start of the subsequent wet season. A possible explanation for this phenomenon is the fact that particle and colloid release from soil is at its highest during the initial irrigation of the soil (El-Farhan et al., 2000). Flushes of volcanogenic material may only occur when both the material itself and sufficient mobile organic matter are present to transport it. Additionally, some studies have suggested that the mobilisation of elements such as lead are linked to the magnitude of rainfall events (Jo et al., 2010). Hartland et al.

(2012) suggest that in regions with large seasonal extremes the kinetic energy of flow may be important to the transport of particulate organic matter and associated elements. Each of these factors would lead to volcanic ash deposition only being recorded in the stalagmite during the first large initial rainfall event of the wet season following the eruption.

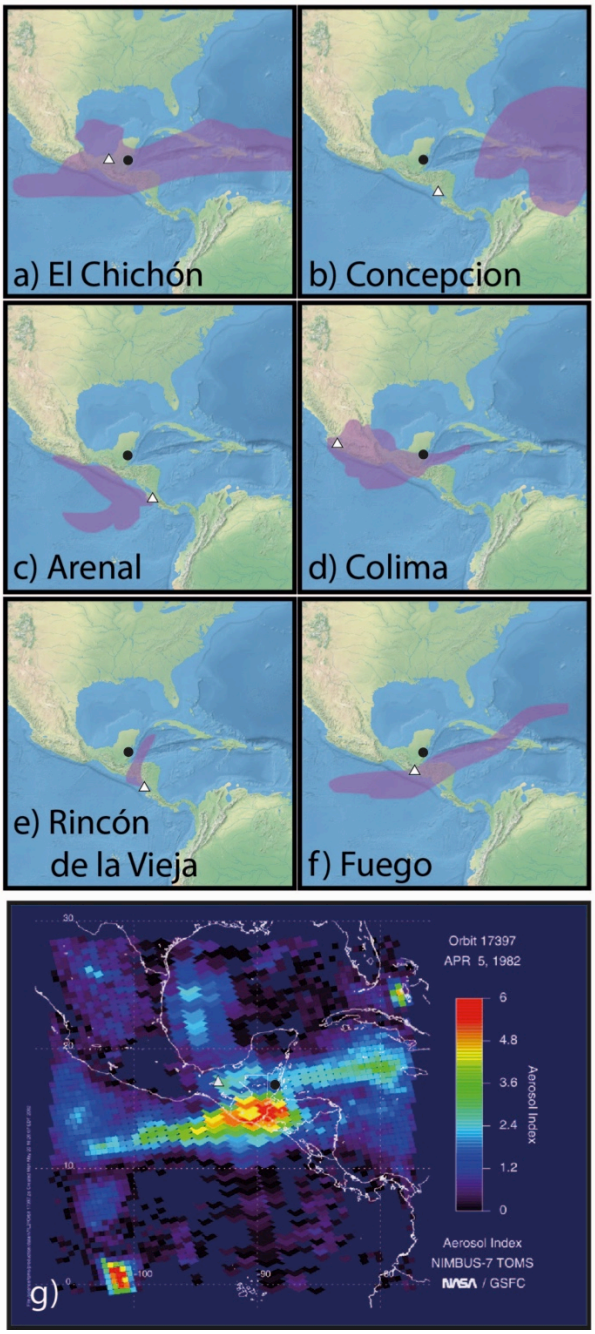


Figure 4.6: HYSPLIT modelling of ash dispersion 48 hours after eruptions of (a) El Chichón, (b) Concepción, (c) Arenal, (d) Colima, (e) Rincón de la Vieja, and (f) Fuego. (g) TOMS Aerosol Index image of El Chichón ash cloud on April 5$^{th}$ 1982 taken approximately one day after the climactic eruption. The triangles mark erupting volcano position, the black circles denote the position of ATM. (a-f) Results of HYSPLIT modelling on the READY system. (g) Courtesy of the NASA TOMS Volcanic Image Archive.

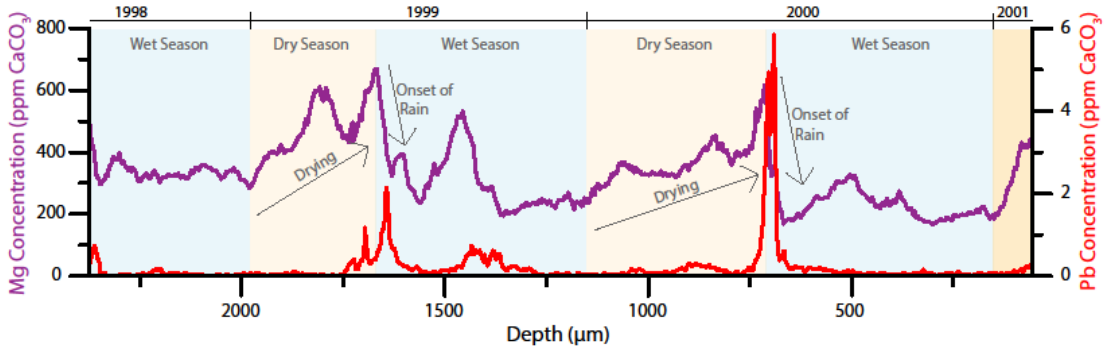


Figure 4.7: Magnesium concentrations (purple) and lead concentrations (red) plotted over time. Seasonality is inferred from fluctuations in magnesium concentrations, assuming abrupt decreases in Mg indicate the onset of the wet season and that the initiation of steadily increasing values marks the more gradual onset of the dry season. Lead concentration spikes occur at the start of the wet season, coincident with PC1 spikes, and are interpreted as representing flushing of volcanogenic compounds accumulated in the soil over the previous dry season.

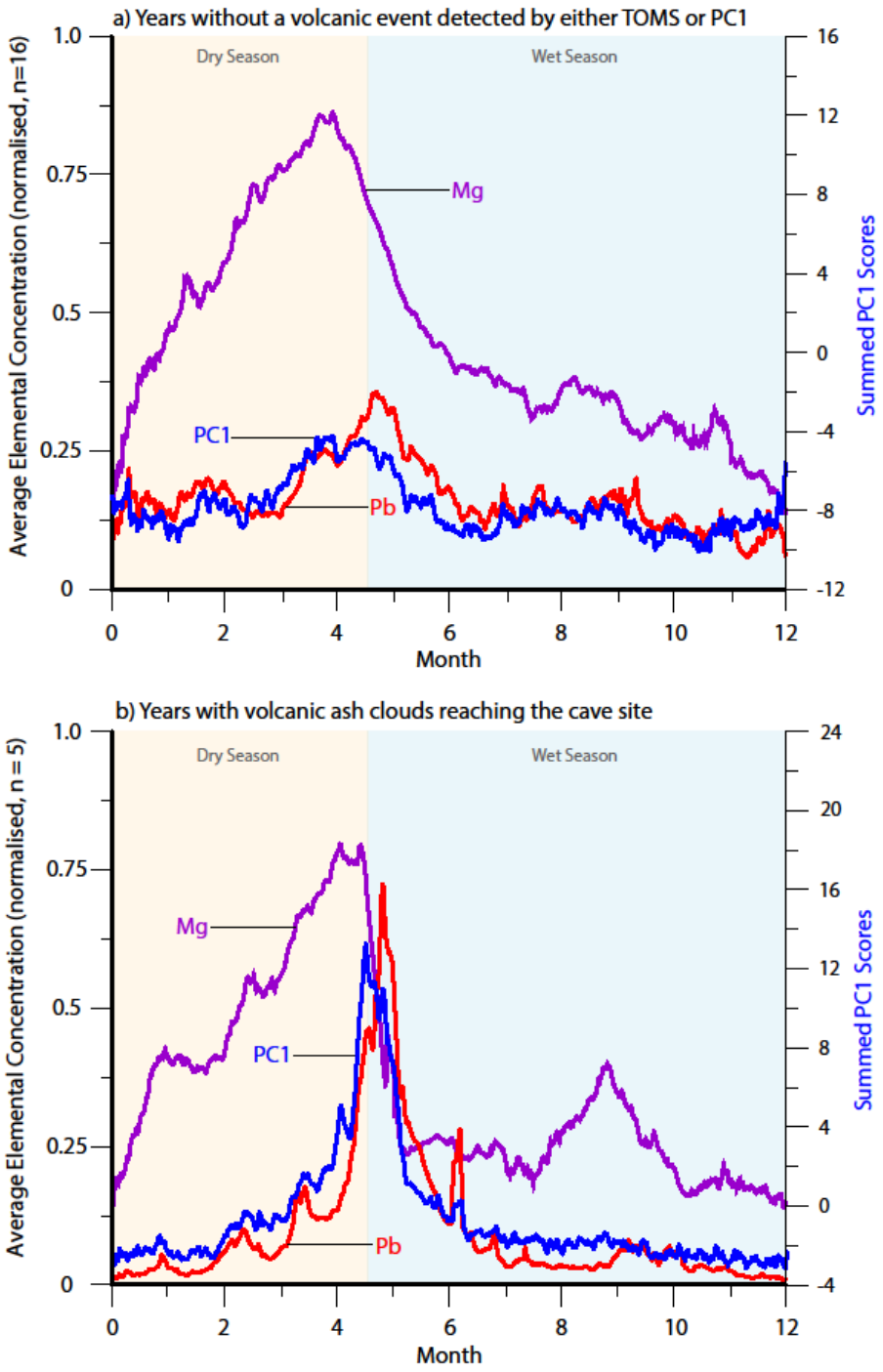


Figure 4.8: a) Average patterns of variation during the sixteen years (out of twenty-one total) without an identified eruption affecting the cave site. Magnesium concentrations (purple) are used to infer seasonality. b) Average patterns of variation during the five years with detectable volcanic ash influence. Spikes in lead (red) and PC1 (blue) occur at the onset of the wet season. Elemental concentrations for each year are normalised such that the maximum concentration in the year is equal to one. PC1 scores in each plot are the summed values over the plotted years.

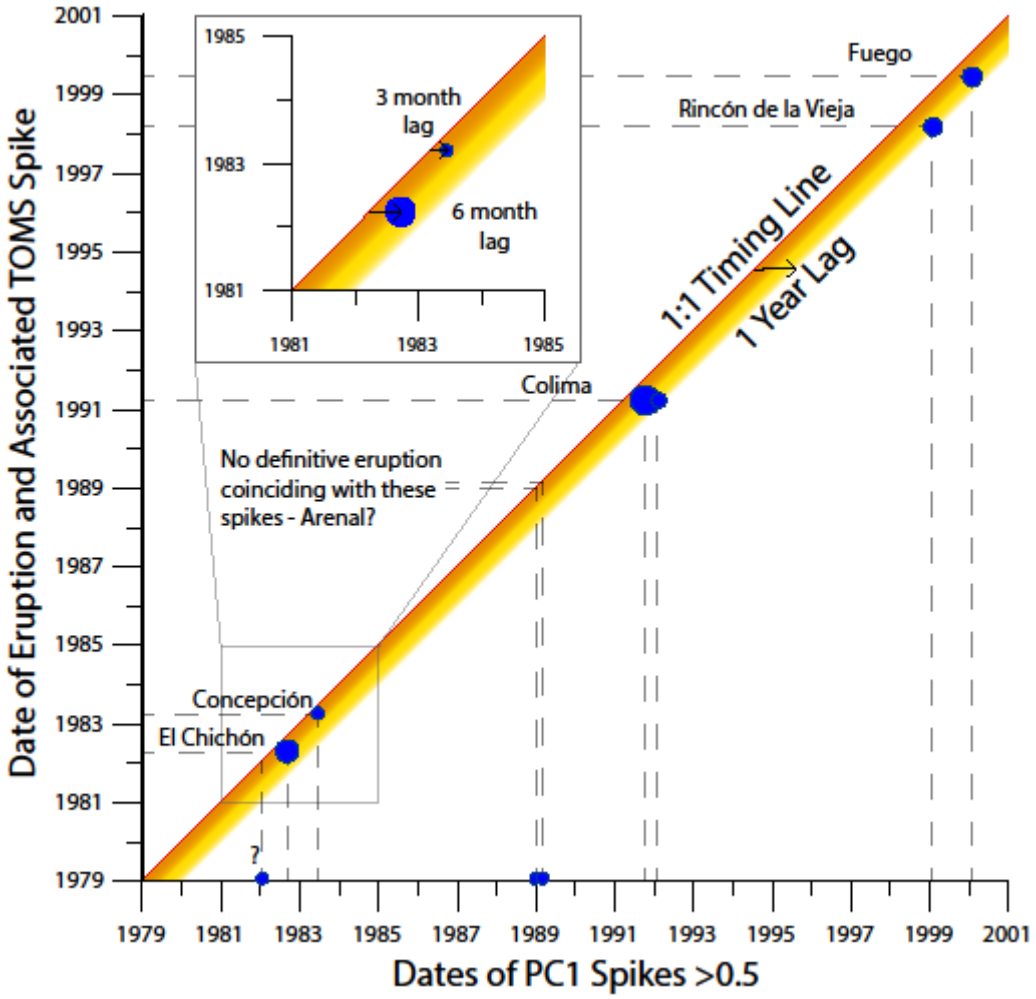


Figure 4.9: Comparison of PC1 spike timings to known eruptions affecting the cave site. Size of markers corresponds to magnitude of PC1 spike. A one-to-one concordance line marks the position where spikes would occur if they were synchronous with the eruptions. All PC1 spikes occur to the right of this line, within up to one year, as expected. Diameter of blue circles is proportional to magnitude of PC1 spike. Markers on x-axis denote PC1 spikes with no definitive corresponding eruption. Insert: length of lag times for El Chichón and Concepción eruptions.

## 4.3.2 Recorded Eruptions

### 4.3.2.1 El Chichón (Mexico)

The very large VEI 5 April 1982 eruptions of El Chichón erupted approximately 0.38km$^3$ direct rock equivalent (DRE) of juvenile material and 0.16km$^3$ DRE of lithic material, much

of which erupted in a 17km high ash cloud which extended across a large area of Central America (Rose and Durant, 2008; Varekamp et al., 1984). TOMS aerosol data (Figure 4.6) demonstrates that an ash cloud extended over Central and northern Belize. Earlier trace element work on ATM-7 using Empirical Orthogonal Function analysis (Frappier, 2006) identified a major perturbation in dripwater chemistry in 1982 that was attributed to the El Chichón eruption. This analysis reproduces that signal using new higher-resolution trace element data whilst also identifying several other comparable events from the rest of the time series.

#### 4.3.2.2 Concepción (Nicaragua)

A VEI 2 Concepción eruption (March 1983) also produced a detectable spike in aerosol levels over Belize. This is followed by a small amplitude spike in PC1. The reduced size of this spike may be the result of a smaller amount of ash delivered to the cave site from this eruption resulting in a weaker signal. Meteorological conditions at the time produced a more diffuse ash cloud which HYSPLIT modelling suggests was carried eastwards over the Caribbean Sea (Figure 4.6). The modelled ash distribution does not show the ash cloud passing over the cave directly, but the small spike in TOMS aerosol data at the time may suggest that some of the ash was deposited over the cave site.

#### 4.3.2.3 Arenal (Costa Rica)

Arenal has been erupting intermittently since 1968 and experienced a significant period of column collapses and pyroclastic flows in 1987-1989 (Cole et al., 2005). These eruptive events are not apparent as large elevations of TOMS aerosol levels, but could conceivably deliver material to the cave site over a sustained period resulting in the low amplitude, longer period signal observed in the PC1 time series. The lack of corroborating TOMS evidence for an ash cloud from Arenal coincident with this signal means that we have low confidence that this eruption is truly recorded. HYSPLIT modelling of one of the larger eruptions of Arenal during this time period shows the ash cloud being carried westwards (Figure 4.6), but this does not preclude the possibility of one of the many smaller eruptive episodes resulting in an ash cloud reaching the cave site at another time. In summary, Arenal can be neither confirmed nor ruled out as the source of this PC1 spike, but remains the most probable source.

#### 4.3.2.4 Colima (Mexico) and Pinatubo (Philippines)

The VEI 2 eruption of Colima in early 1991 is the most distant eruption that apparently influenced the geochemistry of the ATM7 stalagmite. It is recorded largely because of

fortuitous wind conditions following the eruption. HYSPLIT modelling illustrates that the ash cloud passed directly over central Belize (Figure 4.6), very strongly suggesting that Colima is the source of elevated aerosol levels and the initial PC1 signal in 1991. However, the double spike in PC1 is somewhat difficult to explain based on a single eruptive event. This signal suggests either a short period of time when transport of ash sourced elements to the karst stopped prior to a second flush, or a second source of material.

The June 1991 Mount Pinatubo eruption (VEI 6) was the largest volcanic eruption of the late 20$^{th}$ Century (Newhall and Punongbayan, 1996; Torres et al., 1995), erupting 1.8-2.2km$^3$ DRE of tephra as a 40km high column (Wiesner et al., 2003). Although no clear signal of the eruption exists in the TOMS data over Belize it is conceivable that some material from the eruption was capable of reaching the cave site in the months subsequent to the eruption. Mount Pinatubo and Actun Tunichil Muknal are at similar latitudes, of 15° and 17° respectively, and aerosols (although not necessarily ash) from the eruption were detectable in the atmosphere above the Caribbean for over a year after the eruption (Antuña, 1996). Any ash transported this distance would have been diffuse in both concentration and timing so therefore may not have registered above the background summer signal of biomass burning over Belize but could have accumulated in the soil over time. The available data cannot differentiate between Pinatubo or a second flush of remaining material from Colima as the cause of the second PC1 spike.

#### 4.3.2.5 Rincón de la Vieja (Costa Rica)

The February 1998 Rincón de la Vieja eruption (VEI 2), is apparent as a large aerosol spike over the cave site. This is subsequently followed by a large, short-lived spike in PC1 scores at the onset of the subsequent wet season. HYSPLIT modelling demonstrates that the ash cloud from this eruption was carried northwards over the Caribbean Sea over the first 48 hours following the eruption, from where the prevailing easterlies would carry the ash over the cave site (Figure 4.6).

#### 4.3.2.6 Fuego (Guatemala)

Volcán de Fuego in Guatemala began a period of increased activity in May 1999 with a VEI 2 eruption (Lyons et al., 2009). This eruption produced a small but detectable increase in aerosol levels and is subsequently followed by a spike in PC1 scores. HYSPLIT modelling confirms that a significant portion of the ash cloud was blown eastwards towards ATM (Figure 4.6).

### 4.3.3 Unrecorded Eruptions and Potential False Positives

Not all eruptions in Central America during the depositional period are apparent in the ATM-7 trace element record (Figure 4.5). This is clearly attributable to ash only reaching the cave site when wind and ash plume conditions are in the correct configuration. Because prevailing winds in this region are the easterly trade winds (Polzin et al., 2014) this results in the majority of ash clouds being carried away from the cave and over the Pacific Ocean. Eruptions are only recorded when the wind conditions at the time of eruption are such that ash clouds are carried eastwards over the cave site. HYSPLIT modelling for several recorded eruptions demonstrates that wind fields at the time of the recorded eruptions do indeed carry ash clouds over the cave site (Figure 4.6 – a-b,d-f). Whilst HYSPLIT modelling of an unrecorded or uncertain eruption does not show an ash cloud over the cave site (e.g. Arenal – Figure 4.6c).

Several small magnitude spikes in PC1 score occur throughout the record which we have not linked to known eruptions. The spike in 1979 corresponds to a prominent red layer visible in the stalagmite (Figure 4.3), that was deposited during a year of extreme rainfall where precipitation in the area was almost three standard deviations above the mean (reflected by low stable oxygen and carbon isotope values within the same layer). We suggest that this spike occurs due to an area of high levels of detrital material and low density calcite. The lower proportion of calcite in this section of the stalagmite would result in the data reduction procedure applied here overestimating the trace element content. As such, we believe that this spike probably results from extremely atypical weather, rather than a volcanic signal.

The remaining small spikes in late 1981, late 1988/early 1989 and 1995 are very low in amplitude (<0.5), suggesting that the PC1 relationship between variables is much weaker during these events. Indeed, they are at or below background in several of the trace elements measured (e.g. Fe, Rb, Cd, Si and potentially Th). These spikes are not associated with elevated aerosol levels above the cave or known volcanic eruptions, but may result from the diffuse delivery of material, flushing of residual material within the soil or another unknown source that we are unable to identify from the available data.

## 3.4 Geochemistry of Eruptions

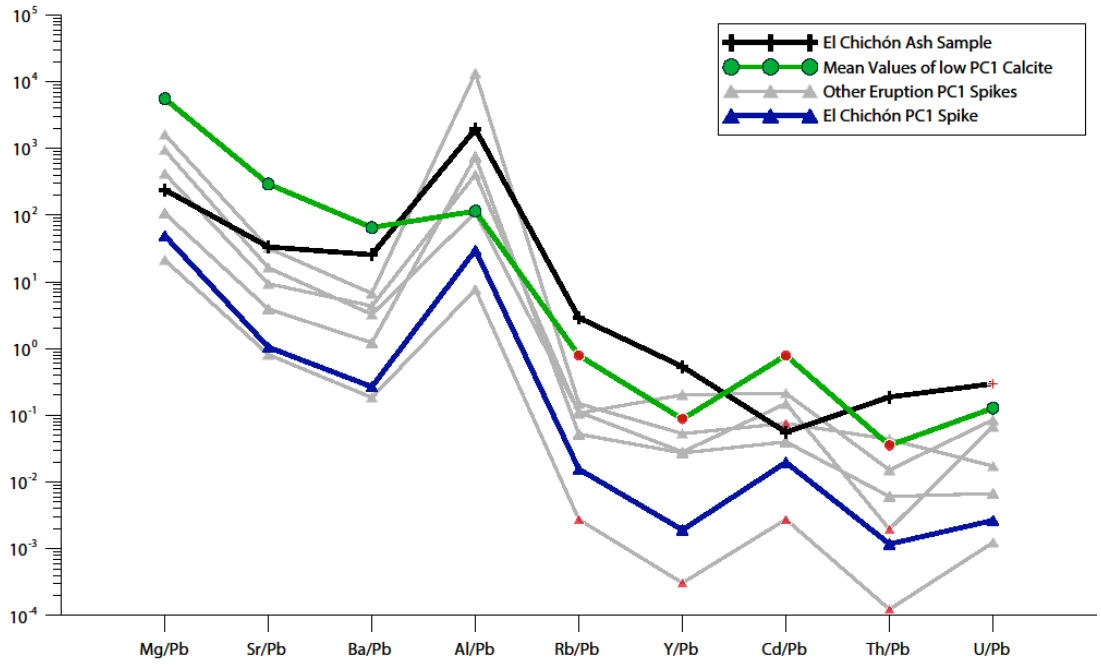


Figure 4.10: Comparison of geochemistry of stalagmite regions containing ash-derived material compared to mean values of calcite containing no ash signal. Also plotted are the results of ICP-MS analysis of an El Chichón ash sample. All elements ratioed to lead to eliminate the effect of varying amounts of ash-derived material within the speleothem. Symbols in red are values where the concentration of the element analysed are below the detection limits; these are plotted at detection limit values for comparison only whilst the actual values will be lower.

Examining the elemental concentrations at the stalagmite depths corresponding to the spikes in PC1 (Figure 4.10) enables comparison of the chemistry of each presumed volcanic ash signal. Elemental concentrations were normalised by ratioing to lead to eliminate differences due to varying amounts of ash incorporation, assuming that the majority of lead incorporated within the speleothem is solely from a volcanic source. These values were also compared to the mean value of calcite with the lowest PC1 scores (n=100) to provide a non-volcanic baseline to compare against. A sample of El Chichón ash obtained from the Smithsonian Institution was analysed by solution ICP-MS to assess the potential for fingerprinting specific eruptions.

Each ash influenced depth interval is broadly similar in elemental profile with similar values of each elemental ratio relative to the other elements measured. This is consistent with broadly similar material (i.e. volcanic ash) being present in each one. Of particular note is the much higher Al/Pb relative to the other elements. In the low PC1 value calcite the Al/Pb ratio is similar to the Ba/Pb and Sr/Pb ratios, whilst in the ash influenced series and ash sample itself the Al/Pb ratio is approximately two orders of magnitude higher. This may suggest the incorporation of aluminosilicate material into the speleothem. This is consistent with the incorporation of clay or feldspar minerals, both common constituents of volcanic ash.

The El Chichón ash sample cannot be definitively matched to the El Chichón PC1 spike rather than the other spikes based on geochemistry alone. This suggests that biogeochemical processing of volcanogenic material in the soil and karst complicates geochemical fingerprinting of eruption- or volcano-specific ash in a speleothem. Several processes between source and sink alter the elemental distributions of the analysed elements. Cycling in the soil and nutrient uptake by overlying vegetation will preferentially lower the concentrations of certain elements. Elements will respond differently to adsorption and chemical reactions in the soil, as well as being flushed through the karst preferentially as a result of binding to different organic matter fractions (Hartland et al., 2012). For example, lead and yttrium have a much greater binding affinity to soil organic matter than most other measured metals (Baldini et al., 2012; Hartland et al., 2012). Future studies focusing on elements that behave similarly between deposition and incorporation may prove more effective. A possible candidate for such a study would be the rare earth elements, although REE measurement challenging by very low concentrations within speleothems and natural waters (Aliaga-Campuzano et al., 2013).

### 4.4.1 Implications and Future Work

Principal component analysis of high-resolution trace element datasets has the potential to produce speleothem eruption records that complement and supplement ice core and sediment tephrochronology, providing a precisely dated, low-latitude, continental, and regional archive of ash deposition even after removal or reworking of surface sediments. Eruptions recorded in ice cores that influence global climate, but which are of unknown location, could be more accurately located to within a specific region using this technique. Additionally, the high precision of speleothem dating allows determination of precise dates of eruptions (such as the Minoan eruption of Santorini), which are disputed or imprecisely

dated by archaeological, stratigraphic or historical records (Friedrich et al., 2006). Geological records of prehistoric records are exceptionally incomplete, with estimates for the percentage of known events less than 0.17% globally for eruptions 5-20Ka and as low as 0.0005% for some regions (Watt et al., 2013). This technique enables the use of speleothems as an additional archive of eruption records, particularly in tropical areas where historical eruption records are often poor. Improved eruption records allow better estimation of recurrence intervals and are essential for assessing volcanic hazards.

In this study remote sensing and meteorological data very strongly suggest that PC1 reflected volcanic ash deposition by linking PC1 spikes to specific historical eruptions. Studies extending further into the past (e.g., beyond the satellite or historical record) will not have this information available. However, these studies could still apply this technique by first calibrating a PC record using modern information, and then extend interpretations back through time. Similar PC spikes as those reflecting historical volcanic ash deposition are interpretable as unknown volcanic eruptions. Furthermore, a modern calibration provides information regarding the proportion of regional eruptions detectable at a specific cave site, as well as any false positives. The proof-of-concept study presented here captured 5 out of 5 volcanic eruptions that produced aerosol clouds that passed over the cave site, and 5 out of 28 total Central American eruptions larger than VEI 2. Studies of older stalagmites that were not growing during historical times could still benefit from the technique, but determination of the stalagmite's sensitivity to eruptions would remain unknown.

Speleothem trace element eruption records can also function as chronological markers. The date of a well-recorded eruption detected in a speleothem can be incorporated into the age model, providing even greater precision in speleothem dating.

Additional future work could focus on further confirming that the trace element spikes recorded in this stalagmite by PC1 are indeed the results of volcanic ash deposition. Geochemical techniques which are impractical for analysis of an entire stalagmite could be employed now that the physical location of the spike within the sample is known. These include employing sulphur isotopes (Frisia et al., 2005; Frisia et al., 2008) or using synchrotron radiation based micro X-ray fluorescence to detect elements diagnostic of volcanism which are only present in low concentrations such as Br or Mo (Badertscher et al., 2014).

### 4.4.2 Comparison to Previous Work

These trace element results are consistent with previous work which suggested that the El Chichón eruption was recorded in the trace elements of ATM-7 (Frappier, 2006), as well as detecting several additional volcanic ash deposition events to the record. Magnesium concentrations are broadly similar to $\delta^{13}C$, showing similar patterns in response to seasonality and El Niño events as in Frappier et al. (2002). Trace elements do not show a clear response to the tropical cyclone events which are observed in the $\delta^{18}O$ record (Frappier et al., 2007b). We suggest that although tropical cyclone rainfall is isotopically distinct from normal rainfall it does not represent a substantial additional volume, and therefore has a much smaller influence on trace element proxies for precipitation.

### 4.5.1 Conclusions

Here we show the potential of Principal Component Analysis as a statistical technique for exploratory analysis of large stalagmite trace element datasets. The technique can deconvolve the different modes of trace element variation and, when principal components are linked to physical processes or inputs, can produce time series of the shifting influence of those modes of variation. For a stalagmite where intermittent signals such as the addition of volcanic ash material are recorded, this technique can clearly identify these discrete events within the record. It is important to note that Principal Component Analysis of individual trace element datasets will produce unique principal components and correlation coefficients. Volcanic ash deposition may not always appear as the first principal component; instead, it may explain a lower proportion of the variability or consist of slightly different elemental distributions due to local soil or plant chemistry. However, for any stalagmite where volcanic ash deposition has a measurable influence on stalagmite geochemistry PCA should produce a corresponding principal component.

We demonstrate that the stalagmite ATM-7 from Actun Tunichil Muknal cave in central Belize records the occurrence of volcanic ash deposition over the cave site. Comparison of ashfall events recorded in speleothems can be used as a tephrochronological tool in conjunction with existing local historical, archaeological or sedimentological records. Additionally, analysis of stalagmites using this technique can yield absolutely dated, high resolution, low latitude records of volcanic eruptions, providing important low latitude counterparts to volcanogenic sulphate records in glacial ice cores.

# Chapter 5

# Intra- and inter-annual uranium concentration variability in a Belizean stalagmite controlled by prior aragonite precipitation: a new tool for reconstructing hydro-climate using aragonitic speleothems

*A version of this chapter has been published in Geochimica et Cosmochimica Acta authored by Robert A. Jamieson [a,*], James U.L. Baldini [a], Marianne J. Brett [a, b], Jessica Taylor [a], Harriet E. Ridley [a], Chris J. Ottley [a], Keith M. Prufer [c], Jasper A. Wassenburg [d], Denis Scholz [d], Sebastian F. M. Breitenbach [e]*

[a] *Department of Earth Sciences, Durham University, United Kingdom*

[b] *Royal Holloway University, London, United Kingdom*

[c] *Department of Anthropology, University of New Mexico, United States of America*

[d] *Institute for Geosciences, Johannes Gutenberg University, Mainz, Germany*

[e] *Department of Earth Sciences, University of Cambridge, United Kingdom*

Chapter 5: Intra- and inter-annual uranium concentration variability in a Belizean stalagmite controlled by prior aragonite precipitation: a new tool for reconstructing hydro-climate using aragonitic speleothems

A version of this chapter has been published in Geochimica et Cosmochimica Acta (Jamieson et al., 2016) with contributions from the following authors:

**Robert A. Jamieson** analysed the sample, processed the data, performed the statistical analyses, interpreted the data, and wrote the manuscript thereby contributing to over 90% of the work presented in this chapter.

**James U.L. Baldini** assisted with interpretation of the data and provided extensive comment on the manuscript.

**Marianne J. Brett** and **Jessica Taylor** performed the analysis of approximately one third of the YOK-G ICP-MS samples as part of MSci Laboratory Dissertation Projects at Durham University under the supervision of **James U.L. Baldini**.

**Harriet E. Ridley** performed stable isotope analyses on the YOK-G samples for her PhD and previous publications on YOK-G (Ridley, 2014; Ridley et al., 2015a; Ridley et al., 2015b)

**Chris J. Ottley** assisted with ICP-MS analysis at Durham University

**Keith M. Prufer** is a principal investigator of the YOK-G study site and enabled collection of the sample.

**Jasper A. Wassenburg** and **Denis Scholz** collaborated on the distribution coefficient calculations, providing data and input on that portion of the manuscript. A more detailed study on aragonite distribution coefficients can be found in (Wassenburg et al., 2016).

**Sebastian F. M. Breitenbach** assisted with the figures.

All authors provided comment and approval on the final manuscript.

**Acknowledgements**

The authors thank Silvia Frisia and Ian Fairchild for productive discussion at the 2015 Summer School on Speleothem Science. Instrumental rainfall records are courtesy of Hydromet Belize.

YOK-G stalagmite was sampled with permission from the Belize Institute of Archaeology.

This work was funded by the ERC (240167) to JULB, NSF (HSD 0827305) and Alphawood Foundation to KP, and DFG (WA3532/1-1) to JAW.

# Chapter 5: Intra- and inter-annual uranium concentration variability in a Belizean stalagmite controlled by prior aragonite precipitation: a new tool for reconstructing hydro-climate using aragonitic speleothems

## Abstract

Aragonitic speleothems are increasingly utilised as palaeoclimate archives due to their amenability to high precision U-Th dating. Proxy records from fast-growing aragonitic stalagmites, precisely dated to annual timescales, can allow investigation of climatic events occurring on annual or even sub-annual timescales with minimal chronological uncertainty. However, the behaviour of many trace elements, such as uranium, in aragonitic speleothems has not thus far been as well constrained as in calcitic speleothems. Here, we use uranium concentration shifts measured across primary calcite-to-aragonite mineralogical transitions in speleothems to calculate the distribution coefficient of uranium in aragonitic speleothems (derived $D_U$ = 3.74 ± 1.13). Because our calculated $D_u$ is considerably above 1 increased prior aragonite precipitation due to increased karst water residence time should strongly control stalagmite aragonite U/Ca values. Consequently, uranium concentrations in aragonitic speleothems should act as excellent proxies for effective rainfall.

We test this using a high-resolution ICP-MS derived trace element dataset from a Belizean stalagmite. YOK-G is an aragonitic stalagmite from Yok Balum cave in Belize with an extremely robust monthly-resolved chronology built using annual $\delta^{13}C$ cycles. We interpret seasonal U/Ca variations in YOK-G as reflecting changes in the amount and seasonality of prior aragonite precipitation driven by variable rainfall amounts. The U/Ca record strongly suggests that modern drying has occurred in Belize, and that this drying was primarily caused by a reduction in wet season rainfall. This is consistent with published stable isotope data from YOK-G also very strongly suggesting modern rainfall reductions, previously interpreted as the result of southward ITCZ displacement. Our results strongly suggest that U/Ca values in aragonitic speleothems are excellent proxies for rainfall variability. This new tool, combined with the exceptional chronological control characteristic of aragonitic stalagmites and the high spatial resolution afforded by modern microanalytical techniques, should facilitate the construction of new exquisitely resolved

rainfall records, providing rare insights into seasonality changes as well as long-term changes in local recharge conditions.

### 5.1.1 Introduction

Speleothems are invaluable continental paleoclimate archives that are amenable to precise and accurate U-Th dating, and can yield high-resolution proxy records. Speleothem-based climate reconstructions are particularly useful for reconstructing effective rainfall, and can provide diverse information about rainfall, including moisture source and trajectory, rainfall amount, seasonality, and karst residence time (Fairchild et al., 2006a). Well-established stable isotope proxies retain each of these variables to varying degrees in different stalagmites. Disentangling these effects in a given sample is challenging, with individual proxies such as $\delta^{18}O$ or $\delta^{13}C$ potentially reflecting multiple climatological and environmental factors in a single proxy record. Therefore, considering multi-proxy approaches when attempting to reconstruct effective rainfall from speleothem records is critical. Trace element proxies for prior carbonate precipitation and/or residence time reflect the volume of water infiltrating through the karst and can help deconvolve these separate signals. In calcite speleothems, the most commonly used trace element proxy for prior calcite precipitation (PCP) is Mg/Ca (Fairchild and Treble, 2009), due to its abundance and strong partitioning between fluid and solid phases (Fairchild et al., 2000). Other element ratios such as Sr/Ca or Ba/Ca also produce complementary information about hydrology (McDonald et al., 2007). In addition, sulphate concentrations in speleothems have been used as tracers of volcanic or anthropogenic inputs to the karst system (Borsato et al., 2015; Frisia et al., 2005; Wynn et al., 2008; Wynn et al., 2010; Wynn et al., 2014). Elements that are less water soluble or less easily incorporated into the calcite crystal lattice, although utilised more rarely, are useful proxies for volcanic or anthropogenic inputs into the karst system (Jamieson et al., 2015) or as chronological markers of seasonal flushing of associated organic material (Borsato et al., 2007; Hartland et al., 2012). Similar mechanisms control trace elements in aragonitic speleothems, although the differing crystal structure of aragonite compared to that of calcite means that elements are incorporated differently between the two minerals. Aragonitic speleothems are particularly useful in paleoclimatic research because their generally high uranium content allows very high U-Th dating precision (Denniston et al., 2013; Kennett et al., 2012; Woodhead et al., 2012). Despite this potential, the relative scarcity of published aragonitic stalagmite trace element records (Finch et al., 2003; Tan et al., 2014; Wassenburg, 2013) means that trace

element partitioning behaviour into their structure remains poorly understood. Research constraining uncertainties in elemental behaviour in aragonitic stalagmite is therefore crucial.

### 5.1.2 Prior Aragonite Precipitation

Prior calcite precipitation is a significant control on dripwater element concentrations before trace element incorporation in speleothems (Fairchild et al., 2001; Fairchild et al., 2000; Fairchild and Treble, 2009; Treble et al., 2015). Precipitation of calcium carbonate up-flow from the speleothem may affect the ratios of various trace elements to calcium in dripwaters (and thus speleothems) depending on the value of their distribution coefficients. This mechanism controls a significant proportion of variability in water-soluble alkaline earth metal concentrations due to their abundance and predictable behaviour. PCP is not a primary control on other elemental variations due to the dominance of other processes such as supply, transport, and/or growth/crystal structure dependencies for incorporation, for example pH (Wynn et al., 2014) or growth rate (Fairchild et al., 2001). Far less is known about the effects of prior aragonite precipitation (PAP) on speleothem geochemistry. However, PAP probably significantly influences speleothem geochemistry in environments where aragonite precipitation is favoured, though currently very few studies have considered PAP controls on speleothem geochemistry. Fairchild and Treble (2009) discussed the potential of PAP as an influence on Sr/Ca, but concluded that it would have a minimal effect on strontium concentrations. Wassenburg et al. (2012) highlighted the potential for PAP to increase dripwater Mg/Ca, and a lack of PCP as an explanation for the decoupling of Sr, Mg and Ba within speleothem aragonite. Wassenburg et al. (2013) identified PAP from monitored dripwaters by observing a negative correlation between Ca and Sr concentrations. These studies established PAP as a process that can affect dripwater and/or speleothem trace element ratios, but did not propose a diagnostic elemental proxy for PAP. The potential of PAP to function as an important hydrologically mediated control on speleothem geochemistry merits further consideration, especially considering that the differing crystal structure of aragonite compared to calcite may favour the incorporation of elements with larger ionic radii, thereby providing proxies for environmental changes that are not available in calcite speleothems. One element incorporated in greater concentrations in aragonite because of the aforementioned reasons is uranium, which is mostly incorporated as $UO_2(CO_3)_3$ (Reeder et al., 2000) and readily substitutes for Ca within the aragonite crystal structure but less so in that of calcite.

U/Ca has not previously been used extensively in speleothem studies as a proxy for paleoenvironmental information, however several groups have measured U/Ca or $^{234}U/^{238}U$ activity ratios in calcite speleothems and discussed the source and mechanisms of incorporation. Bourdin et al. (2011) suggested that uranium in dripwaters is primarily derived from limestone dissolution at their study site, with its incorporation in calcite depending on crystallographic factors such as the presence of kinks or lattice defects. Other groups have suggested that uranium can be derived from an external source such as Saharan dust (Frumkin and Stein, 2004), overlying sediments (Zhou et al., 2005), or anthropogenic sources/disruption (Siklosy et al., 2011). In addition, PCP has been discussed as a possible influence on dripwater U/Ca (Johnson et al., 2006). In summary, very few studies have discussed uranium in detail as a proxy and, to our knowledge, none in aragonitic speleothems.

### 5.1.3 Distribution Coefficients in Speleothem Aragonite and Calcite

One of the key limitations in quantitative speleothem trace element research is imprecise knowledge of the distribution coefficients ($D_{TE}$) controlling the incorporation of elements in speleothems. Existing studies of distribution coefficients in both calcite and aragonite are often non-speleothem specific, and can include biological effects not present in stalagmites (corals), non-comparable fluids (seawater, or other high ionic strength solutions), or implausible growth rates or temperatures (Busenburg and Plummer, 1985; DeCarlo et al., 2015; Meece and Benninger, 1993; Swart and Hubbard, 1982). As such, the applicability of these values to speleothem science is extremely limited.

Recent studies have determined distribution coefficients for speleothem calcite based on karst analogue experiments (Day and Henderson, 2013), or using in-situ measurements of dripwaters and precipitates (Tremaine and Froelich, 2013). These values are more applicable to speleothem studies than earlier efforts, but distribution coefficients are not absolute constants. Instead, distribution coefficients depend on a variety of factors including: temperature, growth rate, competition effects (i.e., solution composition), pH, biological factors, elemental form (e.g., valence state, complexation, etc.), crystallography, and many others (Gabitov et al., 2008; Gabitov et al., 2014; Huang and Fairchild, 2001; Meece and Benninger, 1993; Mucci and Morse, 1983). It is thus likely that cave- or drip-specific distribution coefficient values exist. The concept of a distribution coefficient does

have value for understanding trace element partitioning in a general sense, but is not an absolute constraint on trace element variability in speleothems.

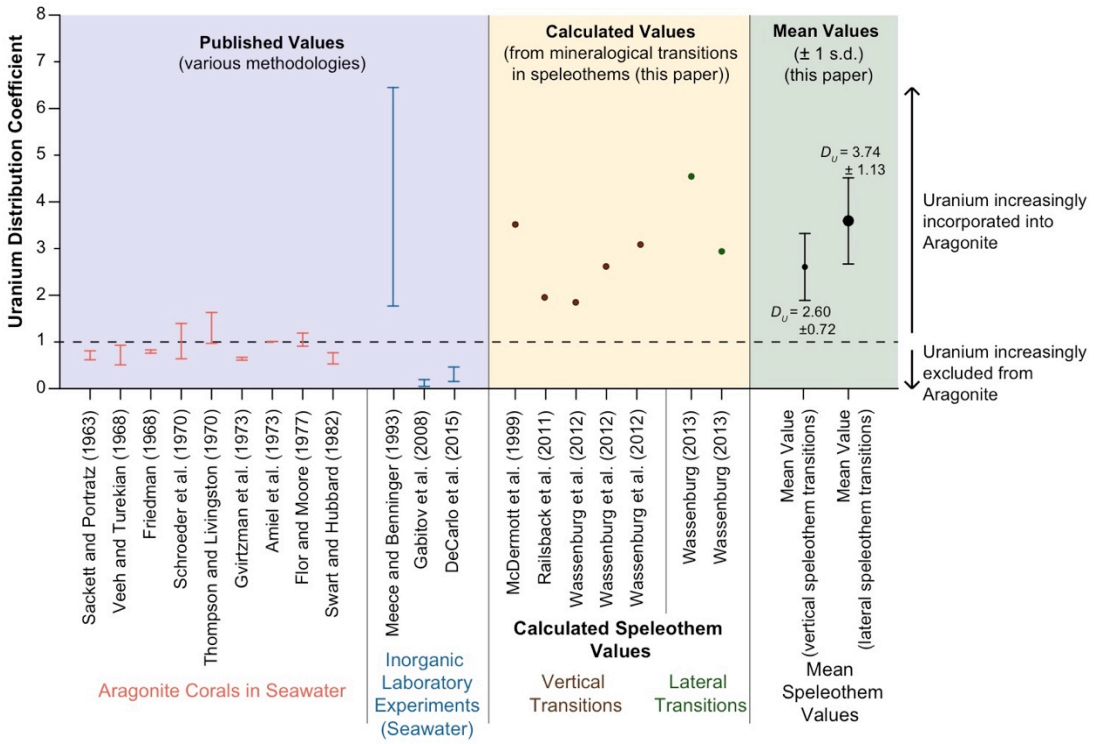


Figure 5.1: A selection of published and newly calculated distribution coefficients for uranium in aragonite. From left to right: published values for aragonite corals in seawater (orange) and inorganic laboratory precipitation experiments (blue), calculated values for vertical transitions in speleothems (brown) and lateral transitions in speleothems (green) calculated as described in Section 5.3.2 (Amiel et al., 1973; DeCarlo et al., 2015; Flor and Moore, 1977; Friedman, 1968; Gabitov et al., 2008; Gvirtzman et al., 1973; McDermott et al., 1999; Meece and Benninger, 1993; Railsback et al., 2011; Sackett and Potratz, 1963; Schroeder et al., 1970; Swart and Hubbard, 1982; Thompson and Livingston, 1970; Veeh and Turekian, 1968; Wassenburg, 2013; Wassenburg et al., 2012). Published coral and experimental values are shown with the range of values reported, calculated values (this study) are shown with ± one standard deviation of the mean of the calculated values (black). The mean value of 3.74 ± 1.13 for lateral transitions (bold circle) is our preferred value (see section 5.4.2).

| Source | Type | n | $D_U^a$ Min | $D_U^a$ Max | $D_U^a$ Mean |
|---|---|---|---|---|---|
| **Sackett and Potratz (1963)** | Aragonitic Corals in Seawater | 2 | 0.62 | 0.81 | 0.72 |
| **Veeh and Turekian (1968)** | Aragonitic Corals in Seawater | 8 | 0.51 | 0.95 | 0.72 |
| **Friedman (1968)** | Aragonitic Corals in Seawater | 2 | 0.76 | 0.83 | 0.80 |
| **Schroeder et al. (1970)** | Aragonitic Corals in Seawater | 6 | 0.64 | 1.42 | 1.02 |
| **Thompson and Livingston (1970)** | Aragonitic Corals in Seawater | 4 | 0.97 | 1.46 | 1.30 |
| **Gvirtzman et al. (1973)** | Aragonitic Corals in Seawater | 3 | 0.61 | 0.67 | 0.64 |
| **Amiel et al. (1973)** | Aragonitic Corals in Seawater | 3 | 1.01 | 1.01 | 1.01 |
| **Flor and Moore (1977)** | Aragonitic Corals in Seawater | 4 | 0.91 | 1.3 | 1.05 |
| **Swart and Hubbard (1982)** | Aragonitic Corals in Seawater | 9 | 0.53 | 0.87 | 0.65 |
| | | | | | |
| **DeCarlo et al. (2015)** | Abiogenic Seawater Lab Experiment | 27 | 0.154 | 0.38 | 0.31 |
| **Gabitov et al. (2008)** | $U^{6+}$ laboratory experiment, inorganic precipitation with ammonium carbonate | 8 | 0.048 | 0.150 | 0.12 |
| **Meece and Benninger (1993)** | Seawater, high $pCO_2$ to saturate with $CaCO_3$ | 11 | 1.77 | 9.85 | 4.11 |
| | | | | | |
| **McDermott et al. (1999)** | Vertical Transition | | | | 3.52 |
| **Railsback et al. (2011)** | Vertical Transition | | | | 1.95 |
| **Wassenburg et al. (2012)** | Vertical Transition | | | | 1.85 |
| **Wassenburg et al. (2012)** | Vertical Transition | | | | 2.62 |
| **Wassenburg et al. (2012)** | Vertical Transition | | | | 3.09 |
| **Mean Value (Vertical Transition)** | | | | | 2.60 ± 0.72 |
| | | | | | |
| **Wassenburg (2013)** | Lateral Change | | | | 4.55 |
| **Wassenburg (2013)** | Lateral Change | | | | 2.94 |
| **Mean Value (Lateral Transition)** | | | | | 3.74 ± 1.13 |

Table 5.1: Values of $D_U^a$ used in Figure 5.1.

In practice, the key piece of information for interpreting speleothem trace element data in terms of PCP and/or PAP is whether the distribution coefficient is greater than or less than one, that is, whether it is preferentially included or excluded from the mineral phase. Even this binary distinction is within the range of estimates for some elements in aragonite within the previously published literature (Figure 5.1); therefore defining clear ranges for these values in speleothems is critical. Without better estimates of these values, it is not possible to determine whether elemental concentrations would increase or decrease in response to increasing amounts of PAP.

Uranium is abundant in aragonitic speleothems but lacks a well-constrained distribution coefficient value. Existing studies generally suggest that uranium is preferentially incorporated into aragonitic stalagmites ($D_U > 1$) and excluded from calcitic stalagmites ($D_U < 1$) (Denniston et al., 2013). If the values of $D_U$ are indeed either side of one in the two mineral phases then uranium represents an ideal geochemical parameter to diagnose the presence, dominance, or variability of PAP as a control on stalagmite geochemistry. PAP variability is (like PCP variability) likely controlled by recharge variability, and may therefore allow U/Ca to function as a palaeorainfall proxy in karst environments where aragonite precipitation occurs. This study is the first to investigate the systematics of U/Ca in an aragonitic speleothem as a proxy for PAP and, in conjunction with $\delta^{13}C$, to use these geochemical indicators to reconstruct past rainfall variability and seasonality.

### 5.2.1 Yok Balum cave site description

Yok Balum cave in southern Belize (16° 12’ 30.78” N, 89° 40’ 24.42”W; 366m above sea level) is a well monitored tropical cave developed in a SW-to-NE trending karst ridge composed of Campur Formation limestone in the Toledo district of southern Belize. The cave is well studied, with cave monitoring records (Ridley et al., 2015b) as well as stable isotope records from two stalagmites already published (Kennett et al., 2012; Ridley et al., 2015a). Here, we supplement these existing records, particularly the YOK-G $\delta^{13}C$ record of Ridley et al. (2015a), with complementary trace element data. That stalagmites taken from this cave are primarily aragonitic in composition (Ridley, 2014), presumably the result of high Mg/Ca values in dripwaters.

The cave consists of a single main trunk passage approximately 540m in length with two entrances. These entrances are a small eastern opening and a larger, higher opening to the southwest formed by a cave roof collapse. The cave ventilates daily through these two

entrances, ensuring that $CO_2$ concentrations in the cave never rise to a level where dissolution of carbonate speleothems would occur. The cave is developed in a tectonically active area, and field observations suggest that it may have formed tracking a local fault. The stalagmite YOK-G was collected in 2006 from an actively dripping area of the cave approximately 80m from the smaller eastern entrance.

Southern Belize has a tropical climate, with seasonal temperatures only ranging approximately 4°C about the annual mean of 22.8°C. Latitude and elevation control rainfall distribution in Belize, with total annual rainfall ranging from 1300mm in the north to 4500mm in the south. Rainfall in the region exhibits a strong seasonality with >80% of the annual rainfall occurring between June and September in the peak of the May-January wet season. February to April receives significantly less rainfall, with evaporation greatly reducing soil and karst infiltration (Kennett et al., 2012).

## 5.3.0 Methods

### 5.3.1 Sample preparation and analysis

For analyses approximately 250µg of speleothem material was milled at 100µm resolution using a computer-controlled ESI/New Wave Micromill, equipped with a 0.8mm tungsten carbide drill bit. Powders were dissolved in 1% Nitric Acid (PWR 67% Nitric Acid Ultrapure Normatom for trace element analysis, diluted with Milli-Q water) and a suite of elements measured using a Thermo Scientific X Series II inductively-coupled plasma mass spectrometer (ICP-MS) at Durham University. The milled analyte used in this analysis is an aliquot of the larger milled volume; the remainder was used for stable isotope measurements (Ridley et al., 2015a), thereby allowing direct comparison with no chronological error between the proxies.

A set of multi-elemental Romil standards and blanks re-run throughout the sequence of samples allow precise quantification and correction for machine drift. Analytical precision on individual samples was <5% RSD for Ca, Mg and U, with Ca precision generally <2% RSD (3 repeat measurements). Detection limits varied by run, but were generally <0.1ppb for Mg and Ca, and <1ppt for U.

Stable isotope analyses were conducted at Durham University using a Thermo-Finnigan MAT 253 Isotope-Ratio Mass Spectrometer coupled with a Gasbench II, external precision of 0.05-0.1‰ as detailed in Ridley et al. (2015a). Each batch of fifty sample aliquots was run

alongside 14 standard powders; NBS18 (carbonatite), NBS19 (limestone), LS VEC (lithium carbonate) and an internal laboratory standard DCSO1. Normalisations and corrections were made to NBS19 and LS VEC. Random samples were re-run to ensure reproducibility between the runs and lend confidence to the results. Values reported are relative to the international VPDB standard.

Clear annual cycles in the monthly resolved $\delta^{13}C$ dataset, anchored to 1955 by detecting the radiocarbon 'bomb spike', were used to construct the monthly-resolution stalagmite age model. Eighteen high-precision U-Th dates produced at the University of New Mexico Radiogenic Isotope Laboratory fall within error of the cycle counting age model confirming the independent chronology. Specifics of the dating and age model construction are detailed in Ridley et al. (2015a). The stalagmite was actively dripping at the time of collection; however, reliable $\delta^{13}C$ cycles are only present until 1982 (approximately 8mm from the stalagmite top). The reasons for this are unclear, and may reflect a cessation or slowdown in growth after 1982, possibly linked to the proximal El Chichón eruption, which is approximately synchronous with this change. Therefore, post-1982 measurements are not considered because of lack of adequate chronological control.

### 5.3.2 Empirical calculation of distribution coefficients in speleothems

We present a method to calculate $D_U^a$ from speleothem calcite to aragonite transitions. Our approach is similar to the method described by Wassenburg et al. (2016), who also provide speleothem aragonite distribution coefficients for Mg, Sr and Ba. Wassenburg et al. (2016) also provide and discuss in detail the uncertainty of the resulting aragonite distribution coefficient taking into account, among other factors, potential changes in the chemical composition of the dripwater through time.

The calculations of the aragonite distribution coefficients involves two-steps: Firstly, a fluid trace element ratio is calculated using the known uranium distribution coefficient for calcite together with the measured uranium concentration in a calcite layer. Secondly, the calculated fluid value, together with the measured U/Ca in the aragonite layer, is then used to calculate the distribution coefficient between the fluid and aragonite (Figure 5.2). The uranium distribution coefficient for calcite used here is calculated from the temperature dependent equation of Day and Henderson (2013) ($D_U^c = 0.14e^{(-0.025*T)}$) and mean annual temperature within each studied cave.

Fluid U/Ca is thus calculated:

$$\frac{U}{Ca}_{fluid} = \frac{U}{Ca}_{calcite} / D_U^c$$

And thus:

$$D_U^a = \frac{U}{Ca}_{aragonite} \Big/ \frac{U}{Ca}_{fluid}$$

This approach operates on the assumption that the U/Ca in the fluid have not changed significantly between the precipitation of the two mineral phases. To minimise the potential effect of variable fluid concentrations we have used values from as close together as are available in the stalagmite, but this does not preclude the possibility of small changes in concentration because of hydrological or climatological variations. This concern can be somewhat ameliorated by examining layers with lateral changes in mineralogy such as those documented by Wassenburg et al. (2012). This approach is more robust as the mineral phases precipitated from the same drip, with only very small changes in fluid chemistry occurring laterally as the minerals precipitate. We calculate several uranium distribution coefficient values in aragonite ($D_U^a$) using this method from speleothems with both lateral and vertical transitions between mineral phases (McDermott et al., 1999; Railsback et al., 2011; Wassenburg, 2013; Wassenburg et al., 2012; Wassenburg et al., 2013). Any speleothems for which petrographic analysis suggests diagenetic alteration (e.g. Green et al. (2015)) were omitted from this analysis due to the recrystallized phase potentially precipitating from a markedly different fluid composition (Perrin et al., 2014).

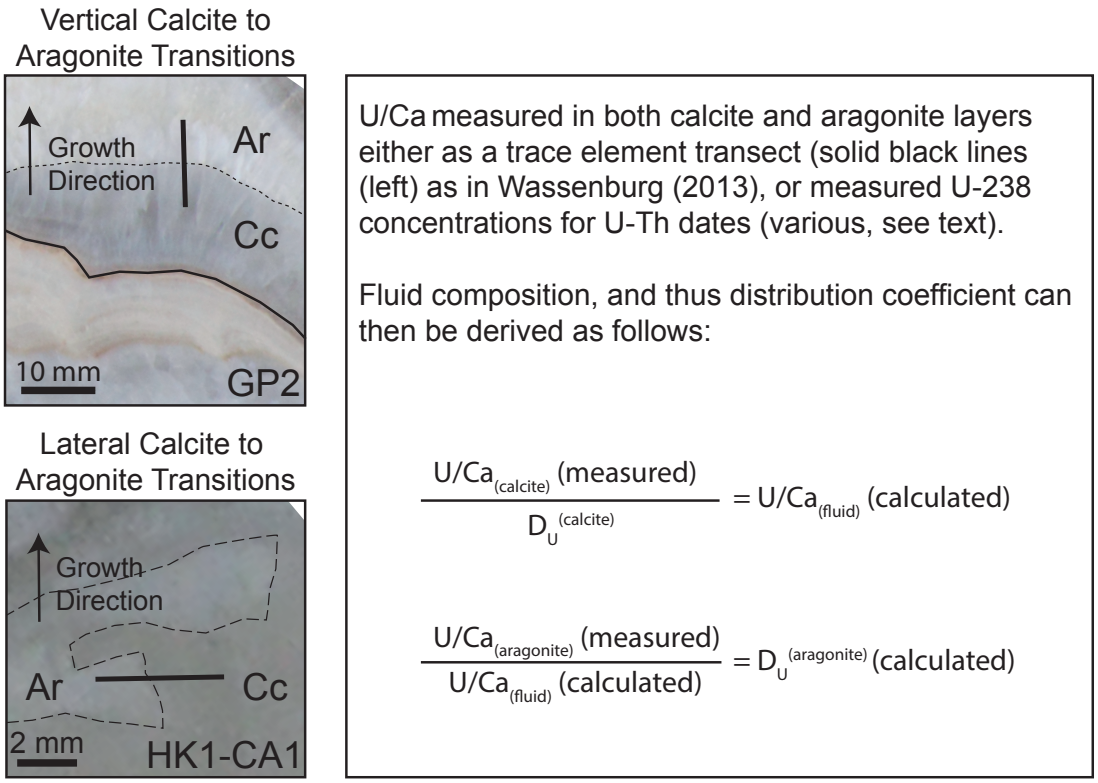


Figure 5.2: Examples of vertical and lateral calcite-aragonite transitions from Wassenburg (2013) (left). Distribution coefficient calculation method used in this chapter (right).

## 5.4.0 Results

### 5.4.1 Stable Isotope and Trace Element Results

From 1669-1983 AD, the YOK-G $\delta^{13}C$ record shows a long term trend towards more positive values, with a shift of approximately 0.5-1‰ in the long term mean over that interval (Figure 5.3). Superimposed on this trend are decadal-scale $\delta^{13}C$ fluctuations of between 0.5-1‰, as well as cyclical intra-annual (seasonal) variability of up to 1‰. U/Ca shows a decrease in the long-term mean from approximately $2x10^{-5}$ to $1x10^{-5}$ from 1669-1983 AD, with several decadal scale fluctuations of similar magnitude. Like $\delta^{13}C$, U/Ca shows annual cycles, with U/Ca cycle amplitudes of approximately $0.2\ x10^{-5}$-$0.5\ x10^{-5}$. Annual U/Ca cycles are generally anti-correlated with those of $\delta^{13}C$, although not exclusively so. The mean annual values of $\delta^{13}C$ and U/Ca anti-correlate throughout the record (1669-1983; $r = -0.70$, $p < 0.0001$).

Mg/Ca values in YOK-G show a very low magnitude long-term decrease in baseline values. Annual spikes of up to 0.0007 above the 0.0001 baseline occur during the wet season, anti-correlated with the annual cycles in $\delta^{13}C$.

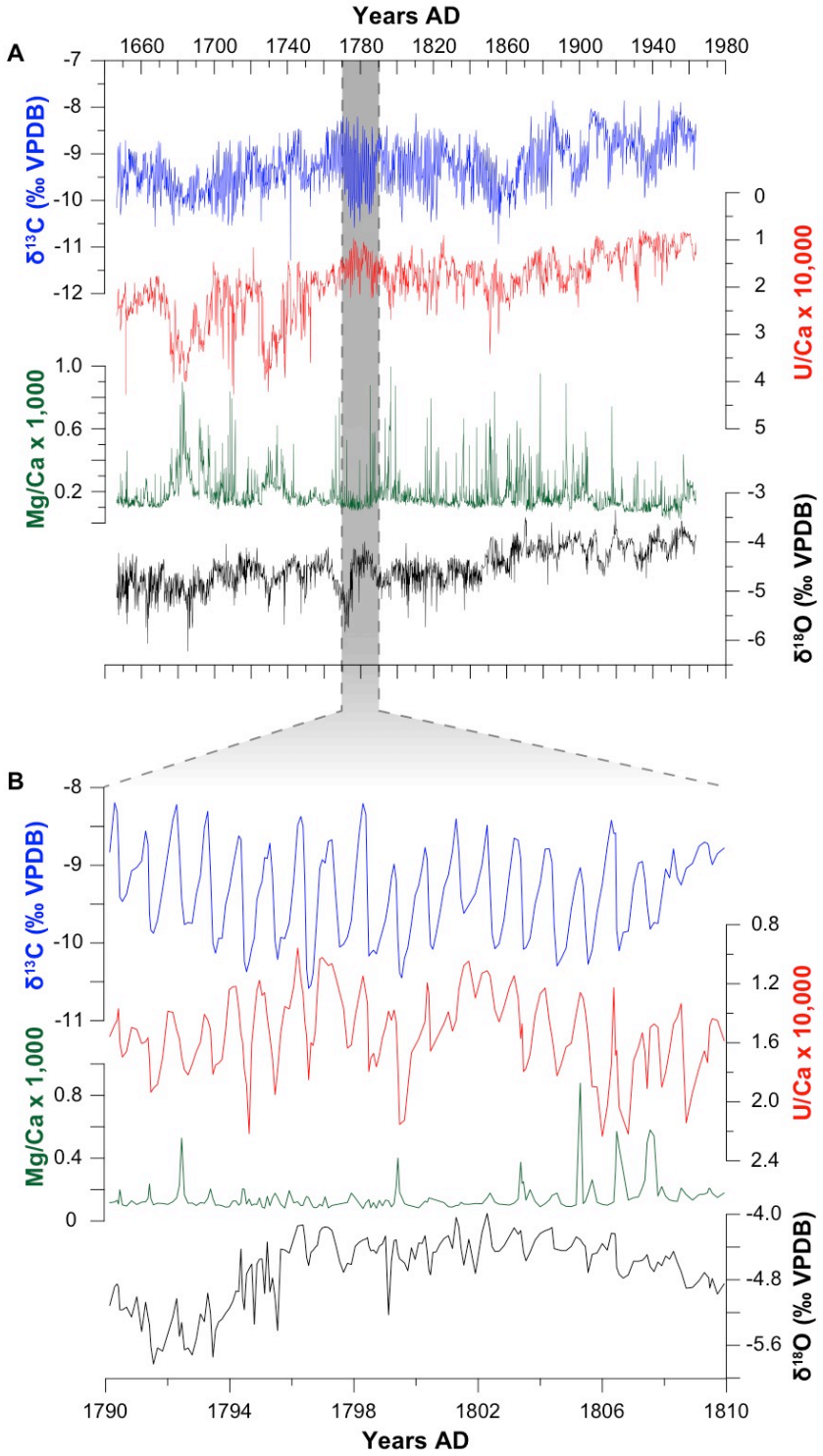


Figure 5.3: A: Time series plot of long-term trends in $\delta^{13}C$ (blue), U/Ca (red), Mg/Ca (green) and $\delta^{18}O$ (black). B: Expanded time series (1790-1810) showing annual cyclicity in proxy values.

### 5.4.2 Uranium Distribution Coefficients

The calculated values for $D_U^a$ are summarised in Figure 5.1 and Table 5.1, where calculations using both vertical and lateral transitions (Table 5.2) show similar value ranges for $D_U^a$ of 1.8-4.5. Our preferred value for $D_U^a$ calculated from this study is 3.74 ± 1.13, as the mean value ± one standard deviation of the two lateral calcite-aragonite transitions used. This value should not be considered an absolute value for the reasons discussed in section 5.1.3, but rather as a useful approximation for modelling and confirmation that the value in aragonitic speleothems is greater than one. Wassenburg et al. (2016) use a similar approach using additional speleothem transitions and report a similar range of distribution coefficients (6.26 ± 4.54). As our calculated values also fall within this range, we can confidently assert that the $D_U^a$ value in speleothem aragonite is greater than one.

| Sample | Location | Publication | Transition Type | Other Notes | Cave Temp (C) | U (Calcite, ppm) | U/Ca Calcite | D(U) (calcite) | Calculated U/Ca Fluid | U (Aragonite, ppm) | U/Ca Aragonite | Calculated D(U) (aragonite) |
|---|---|---|---|---|---|---|---|---|---|---|---|---|
| **CL26** | Grotto de Clamouse (France) | McDermott et al., 1999 | Vertical Layers | Calcite content value is mean of either side of Aragonite layer | 14.5 | 0.1315 | 3.284E-07 | 0.0974 | 3.371E-06 | 4.746 | 1.185E-05 | 3.516 |
| **ESP03** | Cova da Arcoia (NW Spain) | Railsback et al., 2011 | Vertical Layers | Mean values over all dates for definite mineral types | 8.1 | 0.10092 | 2.520E-07 | 0.1143 | 2.204E-06 | 1.724 | 4.306E-06 | 1.953 |
| **GP2** | Grotte de Piste (Morocco) | Wassenburg et al., 2012 | Vertical Layers | Calcite content value is mean of two values close to Aragonite layer | 13 | 0.0752 | 1.878E-07 | 0.1012 | 1.857E-06 | 1.374 | 3.431E-06 | 1.848 |
| **HK3** | Grotte Prison de Chien (Morocco) | Wassenburg et al., 2012 | Vertical Layers | Nearest Calcite values, nearest aragonite value (low) | 14 | 0.239 | 5.969E-07 | 0.0987 | 6.050E-06 | 6.34 | 1.583E-05 | 2.617 |
| **HK1** | Grotte Prison de Chien (Morocco) | Wassenburg et al., 2012 | Vertical Layers | 1 value of each, nearest dates to transition | 14 | 0.353 | 8.816E-07 | 0.0987 | 8.936E-06 | 11.041 | 2.758E-05 | 3.086 |
| **HK1-CA1** | Grotte Prison de Chien (Morocco) | Wassenburg 2013 | Lateral Change | Mean of trace element transect values in each mineralogy | 14 | 0.333 | 8.317E-07 | 0.0987 | 8.430E-06 | 15.342 | 3.831E-05 | 4.545 |
| **HK1-CA2** | Grotte Prison de Chien (Morocco) | Wassenburg 2013 | Lateral Change | Mean of trace element transect values in each mineralogy | 14 | 0.564 | 1.410E-06 | 0.0987 | 1.429E-05 | 16.818 | 4.200E-05 | 2.940 |

Table 5.2: Measured and calculated values for distribution coefficient calculations.

## 5.5.0 Discussion

### 5.5.1 General Trends in U/Ca and $\delta^{13}C$

In general, $\delta^{13}C$ in aragonitic speleothems and in systems where PAP is occurring will behave very similarly to the calcite equivalents. Whilst the exact value of the fractionation factor between precipitated aragonite and bicarbonate in solution may vary slightly from that of calcite, progressive precipitation will still act to increase the $\delta^{13}C$ of the solution (Fairchild et al., 2006a; Polag et al., 2010). As a result, PAP and PCP will both lead to higher $\delta^{13}C$ values in speleothems. Ridley et al. (2015a) interpreted $\delta^{13}C$ values in YOK-G as a palaeorainfall proxy, and noted both a strong intra-annual signal corresponding to seasonality as well as long-term variations resulting from intertropical convergence zone position (ITCZ) shifts linked to anthropogenic and natural (volcanic) aerosol forcing. The $\delta^{13}C$ record shows an increasing drying trend post-1850, which is expressed in both the overall $\delta^{13}C$ signal and particularly in the wet season $\delta^{13}C$ values. This multi-proxy inferred drying trend mirrors the observed decrease in annual rainfall in several meteorological stations near Yok Balum cave (Ridley et al., 2015a).

### 5.5.2 Uranium Distribution Coefficients

Lateral transition values are the basis for our preferred value as they result from small changes in dripwater concentrations due to mineral precipitation rather than potentially large shifts vertically due to changes in climate or flow path, which may result in competition effects modifying the $D_U^a$ value. The range of these values may result from variations in U/Ca in the dripwaters between the precipitation of the two phases (e.g. due to prior carbonate precipitation or varying dissolution) producing variable errors in the calculated $D_U^a$ values. Alternatively, they may be truly different $D_U^a$ values in each stalagmite stemming from the various other factors which influence distribution coefficients (e.g. growth rates (Gabitov et al., 2008) or dripwater pH (Wassenburg et al., 2016)). Similarly high values have been found experimentally (Meece and Benninger, 1993) and in speleothem samples (Wassenburg et al., in revision). However, because these values are all greater than one they indicate that uranium is preferentially incorporated into speleothem aragonite. This is consistent with the general understanding of the uranium incorporation mechanism into the crystal lattice. In aragonite the most common aqueous uranium species, $UO_2(CO_3)_3^{4-}$, is incorporated into the crystal structure intact, whilst to be incorporated into calcite the co-ordination of this unit has to change (Reeder et al., 2000).

This suggests that the distribution coefficients established here are consistent with both the known crystallographic incorporation mechanism, and the generally higher observed concentrations of uranium in aragonitic speleothems. We can conclude that an increase in PAP would result in lowered U/Ca values in dripwater, and thus lower stalagmite concentrations, during drier conditions.

### 5.5.3 Intra-annual variations and inferred controls on U/Ca

Mean monthly U/Ca values demonstrate the presence of a clear annual cyclicity in YOK-G, which is overall anti-correlated with annual $\delta^{13}C$ cycles (Figure 5.4). A mechanism must therefore operate at the YOK-G site that increases dripwater U/Ca values during wetter months of the year. Prior calcite precipitation would have the opposite effect, lowering U/Ca values during wetter months and increasing U/Ca during drier months as uranium is excluded from calcite and dripwater concentrations increase with intensified PCP. Increased residence times of infiltrating water in drier months would also tend to increase uranium concentrations as percolating waters have more time to leach trace elements from the karst rock. The $D_U$ value of 3.74 ± 1.13 calculated above, definitively greater than one (Figure 5.1), confirms that PAP would result in increased U/Ca values during the wet season. As both PCP and/or increased residence times would have the opposite effect to the observed variability, we infer that PAP is the dominant control on seasonal variations in U/Ca concentrations throughout YOK-G (Figure 5.5).

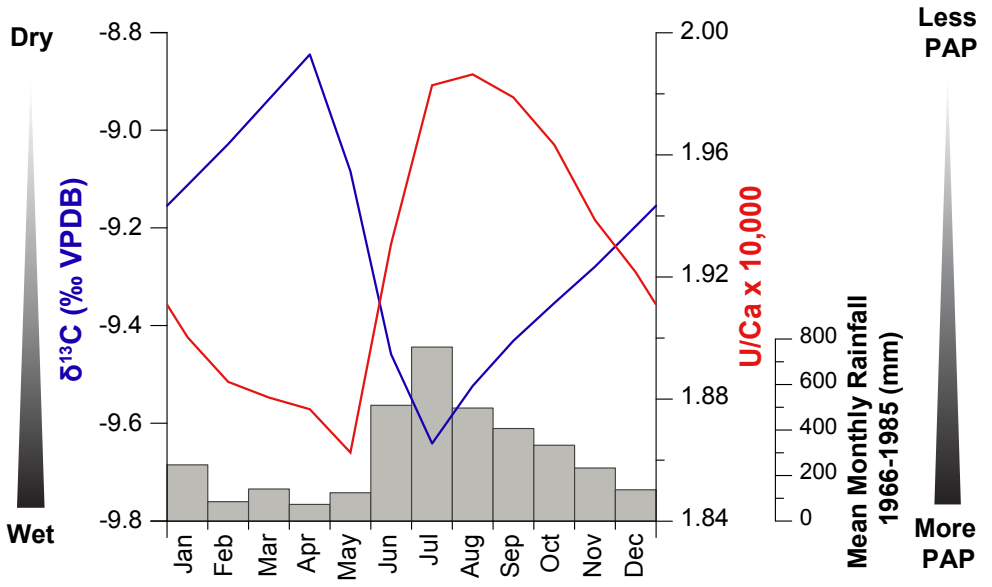


Figure 5.4: Mean monthly variations of U/Ca (red) and $\delta^{13}C$ (blue) in stalagmite YOK-G (means over 1669-1983). Mean monthly rainfall at the Punta Gorda meteorological station from 1966-1985 (grey bars).

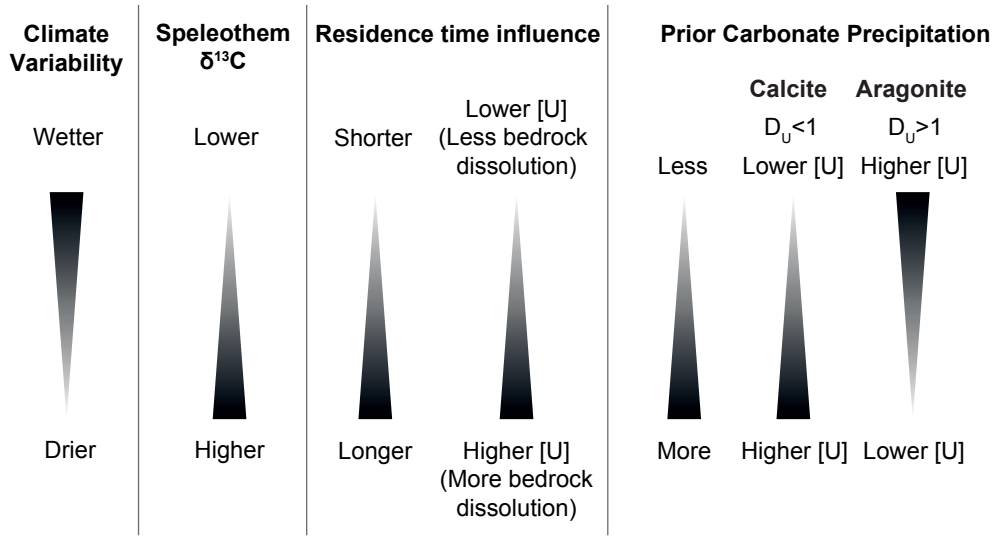


Figure 5.5: Influence of rainfall on $\delta^{13}C$ and factors influencing U/Ca ratios in speleothems.

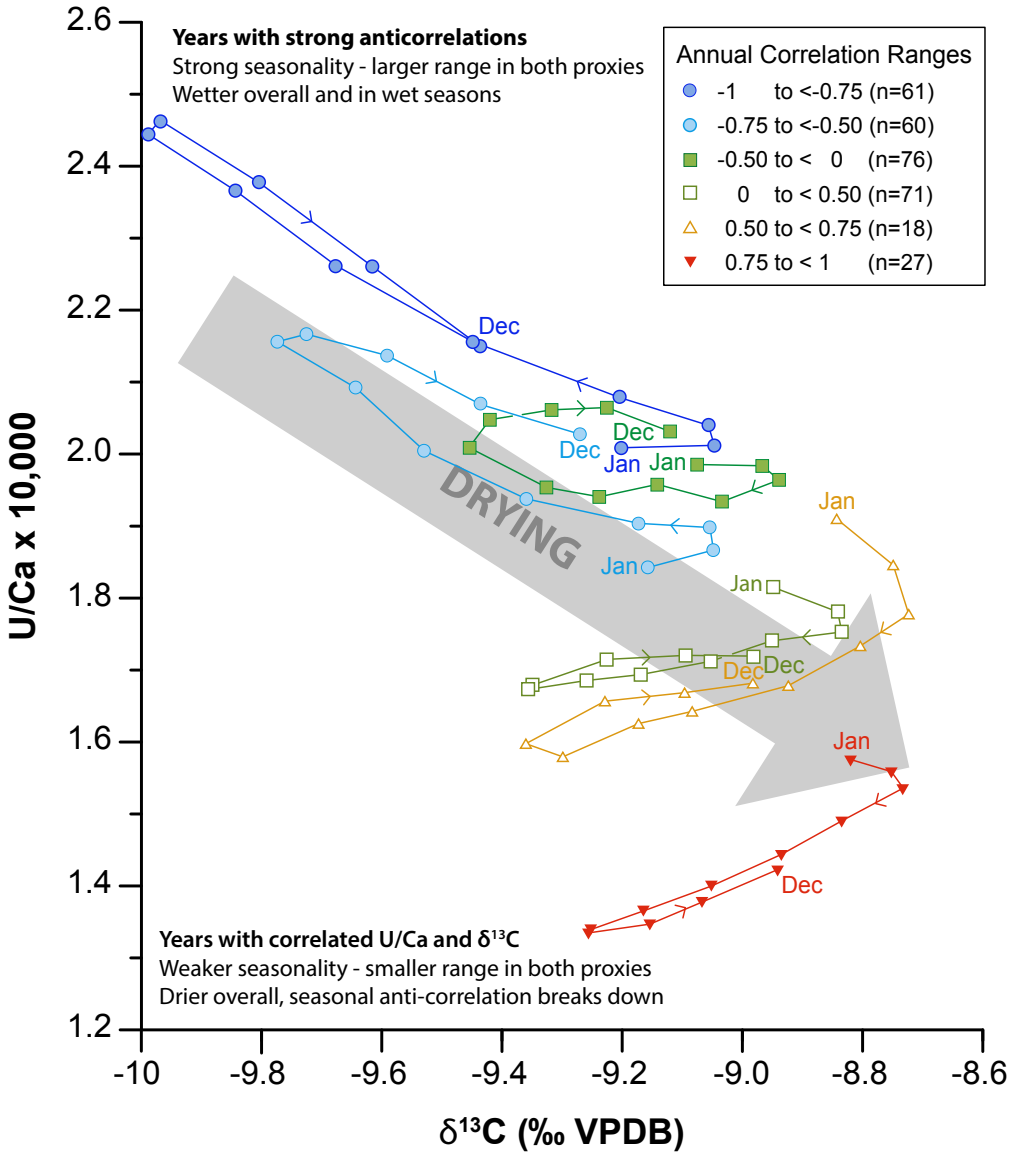


Figure 5.6: Comparison of mean monthly fluctuations in U/Ca and $\delta^{13}C$ in years with varying levels of correlation between the two variables. The dataset is divided into six separate groups based on the correlation between U/Ca and $\delta^{13}C$, then the mean values for each calendar month plotted above. January and December months are labelled, with months joined sequentially.

The mean annual values of $\delta^{13}C$ and U/Ca anti-correlate throughout the record (1669-1983; $r = -0.70$, $p < 0.0001$), consistent with PAP as a dominant control on YOK-G U/Ca on inter-annual timescales. The strength of the anti-correlation between $\delta^{13}C$ and U/Ca varies interannually with some years displaying a very strong anti-correlation but others exhibiting a weaker anti-correlation or occasionally even a positive correlation (Figure 5.6). Overall, U and $\delta^{13}C$ are strongly anti-correlated in 121 years ($r < -0.5$), weakly anti-correlated in 76 years ($-0.5 < r < 0$), weakly positively correlated in 71 years ($0 < r < 0.5$), and strongly positively correlated in 45 years ($0.5 < r < 1$). Positively correlated years are characterised by greatly reduced rainfall seasonality inferred by using both U/Ca and $\delta^{13}C$ (Figure 5.7). This suggests that in years where $\delta^{13}C$ and U/Ca are positively correlated, PAP is no longer the dominant control on the intra-annual U/Ca variability of the speleothem. Monthly and mean annual $\delta^{13}C$ and U/Ca values suggest that these years are drier than the overall mean, as well as exhibiting reduced seasonality. This reflects decreased rainfall, largely in the wet season, where $\delta^{13}C$ and U/Ca are markedly less negative and lower respectively. Therefore, we can infer that in years with reduced wet season rainfall, the dominance of seasonal PAP control on YOK-G geochemistry breaks down because of increased residence time (and thus bedrock dissolution) becoming a more dominant control or simply because of reduced seasonal rainfall contrasts. During drier years increased PAP is still occurring, resulting in lower U/Ca values in those years, it simply does not display the strong seasonal pattern observed in wetter/more seasonal years.

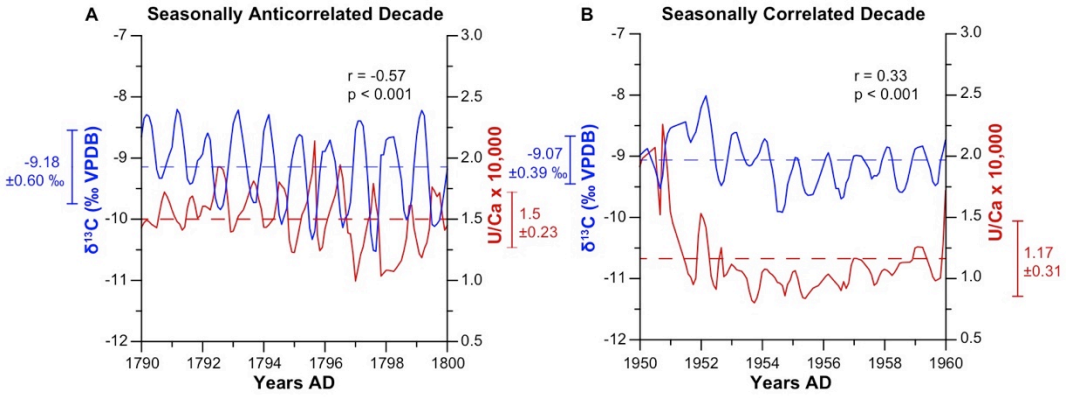


Figure 5.7: Comparison of selected decades where $\delta^{13}C$ and U/Ca are A) seasonally anti-correlated (1790-1800) and B) seasonally correlated (1950-1960). Dashed lines show decadal mean values, with range bars representing ± one standard deviation. Decadal means suggest that, based on both proxies, the seasonally correlated decades are drier overall, with smaller amplitude seasonal variations.

The variability of this seasonal (anti)-correlation varies through time in the stalagmite record (Figure 5.8), and is linked to the inferred amount of summer rainfall. Prior to ~1850, strongly seasonal, wetter, anti-correlated years dominate the record, suggesting that in the pre-industrial period most years in Belize were characterised by strongly seasonal rainfall controlled by the earlier arrival of ITCZ rainfall. Following the mid-1800s, the frequency of years when $\delta^{13}C$ and U/Ca are positively correlated increases, reflecting reduced wet season rainfall, consistent with a more southerly ITCZ (Ridley et al., 2015a).

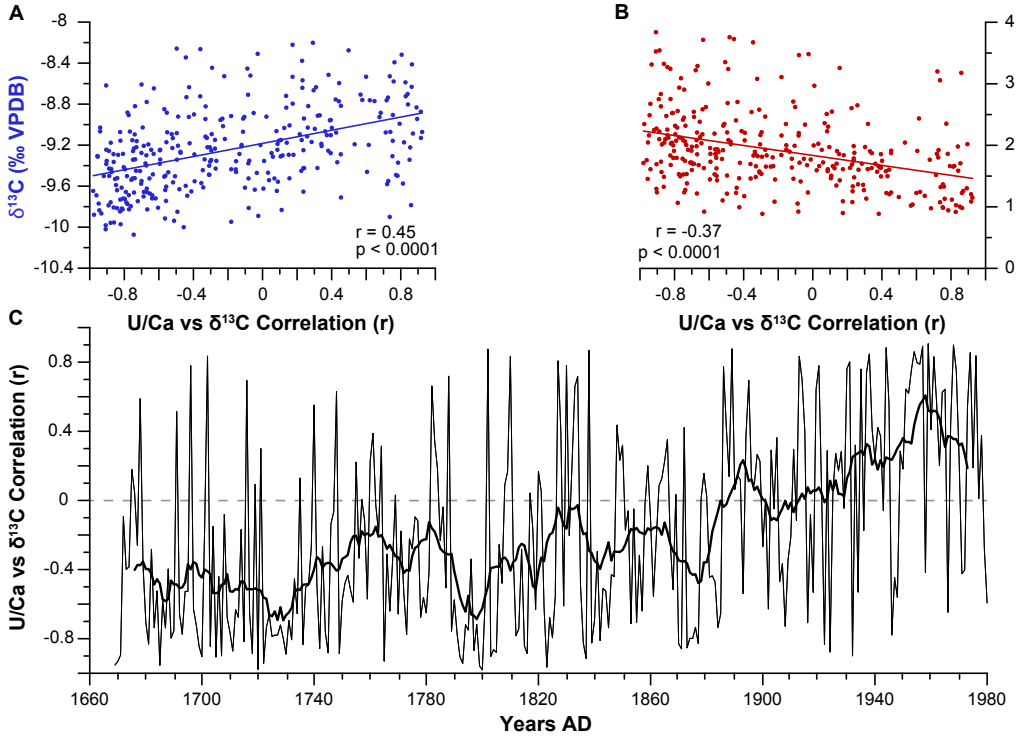


Figure 5.8: A) Mean annual $\delta^{13}C$ vs. seasonal correlation between U/Ca and $\delta^{13}C$ and B) U/Ca vs. seasonal correlation between U/Ca and $\delta^{13}C$. C) U/Ca vs. $\delta^{13}C$ seasonal correlations as an annual time series with 15-year running average. Correlation values shift from negatively correlated towards more positively correlated in recent years.

### 5.5.4 Comparison with meteorological records

Comparison with Punta Gorda rainfall station records (1906-1983) from approximately 30km to the southeast further supports the link between the annual $\delta^{13}C$ versus U/Ca correlation with seasonality. Maximum monthly rainfall and the difference between maximum and minimum monthly rainfall (both measures of rainfall seasonality, because minimum monthly rainfall is reasonably consistent through the record) both anti-correlate with the U/Ca vs $\delta^{13}C$ annual correlation value ($r = -0.26$, $p = 0.03$ and $r = -0.27$, $p = 0.02$ respectively). In other words, years with greater wet season rainfall and increased seasonality resulted in a stronger negative correlation between U/Ca and $\delta^{13}C$, and years with less wet season rainfall and reduced seasonality exhibit a positive correlation because seasonal PAP shifts are muted and consequently is no longer a dominant control on seasonal U/Ca variability. We suggest that this diminished seasonality is enough that residence time and bedrock interaction effects (which positively correlate with $\delta^{13}C$)

overwhelm the lower amplitude seasonal U/Ca variability signal. PAP is still occurring, and indeed is likely intensified in these drier years, however it exhibits reduced variability on intra-annual timescales due to the reduced seasonality. Consequently, dry years have a lower mean U/Ca value due to increased PAP, but positively correlate intra-annually with $\delta^{13}C$ due to reduced variability in PAP (Figure 5.9).

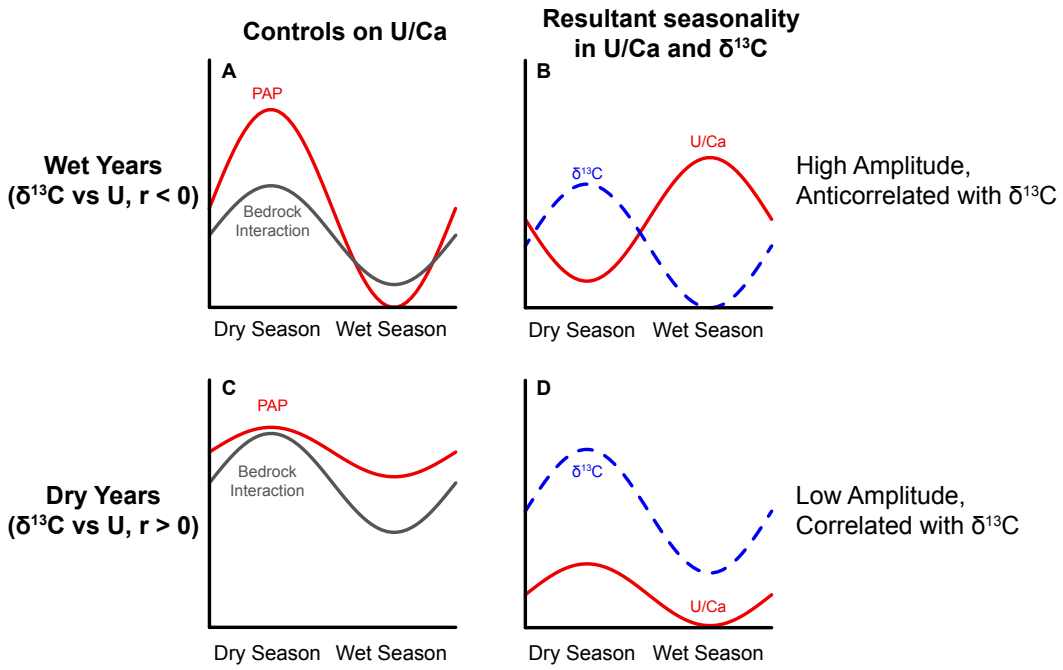


Figure 5.9: Competing controls on U/Ca during wet and dry years. During wet years (A, B) PAP is highly variable seasonally (A), dominating the U/Ca intra-annual variability and anti-correlating with $\delta^{13}C$ (B). During dry years (C, D) PAP is less variable seasonally and the signal is subsumed by bedrock interaction (C), resulting in a seasonal correlation with $\delta^{13}C$ (D).

### 5.5.5 Comparison of proxies with long-term climate records

In the Industrial Period (post-1850), $\delta^{13}C$ and U/Ca both indicate a trend of overall drying and reduced seasonality. As outlined by Ridley et al. (2015a) these variables (annual means, peak wet values, peak dry values and seasonal differences of both proxies) all correlate with increasing Northern Hemisphere Temperature (NHT) (see Table 5.3). Indeed U/Ca displays a stronger and more significant relationship with NHT over this period perhaps suggesting that this proxy is even more sensitive to rainfall shifts than $\delta^{13}C$.

| | r value | p value |
|---|---|---|
| **Peak Wet $\delta^{13}C$** | 0.42 | $4.3x10^{-7}$ |
| **Peak Dry $\delta^{13}C$** | 0.40 | $1.4x10^{-6}$ |
| **Mean Annual $\delta^{13}C$** | 0.46 | $1.8x10^{-8}$ |
| **Seasonal Difference in $\delta^{13}C$** | -0.15 | 0.08 |
| **Peak Wet U/Ca** | -0.59 | $2.5x10^{-14}$ |
| **Peak Dry U/Ca** | -0.65 | $1.3x10^{-17}$ |
| **Mean Annual U/Ca** | -0.68 | $8.1x10^{-20}$ |
| **Seasonal Difference in U/Ca** | -0.19 | 0.030 |
| **$\delta^{13}C$ vs U/Ca Correlation** | 0.34 | $4.52x10^{-5}$ |

Table 5.3: Industrial period (1850-1983) correlations and significance of hydrological proxies with the Northern Hemisphere Temperature reconstruction of Esper et al. (2002).

This shift in both proxies towards drier and less seasonally variable conditions post-1850 supports the interpretation of Ridley et al. (2015a) that the northern maximum extent of the ITCZ has shifted southwards in response to increased anthropogenic sulphate aerosol emissions in the Northern Hemisphere and changing hemispheric temperature contrasts, consequently resulting in drier wet seasons in Belize and reduced hydrological seasonality.

For the pre-industrial period the relationship with NHT is less clear, with only dry season U/Ca showing a weak ($r = -0.16$, $p = 0.003$) anti-correlation to NHT. This suggests that NHT had an influence on dry season moisture balance, possibly in the form of increased dry season evapotranspiration, but did not strongly influence wet season rainfall.

In summary, on inter-annual timescales U/Ca in YOK-G is a proxy for overall dryness in Belize, whilst the annual correlation or anti-correlation of U/Ca and $\delta^{13}C$ reflects changes in intra-annual rainfall seasonality.

### 5.5.6 Mg/Ca variability in YOK-G

Mg/Ca is a more commonly used proxy for prior carbonate precipitation in speleothems, due to its strong partitioning behaviour and abundance in karst environments. We therefore also examine the behaviour of Mg/Ca in YOK-G over the same period of the $\delta^{13}C$ and U/Ca datasets. Having established that PAP is a significant control on the geochemistry

of YOK-G, this is a unique opportunity to improve our understanding of magnesium behaviour in aragonitic stalagmites.

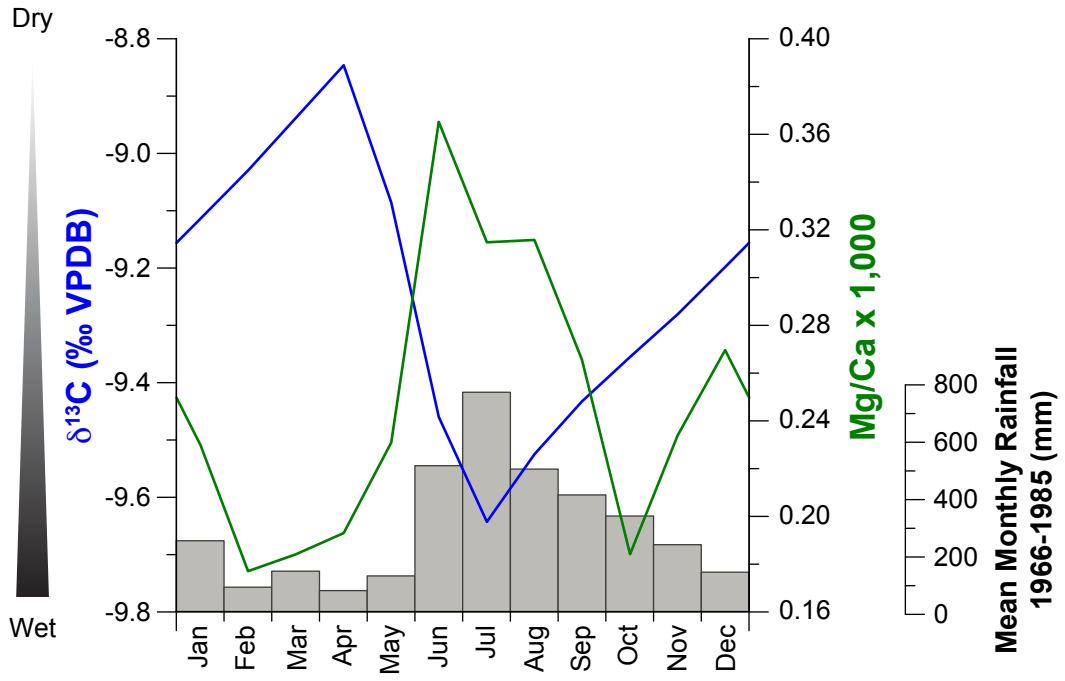


Figure 5.10: Mean monthly variations of Mg/Ca (green) and $\delta^{13}C$ (blue) in stalagmite YOK-G (means over 1669-1983). Mean monthly rainfall at the Punta Gorda meteorological station from 1966-1985 (grey bars).

Prior carbonate precipitation does not appear to control intra-annual Mg/Ca variability in this speleothem. Distribution coefficients for magnesium quoted in the literature are generally below one in both calcite (e.g., $D_{Mg}^{c}$ = 0.012-0.029 (Day and Henderson, 2013), $D_{Mg}^{c}$ = 0.015-0.020 (Fairchild et al., 2010)) and aragonite (e.g., $D_{Mg}^{a}$ = 0.000097 ± 0.00009 (Wassenburg et al., 2016) $D_{Mg}^{a}$ = 0.00002 – 0.00008 (Gabitov et al., 2008), $D_{Mg}^{a}$ = 0.00053 – 0.0149 (Gaetani and Cohen, 2006)), therefore drier intervals should lead to increased stalagmite Mg concentrations, and a positive seasonal correlation with $\delta^{13}C$. However, YOK-G Mg/Ca generally peaks in the wet season, anti-correlating with $\delta^{13}C$, opposite to the predicted relationship if either PCP or PAP were the dominant controls on Mg/Ca in this stalagmite (Figure 5.10). We propose three possible mechanisms for this observation:

1) Elevated wet season Mg/Ca values could result from influx of magnesium rich material from the soil and epikarst during periods of increased rainfall. One candidate for this material is wood ash produced by biomass burning from slash and burn agriculture as practiced in the region. Magnesium is a significant component of wood ash (Etiégni and Campbell, 1991), and could potentially be washed in as either magnesium bearing minerals found in wood ash or as leached ions in dripwaters.

2) Times of higher rainfall and increased water volume in the karst may activate flowpaths sampling from areas of less chemically mature dolomitised limestone material where increased amounts of magnesium are dissolved from the host rock. This overflow pathway, only active during periods of increased rainfall, potentially passes through rocks with elevated magnesium content and/or less weathered surfaces. This explanation, whilst plausible, is extremely difficult to test without extensive additional site hydrology characterisation and country rock sampling within the karst.

3) Because the aragonite crystal lattice strongly excludes magnesium ($D_{Mg}^{a}$ = 0.00002 – 0.00008 Gabitov et al. (2008)) organic colloidal transport, clay mineral incorporation or the presence of fluid inclusions may overprint any hydrological controls on the Mg signal (Wassenburg, 2013; Wassenburg et al., 2012; Yang et al., 2015). This is consistent with the timing of the increased Mg/Ca values, as wet season rainfall would result in both increased flushing of material and potentially increased growth rates. The nature of the long-term Mg dataset, with large amplitude, but short-lived, spikes in Mg concentration superimposed on a relatively low concentration baseline supports sporadic inputs of colloidally associated Mg associated with flush events.

Regardless of the specific mechanism, Mg/Ca is clearly not an effective hydrological proxy in this stalagmite. This further reinforces the concept that the interpretation of proxy records in stalagmites as rainfall variability often requires more information than a single proxy record. Multi-proxy approaches using trace elements in conjunction with stable isotopes (this study), other trace element proxies (Wassenburg et al., 2012) , or dripwater monitoring (Rutlidge et al., 2014), are vital to support any palaeoclimatic interpretation.

## 5.6.0 Conclusions

We calculate a distribution coefficient of uranium in aragonitic speleothems of 3.74 ± 1.13, which is in agreement within error with the value derived by Wassenburg et al. (2016). We infer that prior aragonite precipitation results in lower U/Ca in speleothems. Aragonitic speleothems contain relatively high concentrations of uranium and thus have great potential to provide exceptionally precise U-Th ages. In addition, they grow in environments where varying aragonite precipitation along the flow pathway can exert a strong control on dripwater uranium content with little additional noise in the signal from varying external inputs. We therefore suggest that in aragonitic speleothems uranium concentrations are a powerful proxy for rainfall variability.

The unusually high temporal resolution of the YOK-G trace element record enables an examination of seasonal geochemical variations in aragonitic stalagmites and the development of a new proxy for rainfall. U/Ca hydrological variations occur on both intra- and inter-annual timescales, and are therefore useful for assessing seasonal changes in rainfall patterns. We demonstrate that U/Ca correlates with other rainfall proxies such as $\delta^{13}C$, can be linked to instrumental rainfall records, correlates with other climatic variables (e.g., NHT), and reflects previously inferred trends in Belizean paleo-rainfall. Mg/Ca in YOK-G does not appear to be a viable paleo-rainfall proxy, emphasising the importance of considering multiple proxies.

The development of an additional hydrological proxy in aragonitic speleothems, which is easily measured at extremely high spatial resolution and appears extremely sensitive to rainfall amount and seasonality, is an important addition to the set of tools available with which to reconstruct climate. Aragonitic speleothems, with their precise age controls, are ideal for this purpose as they minimise age uncertainty. This study presents a valuable new method for estimating paleo-rainfall in low-latitude regions where few high quality rainfall proxy archives of climate are available.

# Chapter 6

# 630 years of trace element records from a Bermudan stalagmite linked to effective rainfall, soil bioproductivity and NAO state

*This chapter is presented in manuscript form, and is intended for future publication.*

**Robert A. Jamieson** analysed the sample, processed the data, performed the statistical analyses, interpreted the data, and wrote the manuscript thereby contributing to over 95% of the work presented in this chapter.

**James U.L. Baldini** assisted with interpretation of the data and provided extensive comment on the manuscript.

**Izabela Walczak** conducted fieldwork and collected the sample. In addition, she performed cave monitoring and milled the sample for dates. Monitoring data, as well as stable isotope results for this sample are included in her thesis (Walczak, 2016).

**Wolfgang Müller** assisted with the LA-ICP-MS analysis at Royal Holloway University, London

**Franziska Lechleitner and Cameron McIntyre** produced the radiocarbon dates used for this sample.

**Acknowledgements**

Thanks to Viola Warter and Damiano Della Lunga for their assistance with LA-ICP-MS measurements at Royal Holloway University, London.

Bermuda Weather Service graciously provided weather station data used in Figure 6.1.

Thanks to the owners of Leamington Cave and the overlying property for granting us access to the cave. We also thank Gil Nolan and Robbie Smith for their assistance with cave site selection, local access and fieldwork assistance.

Export permit for BER-SWI-13 provided by Bermuda Aquarium.

This work was in part funded by the ERC (240167).

# Chapter 6: 630 years of trace element records from a Bermudan stalagmite linked to effective rainfall, soil bioproductivity and NAO state

## Abstract

Speleothem trace elements are a set of proxies, which record a diverse set of palaeoenvironmental information. They are generally used to reconstruct palaeoclimatic information, principally effective rainfall. However, they can also reflect more complex processes such as bioproductivity, changing external inputs, and anthropogenic influences on a cave site. This study presents a high-resolution 630-year record of multiple trace elements from a Bermudan stalagmite.

In this stalagmite, magnesium concentrations record, via varying prior calcite precipitation, changes in local rainfall which appear to correspond to variation in the North Atlantic Oscillation (NAO). Through a different mechanism, phosphorous also correlates with changes in the NAO. We infer that local effective rainfall changes, influenced by NAO state, influence bioproductivity above the cave and thus the amount of phosphorous in dripwaters. Surprisingly, for a location such as Bermuda, we see no evidence of clear direct anthropogenic influence on speleothem chemistry.

These results suggest that Bermudan speleothems are well situated to record basin scale climate changes in the North Atlantic. High-resolution speleothem trace element records continue to be extremely valuable tools for reconstructing effective rainfall.

## 6.1 Introduction

Speleothems are important terrestrial archives of high-resolution palaeoenvironmental information. They are dateable using a variety of techniques and with dating precision that arguably exceeds that of any other palaeoclimate archive. Additionally, speleothems are multi-proxy archives hosting a variety of complementary proxy systems which can be compared to disentangle multiple palaeoenvironmental controls. Stable isotope ratios are the proxies most frequently used in speleothem research to reconstruct climate variability. However, other proxies including laminae thickness (Baker et al., 2008), optical properties (Proctor et al., 2000), trace element concentrations (Fairchild and Treble, 2009), and crystallography (Frisia, 2015) also record various climatic and hydrological information. Trace element proxies preserve diverse information including both climate (Cruz Jr. et al., 2007) and non-climatic signals such as volcanism (Frisia et al., 2008), land use changes (Borsato et al., 2007) and anthropogenic emissions (Tan et al., 2014).

### 6.1.1 Speleothem Trace Elements

Trace element proxies in speleothems, although often considered only as a supplement to the more widely used stable isotope proxies, are a suite of tools which are being increasingly used to reconstruct environmental information. The majority of trace element studies in speleothems utilise the Group II (alkali earth) elements which are commonly incorporated into calcite (Fairchild and Treble, 2009). Magnesium is the most commonly utilised element, due to both its abundance in cave dripwaters as well as its well understood behaviour in speleothem systems (Fairchild and Baker, 2012). Correlations between speleothem magnesium content and climate have been reported extensively in the literature, and the concept of Prior Calcite Precipitation is well established as a climate dependent mechanism in karst environments that mediates dripwater, and thus speleothem, magnesium concentrations. The same mechanism has been proposed as a control on strontium and barium variability in stalagmites, however interpretation of their behaviour is complicated by other influences on their incorporation, including growth rate and competition effects (Fairchild and Treble, 2009).

### 6.1.2 Site Description

The Bermuda islands are a carbonate platform developed atop a volcanic seamount in the North Atlantic. The modern subaerial exposure in Bermuda consists almost entirely of carbonate rocks, the majority of which are either aeolianites with clear dune structures, or more massive limestones. Facies changes in Bermudan geology generally result from

eustatic sea level changes during the Pleistocene. Caves in Bermuda develop almost exclusively in the highly weathered and karstified Walsingham Formation (Swinnerton, 1929), some of the oldest rocks on the island (deposited approximately 1.1-0.8Ma (Hearty and Vacher, 1994)), which outcrop in a narrow band along the North-East coast of the main island between Harrington Sound and Castle Harbour.

Leamington Cave is one such cave, a privately owned former show cave that is richly decorated with actively growing speleothems and which has been continuously monitored for CO2 fluctuations, temperature, and drip rate changes for a year (Walczak, 2016). The cave pool, which dominates the main cave chamber (Figure 2.6), connects to the ocean and causes the cave to ventilate daily thanks to a tidal flushing mechanism. This suggests that speleothems in Leamington Cave are unlikely to undergo dissolution due to build-up of $CO_2$. Stalagmite BER-SWI-13 (or 'Swizzle') was selected based on its hydrology (e.g., active but moderate response to rainfall) and a favourable internal structure as revealed by CT scans (Walczak, 2016).

### 6.1.3 Climate of Bermuda

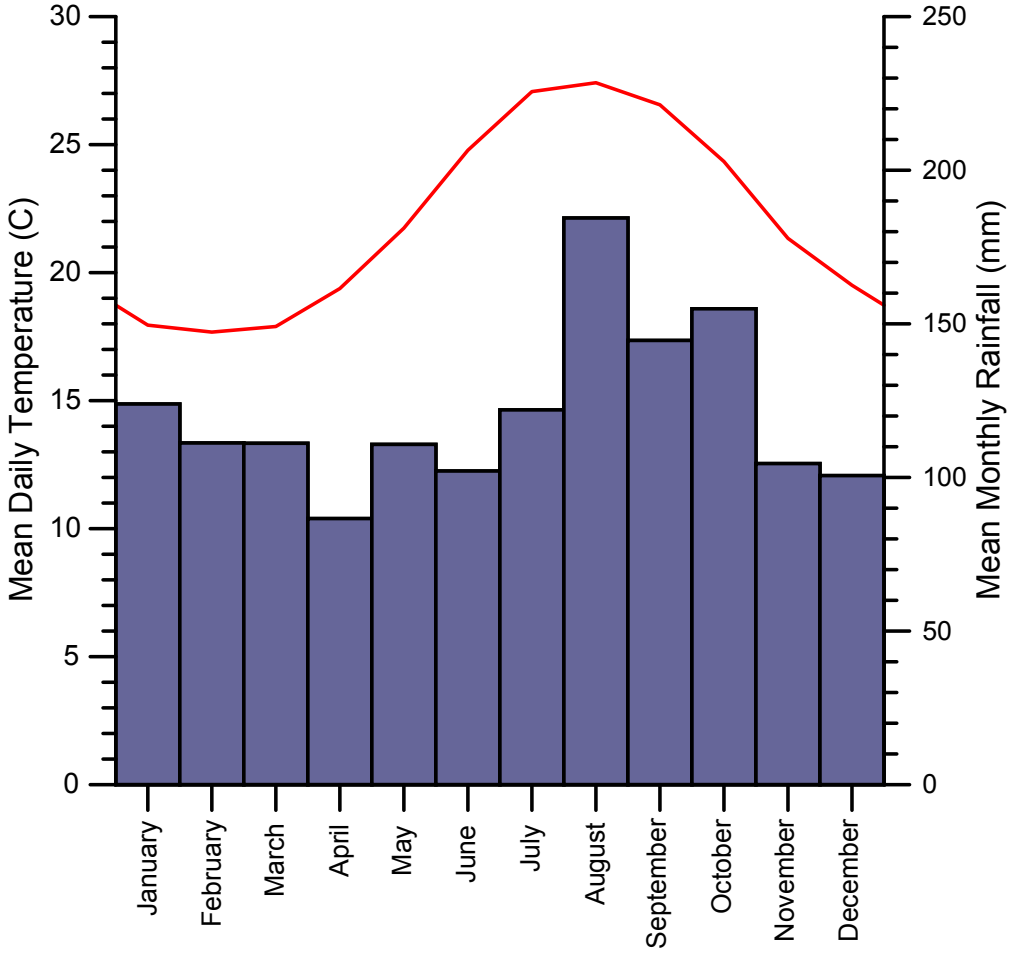


Figure 6.1: Climate of Bermuda. Mean Daily Temperature in degrees Celsius (red) and Mean Monthly Rainfall in mm (blue). Source: Bermuda Weather Service. Mean monthly values 1996-2015AD

Bermuda is located at 32°N in the North Atlantic, and has a humid subtropical climate. The island group's position on the eastern edge of the Gulf Stream results in warmer temperatures and slightly wetter conditions than latitude alone accounts for. This position also puts Bermuda on the south-eastern side of the Atlantic hurricane belt which often influences Bermudan weather. Seasonally, temperatures vary by approximately 10°C with a clear seasonal contrast between summer and winter. Rainfall is more uniform throughout the year with no pronounced dry season, however rainfall does increase somewhat in autumn (Figure 6.1).

Bermuda's position in the mid-Atlantic means that its climate is strongly influenced by basin scale climate factors which influence the position and strength of the Gulf Stream (such as NAO state). The influence of the North Atlantic Oscillation on hydroclimate is generally considered primarily in the context of storm track positioning and influence on the weather of Western Europe. Positive NAO values generally reflecting more northerly storm track positioning, and thus increased precipitation in Northern Europe. The influence of the NAO over the rest of the Atlantic basin can be more complex, influencing hurricane storm tracks, weather on the Eastern seaboard of North America, and sea surface temperatures (SST) throughout the Atlantic basin. NAO variability may be controlled to some degree by fluctuations in SST, with persistent SST anomalies leading changes in NAO state by up to 6 months (Czaja and Frankignoul, 2002).

## 6.2 Methodology

### 6.2.1 U-Th dates

BER-SWI-13 was sectioned along the central growth axis determined using reconnaissance CT scanning following the methods described in Walczak et al. (2015), polished, and then cleaned in an ultrasonic bath of deionised water. Samples of ~400 mg weight were milled from BER-SWI-13 along the growth axis for U-series dating. They were consecutively dated at the Department of Earth Sciences, University of Bristol, and at the St. Andrews Isotope Geochemistry (STAiG) lab using multi- collector-inductively coupled plasma mass spectrometer (MC-ICPMS), following the chemical separation procedure described in Hoffmann et al. (2007). All dates were in stratigraphic order within errors.

### 6.2.2 Radiocarbon dates

25 carbonate samples for $^{14}C$ analysis were milled along the growth axis using a semi-automatic high-precision drill (Sherline 5400 Deluxe) at ETH Zurich. All equipment and the stalagmite surface were cleaned using methanol and dried using compressed air prior to sampling, to minimize external contamination.

Graphitization was performed on ~8-12 mg of carbonate samples using an automatic graphitization system fitted with a carbonate handling system (CHS-AGE, Ionplus) at the Laboratory for Ion Beam Physics (LIP) at ETH Zurich. The sample $^{14}C$ content was then measured using accelerator mass spectrometry (AMS) at LIP (MICADAS, Ionplus). The normalizing standard was Oxalic acid II (NIST SRM 4990C), measured to a precision better than 2‰. We used IAEA-C1 as a blank and IAEA-C2 and a modern coral standard as secondary standards. The procedural blank was established using a $^{14}C$-free stalagmite (MAW-1, ~170 Kyr old).

### 6.2.3 Laser ablation

Trace element concentrations were measured using a prototype RESOlution M-50 excimer (193 nm) laser-ablation system with two-volume laser-ablation cell coupled to an Agilent 7500ce/cs quadrupole ICPMS at Royal Holloway University, London. Full description of the analytical setup, as well as initial performance metrics can be found in Müller et al. (2009).

Ablation tracks were measured using a 140 by 10µm rectangular laser slit across 50mm sectioned blocks of BER-SWI-13, all tracks were pre-ablated to remove any superficial contamination. Stalagmite sectioning was done at an angle slightly off perpendicular to

growth direction to allow for overlap between sectioned blocks and subsequent combination of transect data without missing data between sections. A 15Hz repetition rate of a 90mJ laser spot and a stage scan speed of 10µm $s^{-1}$ were used during the main track measurement. Speleothem analyses were bracketed by analyses of NIST 612, NIST 610, and MACS3 standards for quantification and quality control.

Data reduction was performed using the Iolite software package using NIST 610/612 standards for external standardisation (Paton et al., 2011). Calcium-43 was measured throughout the sample runs as an internal standard. MACS3 analyses were used for quality control.

## 6.3 Results

### 6.3.1 Age Model

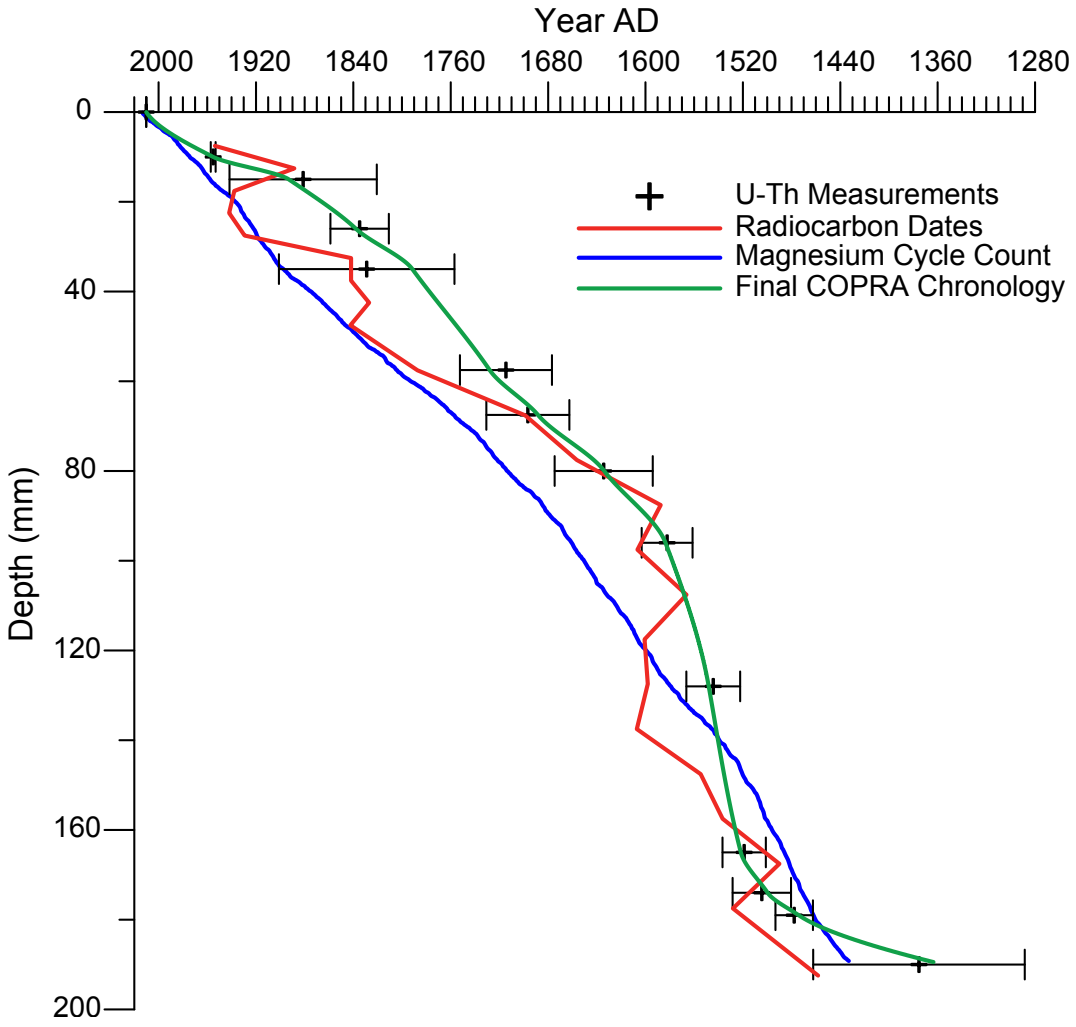


Figure 6.2: U-Th (black) and radiocarbon dates (with constant DCF correction to bomb spike) (red). Final COPRA generated age model (green) using U-Th points, radiocarbon bomb spike and date of collection. Magnesium cycle count (blue) shown for comparison (not used in final chronology).

The final age model for BER-SWI-13 was constructed using a combination of reliable U-Th dates (omitting any samples with problematic indications such as high detrital thorium content, or reversals), the radiocarbon bomb spike and the date of collection. An age-depth model was generated using COPRA (Breitenbach et al., 2012) and applied to the proxy measurements.

Two semi-independent chronologies are also shown in Figure 6.2 as cross-checks on the U-Th records. Radiocarbon dates show a good agreement with the COPRA generated age-depth model, albeit with some discrepancies and a general bias towards younger ages. This is presumably due to variations in the true dead carbon fraction (DCF) contribution to the stalagmite that differ from the generalized DCF correction applied to the data. This chronology is only semi-independent, since the radiocarbon bomb spike was used in the COPRA age model and DCF estimates were informed by the known dates, however, the similarity of growth rates and age model "shape" corroborate the U-Th age model well.

Preliminary cycle counts of the magnesium trace element dataset suggested an approximately annual cyclicity relative to estimated growth rates from early dates. However, magnesium cycles are not consistent throughout the record with cyclicity unclear or perhaps absent in some regions of the stalagmite. A subjective manual count of all cycles, including some equivocal cycles of similar length to clearer cycles, produces a cycle count chronology relative to collection date which is broadly similar to the radiocarbon and U-Th chronologies. However, the cycle count undercounts significantly, suggesting that identifiable magnesium cycles do not occur in all years of the record. This is particularly evident in the youngest part of the record, where the absolute date of collection and near absolute date of the radiocarbon bomb spike produces an extremely accurate chronology; in this section there is a cycle undercount of approximately 20 cycles. The magnesium cycle chronology therefore supports the growth rates of the U-Th age model, but cannot be used as an absolute chronology because cycles are either not consistently annual in length, or not consistently recorded.

### 6.3.2 Long Term Trace Element Trends

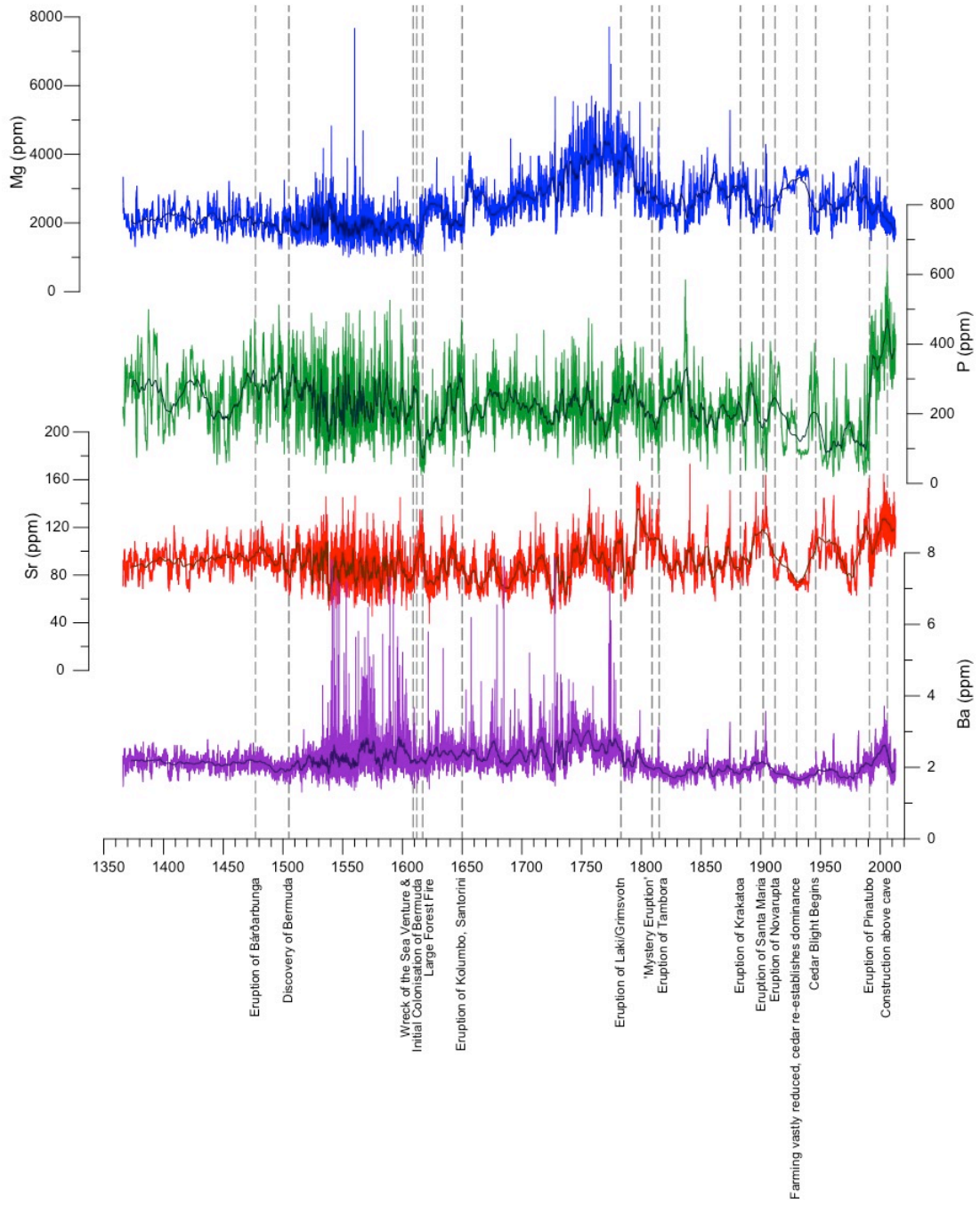


Figure 6.3: Full records of key trace elements: magnesium (blue), phosphorous (green), strontium (red), and barium (purple). Darker lines show 99 point running means of the data to highlight longer-term trends. Also shown are the timings of significant events that could potentially have influenced trace element concentrations in Bermudan cave dripwaters.

Magnesium concentrations in BER-SWI-13 are highly variable with approximately annual fluctuations of several hundred ppm about the long-term mean of ~2400ppm (Figure 6.3). Variability is highest between approximately 1500-1775, the latter part of this period also exhibiting a substantial increase in the longer-term baseline to almost 4000ppm. The record also shows variability on a multi-decadal timescale with clear long-term variations in the mean annual concentrations of several hundred ppm.

Phosphorous concentrations throughout the record fluctuate around a long-term mean of approximately 225ppm, with short-term fluctuations of plus or minus around 200ppm (Figure 6.3). This dataset appears to be relatively noisy, but has a few distinct anomalies such as a substantial decrease around 1610-1620AD, a general decrease in concentration and variability in the 20$^{th}$ century, and a marked increase to a new multi-year mean value of approximately 400ppm from 1990AD to the date of collection.

Strontium concentrations fluctuate about a mean value of approximately 90ppm throughout the record, with short-term fluctuations of plus or minus 20ppm throughout the record (Figure 6.3). Larger, longer-term fluctuations from the mean increase somewhat through time with shifts in long term mean of as much as 20-30ppm which persist for decades, appearing in the record from around 1800AD onwards.

Barium concentrations have a baseline value of approximately 2ppm, with occasional large short-lived spikes of several ppm throughout the record but most frequently between approximately 1500-1800AD (Figure 6.3). Baseline levels decrease very slightly from 1800AD onwards, with an associated fall in variability, but begin to increase again slightly between 1980AD and 2000AD.

Trace element concentrations in the stalagmite show no obvious correspondence with visible colour or density changes in the stalagmite, with the possible exception of the late 20$^{th}$ century where a whitening of the calcite corresponds to increases in P and Sr.

## 6.4 Discussion

### 6.4.1 Magnesium Variability

Magnesium concentrations in BER-SWI-13 display an apparently annual cyclicity throughout almost the entire record. However, magnesium annual cycles do not occur in every year of the record with a maximum count of approximately 580 cycles occurring in the 630 years of the record (Figure 6.2). This disparity may be partially due to the subjective nature of a manual cycle count, but the varying prominence of cycles suggests that magnesium cyclicity is the result of an annual (presumably seasonal) process which varies in amplitude throughout the record. Annual cycles may not occur in years with reduced seasonality, or may perhaps be disrupted intermittently by other processes overprinting the record.

Several seasonal environmental variables can influence trace element concentrations including temperature, rainfall, evapotranspiration, and anthropogenic factors. Temperature is generally only a factor where it influences cave ventilation or evaporation and is unlikely to be a factor in the case of Bermuda where temperature variations are not particularly extreme and cave ventilation is controlled by tidal action (Walczak, 2016) rather than temperature gradients as is the case in some caves (Ridley et al., 2015b). No significant seasonally varying anthropogenic factors affect the cave (e.g., seasonal tourist openings or agriculture). Rainfall amount in Bermuda does vary seasonally (Figure 6.1) and this is reflected by drip rates within the cave (Walczak, 2016). This suggests that variations in effective rainfall amount are the most likely candidate as a seasonal control on annually cyclical trace element variations.

Dripwater magnesium concentration variability (and resultant speleothem concentrations) is related to rainfall amount in numerous speleothem studies (Fairchild and Treble, 2009; Treble et al., 2003). Generally, the mechanism invoked to explain this is that of Prior Calcite Precipitation (Fairchild et al., 2001; Fairchild et al., 2000). The distribution coefficient for magnesium in calcite is less than one, suggesting that reduced calcite precipitation up-drip path from the stalagmite will result in lower concentrations of magnesium. In conditions of increased rainfall there is a reduced potential for calcite precipitation in the karst due to reduced opportunities for degassing, as well as potentially decreased residence times. Similarly, increased rainfall results in both increased dilution as well as reducing the potential for water-rock interactions. All three of these processes act to reduce magnesium concentrations in response to increased rainfall.

BER-SWI-13's seasonal magnesium cyclicity is difficult to link directly to rainfall with limited rainfall records to correlate against, and a chronology which, whilst reasonably precise on a multi-decadal scale, cannot reliably be used on an annual or subannual basis for comparison with weather station data. However, other processes that influence regional rainfall amounts over longer timescales can be linked to the record. The North Atlantic Oscillation, a fluctuation in sea level atmospheric pressure differential between the Icelandic low and the Azores high (sometimes referred to as the Bermuda-Azores high), which strongly influences climate variability throughout the North Atlantic basin, exerts a significant control on North Atlantic storm tracks. Positive NAO index winters are associated with north-eastward shifts in Atlantic storms reaching Europe, with negative NAO index winters exhibiting more southerly storm tracks. Proxy NAO reconstructions generally rely on localised reconstructions of either rainfall or temperature (generally in terrestrial and marine settings respectively) and extrapolating from good correlations with instrumental records of NAO index that the NAO is the dominant forcing of that climate record. Bermuda's position on the edge of the Gulf Stream suggests that local weather patterns may be sensitive to shifts in the NAO index.

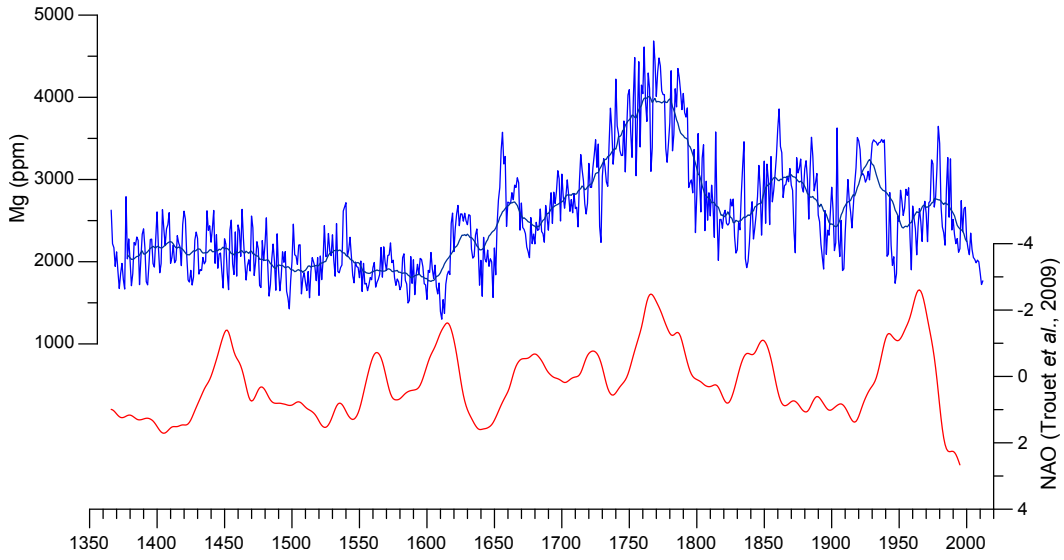


Figure 6.4: Magnesium (blue) plotted against the NAO index of Trouet et al. (2009)(red, flipped).

Annual mean magnesium concentrations in BER-SWI-13 anti-correlate with the NAO index reconstruction of Trouet et al. (2009) ($r = -0.33$, $p < 0.0001$). This suggests that when the

NAO is in a positive phase increased effective rainfall in Bermuda lowers magnesium concentrations in BER-SWI-13 (Figure 6.4).

Goodkin et al. (2008) used Sr/Ca variability in a Bermuda coral to reconstruct SSTs around Bermuda from 1781-1999, using this record to reconstruct NAO variability. Their results, when compared to previous NAO reconstructions, suggested that inter-annual variability in SSTs were correlated positively with NAO state but that multi-decadal variability correlated negatively with NAO state.

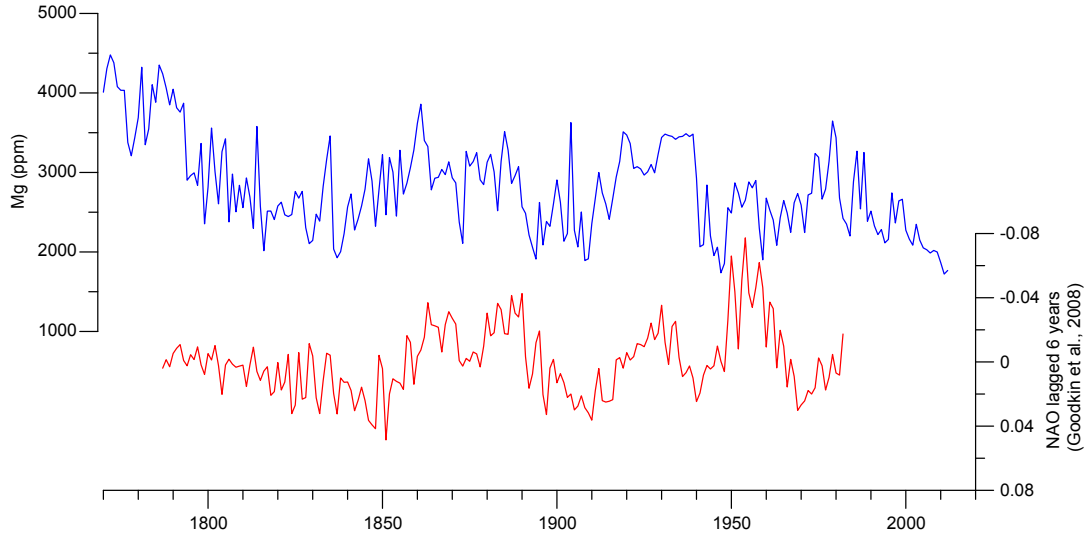


Figure 6.5: Magnesium (blue) plotted against the Sr/Ca derived NAO reconstruction of Goodkin et al. (2008), lagged by 6 years (red, flipped)

The magnesium record in BER-SWI-13 does show some broad similarities with the record of Goodkin et al. (2008). For the period of overlap between the records they are somewhat anticorrelated (Figure 6.5), although the best correlation occurs when the Goodkin et al. (2008) record is lagged by 6 years ($r = -0.213$, $p < 0.01$). This lag is within the overlap of uncertainties between the age models of the two records. This again suggests that during positive NAO states magnesium concentrations fall in BER-SWI-13, suggesting that positive NAO states lead to increased rainfall in Bermuda.

This is consistent with modelling results which suggest that positive NAO states correlate with increased jet stream strength (Woollings and Blackburn, 2012), and thus potentially increased rainfall over Bermuda. This is also consistent with locally increased SSTs as a result of positive NAO state as recorded by Goodkin et al. (2008).

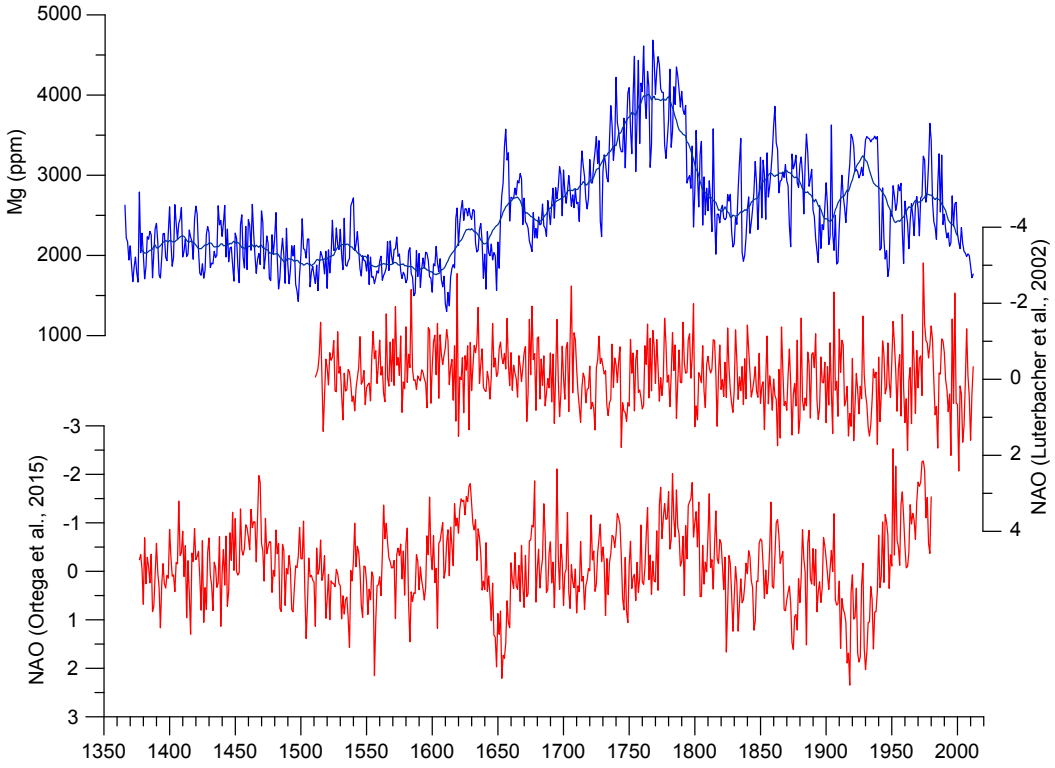


Figure 6.6: Mg (blue) plotted against the NAO reconstructions of Luterbacher et al. (2002) (red, flipped, top) and (Ortega et al., 2015) (red, flipped, bottom).

Other NAO reconstructions do not show clear correlations with the Mg record from this stalagmite (Figure 6.6). Neither the record of Luterbacher et al. (2002) (r = 0.05m p = 0.23), nor that of Ortega et al. (2015) (r = -0.08, p = 0.056) show clear correlations with magnesium in BER-SWI-13. The reasons for this are unclear, and may be primarily due to age model offsets. However, it may also be that the local record of Goodkin et al. (2008) and the longer term average of Trouet et al. (2009) better reflect that variations in NAO influencing this particular site.

### 6.4.2 Other Trace Elements

Neither strontium nor barium show annual correlations with either the NAO index of Trouet et al. (2009) or the local SST derived NAO record of Goodkin et al. (2008). This suggests that they are not controlled by the same climatic factors as the magnesium record, or perhaps that any climate derived signal is overprinted by other factors such as growth rate, competition effects or anthropogenic inputs. Indeed the largest variability in

the barium record occurs in the late 1500s, approximately coinciding with the highest growth rates of the stalagmite (Figure 6.2, Figure 6.3).

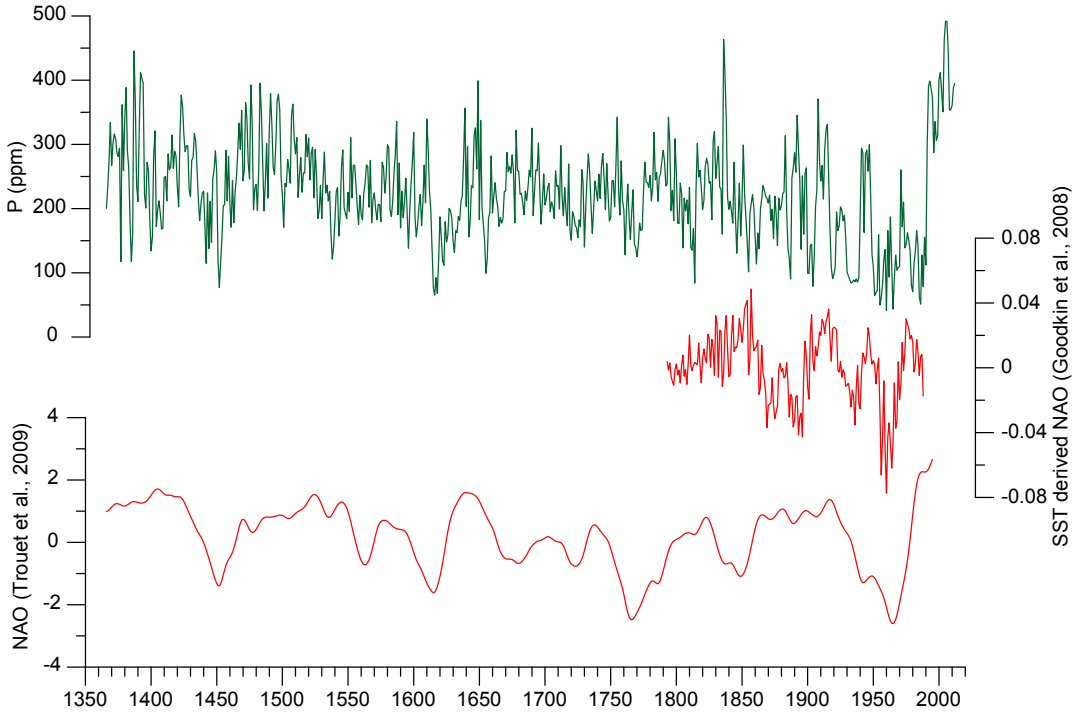


Figure 6.7: Comparison of mean annual phosphorous concentrations in BER-SWI-13 (green) with the NAO reconstructions of Goodkin et al. (2008) and Trouet et al. (2009) (red, top and bottom respectively).

Intriguingly, phosphorous exhibits a positive correlation with both the Trouet et al. (2009) NAO record ($r = 0.28$, $p < 0.0001$ ) and the Goodkin et al. (2008) record ($r = 0.28$, $p < 0.0001$) (Figure 6.7). Phosphorous is not commonly used as a climate proxy in stalagmite records, with comparatively few studies utilising the element. Several studies have documented the presence of phosphorous in dripwaters (e.g., Baldini et al. (2012)), and even identified seasonal cycles in the element (Borsato et al., 2007) that have been interpreted as seasonal flushing of colloidally transported material. Treble et al. (2003) demonstrated that in an Australian speleothem phosphorous correlated positively with rainfall, and attributed this to changes in soil moisture content influencing bioproductivity. This is consistent with the record of BER-SWI-13 where higher phosphorous concentrations correlate with positive NAO states and thus inferred locally increased rainfall. The area

above the cave is heavily vegetated and has been for most of the island's history, albeit with some changes due to deforestation and the cedar blight, suggesting that dripwater elemental concentrations may be susceptible to climate induced changes in bioproductivity.

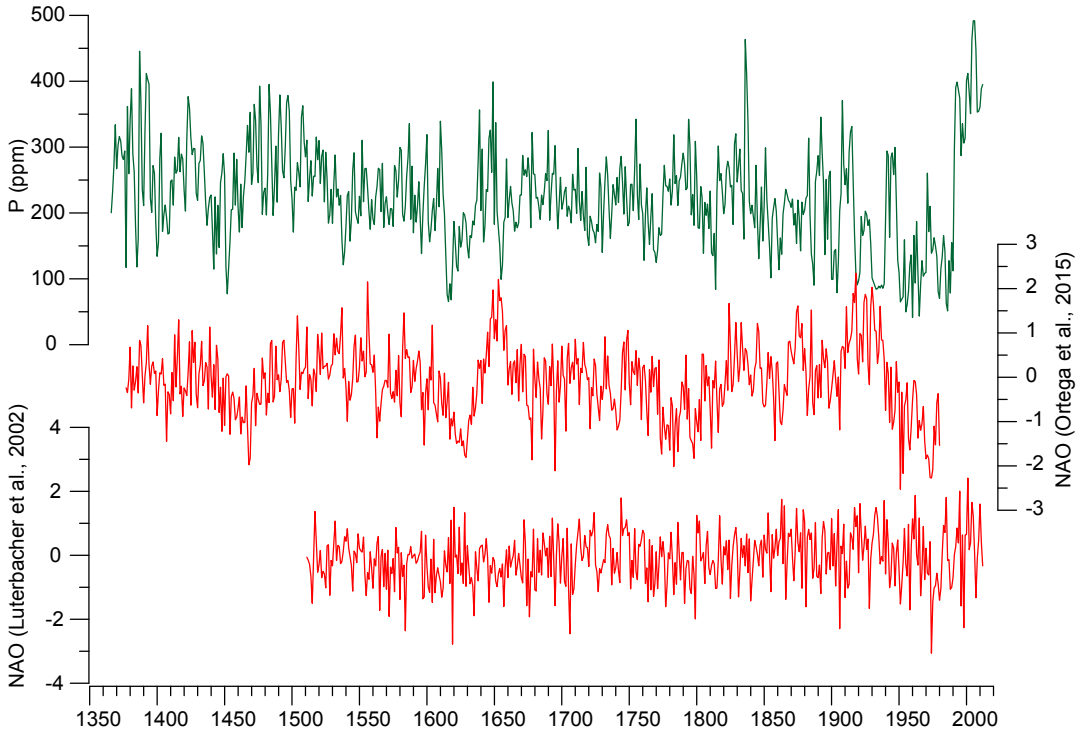


Figure 6.8: Comparison of mean annual phosphorous concentrations in BER-SWI-13 (green) with the NAO reconstructions of (Ortega et al., 2015) and (Luterbacher et al., 2002) (red, top and bottom respectively).

As with magnesium, this relationship is not seen as clearly in other NAO records (Figure 6.8). Phosphorous in BER-SWI-13 does not correlate with the NAO reconstruction of Luterbacher et al. (2002) ($r = 0.02$, $p = 0.61$). However, it does show a relationship with the reconstruction of Ortega et al. (2015), albeit a weaker one ($r = 0.15$, $p < 0.0001$).

### 6.4.3 Anthropogenic Influences

Bermuda has the 9th highest population density of any country or territory in the world, beaten only by a handful of other densely populated islands and city-states. As a result, anthropogenic influence on climate records derived from Bermudan archives is almost inevitable. Leamington cave is not an isolated cave that can be considered independent from human activity, but is a former show cave located near several residences and a road, which may influence the geochemistry of waters infiltrating the cave.

Notable natural or anthropogenic events, both global and local, which may influence trace element concentrations at the cave site, are plotted in Figure 6.3 alongside the high-resolution records of Mg, Sr, Ba and P in BER-SWI-13. These events include large volcanic eruptions, historical land use changes relating to the colonisation and development of Bermuda, as well as biological changes such as the cedar blight which dramatically altered the arboreal make up of Bermuda's vegetation (Bretz, 1960; Hearty and Vacher, 1994; Sterrer, 1998; Swinnerton, 1929).

Although the age model for BER-SWI-13 is likely very accurate, the precision on any particular date is at best +/- approximately 10 years. This is sufficient for confident comparison to long-term climate phenomena such as the NAO, however cannot be used to definitely link near point events (e.g., local anthropogenic disruptions) or short term events such as volcanic forcing (Ridley et al., 2015a) to individual fluctuations in trace element concentrations.

Some general inferences can be made based on longer-term trends in trace element data. In general, variability in Sr and Ba seems to be highest in the period following the discovery of Bermuda and then over time decreases back towards pre-discovery levels (Figure 6.3). Whether this can be attributed to human activity is debatable, as the island was only sporadically visited during this period, however the timing is suggestive. The discovery of Bermuda was the beginning of large-scale changes to the ecology of the island as large numbers of invasive species began to alter ecosystems (Sterrer, 1998). Other key events in the human history of the islands show surprisingly little impact on the trace element variations in BER-SWI-13. The early years of the colony (1609 onwards) would have been a time of great disruption on the island, with trees felled for lumber and planting, as well as fires and dramatic disruptions to the ecology of the island. However, this has surprisingly little apparent impact on trace element concentrations in BER-SWI-13 over this period. A prominent drop in phosphorous concentration does follow the initial colonisation, however

this drop appears to be the result of a significant negative NAO index at this time, resulting in reduced bioproductivity, rather than any anthropogenic factor. This holds true throughout the record, with even its use as a showcave in the 20th century and modern construction proximal to the cave in the 21st century having minimal apparent impact on trace element variation compared to that of broader climate influences. This is somewhat surprising, as several authors have documented trace element variations in speleothems in response to deforestation and ecosystem disruption in other areas. Borsato et al. (2007), for example, documented a marked increase in several trace elements in response to deforestation in the early 20th century above Grotta di Ernesto in NE Italy.

Whilst increased variability in speleothem trace elements, as well as an increased growth rate, is apparent shortly following the discovery of the island (post ~1500AD) it is unclear to what extent this is the result of anthropogenic influence. These changes predate the actual colonisation of the island, and it would seem unlikely that the changes would result from post-discovery visits when the 20th century use of the cave appears to have comparatively minimal effect. Whilst human influence cannot be ruled out, an anthropogenic cause for this variability and growth appears unlikely, particularly given that this variability subsides post-colonisation.

Large volcanic eruptions do not appear to have a significant effect on trace element concentrations in BER-SWI-13, either through a detectable volcanic ash component or through unambiguous climate forcing. Any effect on the cave site is indistinguishable from background variability due to being small in magnitude and uncertain in exact timing in the record. Furthermore, the cave's location away from either active volcanism or a major climatic transition zone implies that volcanic influences should be minimal.

In general it appears that Leamington cave is surprisingly resilient to anthropogenic influence on its dripwater chemistry despite being located in close proximity to a residential area. The cave itself is not directly overlain by any buildings and is located underneath vegetation, perhaps ensuring that dripwaters are relatively uncontaminated by human influence. In any case, the robust correlations of both phosphorous and magnesium to large-scale climate suggest that this speleothem records a fairly unmodified signal.

## 6.5 Conclusions

Trace elements in BER-SWI-13 appear to be faithful recorders of basin scale climate in the Atlantic. Two separate trace element systems, magnesium and phosphorous, are both correlated with changes in the North Atlantic Oscillation as recorded in both local (Goodkin et al., 2008) and basin (Trouet et al., 2009) scale reconstructions. We suggest that changes in effective rainfall to the cave influence magnesium concentrations in the stalagmite by means of a Prior Calcite Precipitation mechanism. Phosphorous variability is likely controlled by changes in bioproductivity in the soil or surface vegetation as a result of changes in rainfall and local temperatures.

These two semi-independent proxy systems demonstrate that hydroclimate in Bermuda has been strongly influenced by the North Atlantic Oscillation and its resultant effects on the strength and positioning of the North Atlantic drift. Positive NAO periods result in increased rainfall and local SSTs around Bermuda, noticeably influencing local rainfall and bioproductivity. The sensitivity of Bermudan speleothems to basin scale climate processes illustrates their potential use in extending our understanding of how the NAO responds to climate forcings over the last few thousand years and may prove to be a vital resource in developing models of NAO response to anthropogenic climate change.

# Chapter 7 Conclusions and Summary

# Chapter 7: Conclusions and Summary

## Summary

This thesis presents three high-resolution modern speleothem records from three Northern Hemisphere cave sites located in and around the Atlantic Basin. Each record utilises trace element proxies in different ways to reconstruct palaeoenvironmental information including volcanism, seasonal flushing of material, prior aragonite precipitation linked to variable rainfall, prior carbonate precipitation linked to basin scale climate variability, and bioproductivity changes results from same.

The aim of this thesis is primarily to further understanding of the various processes controlling trace element variability in speleothems. This includes developing methods of processing multi-proxy trace element data (Chapter 4), better constraining chemical processes which control trace element concentrations (Chapter 5), and highlight the manner in which multiple proxies can be used to reconstruct climate information via different mechanisms (Chapter 6).

This thesis was written as a series of papers, two of which have already been published (Jamieson et al., 2016; Jamieson et al., 2015) and one which is presented here in a currently unpublished form (Chapter 6). As such, each chapter has its own conclusions on the particular record and topic. This chapter summarises and consolidates the conclusions of each, as well as providing a brief overview of the contributions they provide to our overall understanding of speleothem science. Finally, some brief comments are made about potential future work leading on from the work presented herein.

## Main Conclusions

### On interpretation and analysis of trace element records

- PCA can simplify exploration of large laser ablation datasets, and is a valuable tool for identifying the dominant controls on stalagmite trace element chemistry. The technique can deconvolve the different modes of trace element variation and, when principal components are linked to physical processes or inputs, can produce time series of the shifting influence of those modes of variation. For a stalagmite where intermittent signals such as the addition of volcanic ash material are

recorded, this technique can clearly identify these discrete events within the record.

- The stalagmite ATM-7 from Actun Tunichil Muknal cave in central Belize records the occurrence of volcanic ash deposition over the cave site. The discovery of a volcanic ash deposition record in speleothems potentially adds tephrochronology to the stalagmite dating toolkit or, conversely, opens the door to using stalagmites to identify previously unknown or uncertainly dated eruptions.
- In stalagmite BER-SWI-13 two separate trace element systems, magnesium and phosphorous, are both correlated with changes in the North Atlantic Oscillation as recorded in both local and basin scale reconstructions. Changes in effective rainfall to the cave influence magnesium concentrations in the stalagmite by means of a Prior Calcite Precipitation mechanism, whilst phosphorous variability is likely controlled by changes in bioproductivity in the soil or surface vegetation as a result of changes in rainfall and local temperatures. The use of two separate proxy systems within a single archive increases the confidence of any climate interpretation, and underscores the value of multi-proxy stalagmite reconstructions.

### On aragonitic stalagmites and the chemistry of Prior Aragonite Precipitation

- We calculate a distribution coefficient of uranium in aragonitic speleothems of 3.74 ± 1.13, which is in agreement within error with the value derived by Wassenburg et al. (2016). We infer that prior aragonite precipitation results in lower U/Ca in speleothems.
- The unusually high temporal resolution of the YOK-G trace element record enables an examination of seasonal geochemical variations in aragonitic stalagmites and the development of a new proxy for rainfall. U/Ca hydrological variations occur on both intra- and inter-annual timescales, and are therefore useful for assessing seasonal changes in rainfall patterns. We demonstrate that U/Ca correlates with other rainfall proxies such as $\delta^{13}C$, can be linked to instrumental rainfall records, correlates with other climatic variables (e.g., NHT), and reflects previously inferred trends in Belizean paleo-rainfall. On inter-annual timescales U/Ca in YOK-G is a proxy for overall dryness in Belize, whilst the annual correlation or anti-correlation of U/Ca and $\delta^{13}C$ reflects changes in intra-annual rainfall seasonality.

### On large-scale climate variation in the speleothem record.

- In the Industrial Period (post-1850), $\delta^{13}C$ and U/Ca in stalagmite YOK-G both indicate a trend of overall drying and reduced seasonality. As outlined by Ridley et al. (2015a) these variables (annual means, peak wet values, peak dry values and seasonal differences of both proxies) all correlate with increasing Northern Hemisphere Temperature (NHT). Indeed U/Ca displays a stronger and more significant relationship with NHT over this period, perhaps suggesting that this proxy is even more sensitive to rainfall shifts than $\delta^{13}C$. This shift in both proxies towards drier and less seasonally variable conditions post-1850 supports the interpretation of Ridley et al. (2015a) that the northern maximum extent of the ITCZ has shifted southwards in response to increased anthropogenic sulphate aerosol emissions in the Northern Hemisphere and changing hemispheric temperature contrasts, consequently resulting in drier wet seasons in Belize and reduced hydrological seasonality.
- Hydroclimate in Bermuda has been strongly influenced by the North Atlantic Oscillation and its resultant effects on the strength and positioning of the North Atlantic drift. Positive NAO periods result in increased rainfall and local SSTs around Bermuda, noticeably influencing local rainfall and bioproductivity. The sensitivity of Bermudan speleothems to basin scale climate processes illustrates their potential use in extending our understanding of how the NAO responds to climate forcings over the last few thousand years and may prove to be a vital resource in developing models of NAO response to anthropogenic climate change.

## Future Work

Future studies should evaluate how transferable the technique of using PCA to isolate signals of volcanic ash deposition is to other sites with different environmental conditions where volcanic ashfall has occurred. Ideally sections of speleothems coinciding with historical eruptions can be used to validate the technique, and then older sections of the speleothem used to produce records of previously unknown or uncertain eruptions.

With greater understanding of the geochemical processes controlling trace element variation in environments depositing aragonitic speleothems it should now be possible to generate high quality palaeoenvironmental records from these environments. Aragonitic

speleothems, with their precise age controls, are ideal for this purpose as they minimise age uncertainty. This study presents a valuable new method for estimating paleo-rainfall in low-latitude regions where few high quality rainfall proxy archives are available. Future studies can expand on this technique by generating additional U/Ca records from aragonitic stalagmites. Additionally, the response of U/Ca as a PAP proxy could be further explored and documented using dripwater monitoring studies.

Very few climate reconstructions from Bermuda have been previously produced. This work and that of Walczak (2016) establish that Bermudan stalagmites can produce high quality climate records. The position of Bermuda with respect to the Gulf Stream, hurricane belts and the "centre of action" of the NAO suggests that it is an area sensitive to large scale climate variability in the Atlantic and worthy of further study to reconstruct Atlantic basin climate.

## Concluding Remarks

This thesis presents a selection of trace element tools and proxies for reconstructing recent palaeoenvironmental change. This area of research, which is often overlooked in favour of stable isotope ratios in speleothems, shows a great deal of promise for future development. This thesis demonstrates that there are still new trace element proxies being developed, as well as far greater potential for multi-proxy analyses to extract additional information from speleothem records in a variety of settings. The future of speleothem science is bright, with trace elements in particular displaying a wealth of future potential for both new proxies and the production of high quality palaeoenvironmental records. Several trace element proxies are now well developed, and our understanding sufficient to produce confident records of climate processes. These records have the potential to give unprecedented insight into climate processes at resolutions which have previously been unobtainable.

# Appendix 1: Other Associated Work

In the course of producing this thesis, I have also contributed data or participated in the production of several associated works. These, along with my contributions are summarised here:

## Lechleitner et al. (2016a)

This work presents a study of carbon cycling and controls on the stalagmite dead carbon fraction (DCF) at Yok Balum Cave. $^{14}C$, $\delta^{13}C$ and U/Ca measurements from stalagmite YOK-I are used in concert to examine the controls on DCF variability in this stalagmite, and examining the potential use of $\delta^{13}C$ and U/Ca to estimate the required DCF correction to speleothem radiocarbon measurements.

My contribution to this work was in the production and processing of trace element data, providing the 184 sample U/Ca record from YOK-I presented alongside the radiocarbon and stable isotope time series.

## Lechleitner et al. (2016b)

This work presents a novel approach for developing radiocarbon based chronologies for stalagmites. The model estimates average stalagmite growth rates from 14C ages, accounting for atmospheric 14C changes and produces a chronology relative to a known anchor point.

My contribution to this work was in the production and processing of trace element data, generating a high-resolution LA-ICP-MS dataset from stalagmite NIED08-05, Niedzwiedzia Cave, Poland. This data is used to evaluate the relationships between δ13C, Mg/Ca, and their relationship to dripwater degassing rate. Additionally, it is used to identify the likely position of a growth hiatus.

## Wassenburg et al. (2016)

This work presents a novel method for determining aragonite trace element distribution coefficients in stalagmites with calcite-aragonite transitions. It reports distribution coefficients for several elements, as well as a robust determination of their likely range of variability.

Appendix 1: Other Associated Work

This paper was produced in conjunction with Jamieson et al. (2016), and published together in an issue of Geochimica et Cosmochimica Acta. Together the two papers provide vital new insights into the behaviour of trace elements in aragonitic speleothems. My contribution to Wassenburg et al. (2016) primarily consisted of discussion of U/Ca behaviour, and the subsequent application of this knowledge to the use of U/Ca as a PAP proxy.

# Appendix 2: Data Appendices

Data appendices are not reproduced in printed form in this thesis, due to the challenge of printing large, multivariate laser ablation time series. Instead they are included as Microsoft Excel files on an associated CD-ROM.

## References

Abdi, H. and Williams, L.J. (2010) Principal component analysis. Wiley Interdisciplinary Reviews: Computational Statistics 2, 433-459.
Acker, J.G. and Leptoukh, G. (2007) Online Analysis Enhances Use of NASA Earth Science Data. EOS, Transactions, American Geophysical Union 88, 14-17.
Aliaga-Campuzano, M.P., Bernal, J.P., Briceno-Prieto, S.B., Perez-Arvizu, O. and Lounejeva, E. (2013) Direct analysis of lanthanides by ICPMS in calcium-rich water samples using a modular high-efficiency sample introduction system-membrane desolvator. Journal of Analytical Atomic Spectrometry 28, 1102-1109.
Allan, M., Fagel, N., Van Rampelbergh, M., Baldini, J., Riotte, J., Cheng, H., Edwards, R.L., Gillikin, D., Quinif, Y. and Verheyden, S. (2015) Lead concentrations and isotope ratios in speleothems as proxies for atmospheric metal pollution since the industrial revolution. Chemical Geology 401, 140-150.
Amiel, A.J., Miller, D.S. and Friedman, G.M. (1973) Incorporation of uranium in modern corals. Sedimentology 20, 523-528.
Antuña, J.C. (1996) Lidar measurements of stratospheric aerosols from Mount Pinatubo at Camaguey, Cuba. Atmospheric Environment 30, 1857-1860.
Badertscher, S., Borsato, A., Frisia, S., Cheng, H., Edwards, R.L., Tüysüz, O. and Fleitmann, D. (2014) Speleothems as sensitive recorders of volcanic eruptions – the Bronze Age Minoan eruption recorded in a stalagmite from Turkey. Earth and Planetary Science Letters 392, 58-66.
Baker, A. and Bradley, C. (2010) Modern stalagmite δ18O: Instrumental calibration and forward modelling. Global and Planetary Change 71, 201-206.
Baker, A., Smart, P.L., Barnes, W.L., Edwards, R.L. and Farrant, A. (1995) The Hekla 3 volcanic eruption recorded in a Scottish speleothem? The Holocene 5, 336-342.
Baker, A., Smith, C.L., Jex, C.N., Fairchild, I.J., Genty, D. and Fuller, L. (2008) Annually Laminated Speleothems: a Review. International Journal of Speleology 37, 193-206.
Baker, A.J., Mattey, D.P. and Baldini, J.U.L. (2014) Reconstructing modern stalagmite growth from cave monitoring, local meteorology, and experimental measurements of dripwater films. Earth and Planetary Science Letters 392, 239-249.
Baldini, J., McDermott, F., Baker, A., Baldini, L., Mattey, D. and Railsback, L. (2005) Biomass effects on stalagmite growth and isotope ratios: A 20th century analogue from Wiltshire, England. Earth and Planetary Science Letters 240, 486-494.
Baldini, J.U.L., McDermott, F., Baldini, L.M., Ottley, C.J., Linge, K.L., Clipson, N. and Jarvis, K.E. (2012) Identifying short-term and seasonal trends in cave drip water trace element concentrations based on a daily-scale automatically collected drip water dataset. Chemical Geology 330, 1-16.
Baldini, J.U.L., McDermott, F. and Fairchild, I.J. (2002) Structure of the 8,200-Year Cold Event Revealed by a Speleothem Trace Element Record. Science 296.
Baldini, L.M., McDermott, F., Baldini, J.U.L., Arias, P., Cueto, M., Fairchild, I.J., Hoffmann, D.L., Mattey, D.P., Müller, W., Nita, D.C., Ontañón, R., Garciá-Moncó, C. and Richards, D.A. (2015) Regional temperature, atmospheric circulation, and sea-ice variability within the Younger Dryas Event constrained using a speleothem from northern Iberia. Earth and Planetary Science Letters 419, 101-110.
Barats, A., Pecheyran, C., Amouroux, D., Dubascoux, S., Chauvaud, L. and Donard, O.F. (2007) Matrix-matched quantitative analysis of trace-elements in calcium carbonate shells

by laser-ablation ICP-MS: application to the determination of daily scale profiles in scallop shell (Pecten maximus). Anal Bioanal Chem 387, 1131-1140.
Barker, S., Cacho, I., Benway, H. and Tachikawa, K. (2005) Planktonic foraminiferal Mg/Ca as a proxy for past oceanic temperatures: a methodological overview and data compilation for the Last Glacial Maximum. Quaternary Science Reviews 24, 821-834.
Bernal, J.P., Cruz, F.W., Stríkis, N.M., Wang, X., Deininger, M., Catunda, M.C.A., Ortega-Obregón, C., Cheng, H., Edwards, R.L. and Auler, A.S. (2016) High-resolution Holocene South American monsoon history recorded by a speleothem from Botuverá Cave, Brazil. Earth and Planetary Science Letters 450, 186-196.
Blaauw, M. (2012) Out of tune: the dangers of aligning proxy archives. Quaternary Science Reviews 36, 38-49.
Blyth, A.J., Baker, A., Collins, M.J., Penkman, K.E.H., Gilmour, M.A., Moss, J.S., Genty, D. and Drysdale, R.N. (2008) Molecular organic matter in speleothems and its potential as an environmental proxy. Quaternary Science Reviews 27, 905-921.
Blyth, A.J., Hartland, A. and Baker, A. (2016) Organic proxies in speleothems – New developments, advantages and limitations. Quaternary Science Reviews 149, 1-17.
Borsato, A., Frisia, S., Fairchild, I.J., Somogyi, A. and Susini, J. (2007) Trace element distribution in annual stalagmite laminae mapped by micrometer-resolution X-ray fluorescence: implications for incorporation of environmentally significant species. Geochimica et Cosmochimica Acta 71, 1494-1512.
Borsato, A., Frisia, S., Wynn, P.M., Fairchild, I.J. and Miorandi, R. (2015) Sulphate concentration in cave dripwater and speleothems: long-term trends and overview of its significance as proxy for environmental processes and climate changes. Quaternary Science Reviews 127, 48-60.
Borsato, A., Johnston, V.E., Frisia, S., Miorandi, R. and Corradini, F. (2016) Temperature and altitudinal influence on karst dripwater chemistry: Implications for regional-scale palaeoclimate reconstructions from speleothems. Geochimica et Cosmochimica Acta 177, 275-297.
Bourdin, C., Douville, E. and Genty, D. (2011) Alkaline-earth metal and rare-earth element incorporation control by ionic radius and growth rate on a stalagmite from the Chauvet Cave, Southeastern France. Chemical Geology 290, 1-11.
Box, G.E. and Draper, N.R. (1987) Empirical model-building and response surfaces. Wiley New York.
Brasier, A.T. (2011) Searching for travertines, calcretes and speleothems in deep time: Processes, appearances, predictions and the impact of plants. Earth-Science Reviews 104, 213-239.
Breitenbach, S.F.M., Rehfeld, K., Goswami, B., Baldini, J.U.L., Ridley, H.E., Kennett, D.J., Prufer, K.M., Aquino, V.V., Asmerom, Y., Polyak, V.J., Cheng, H., Kurths, J. and Marwan, N. (2012) COnstructing Proxy Records from Age models (COPRA). Climate of the Past 8, 1765-1779.
Bretz, J.H. (1960) Bermuda - a Partially Drowned, Late Mature, Pleistocene Karst. Geological Society of America Bulletin 71, 1729-1754.
Buckles, J. and Rowe, H.D. (2016) Development and optimization of microbeam X-ray fluorescence analysis of Sr in speleothems. Chemical Geology 426, 28-32.
Busenburg, E. and Plummer, L.N. (1985) Kinetic and thermodynamic factors controlling the distribution of SO4^2- and Na^+ in calcites and selected aragonites. Geochimica et Cosmochimica Acta 49, 713-725.
Carn, S.A., Krueger, A.J., Bluth, G.J.S., Schaefer, S.J., Krotkov, N.A., Watson, I.M. and Datta, S. (2003) Volcanic eruption detection by the Total Ozone Mapping Spectrometer (TOMS) instruments: a 22-year record of sulphur dioxide and ash emissions. Geological Society, London, Special Publications 213, 177-202.

Cole, P.D., Fernandez, E., Duarte, E. and Duncan, A.M. (2005) Explosive activity and generation mechanisms of pyroclastic flows at Arenal volcano, Costa Rica between 1987 and 2001. Bulletin of Volcanology 67, 695-716.
Condomines, M. and Rihs, S. (2006) First 226Ra–210Pb dating of a young speleothem. Earth and Planetary Science Letters 250, 4-10.
Crowell, B. and White, W. (2012) Measurement of luminescent banding in speleothems: some techniques and limitations. International Journal of Speleology 41, 51-58.
Cruz Jr., F.W., Burns, S.J., Jercinovic, M., Karmann, I., Sharp, W.D. and Vuille, M. (2007) Evidence of rainfall variations in Southern Brazil from trace element ratios (Mg/Ca and Sr/Ca) in a Late Pleistocene stalagmite. Geochimica et Cosmochimica Acta 71, 2250-2263.
Czaja, A. and Frankignoul, C. (2002) Observed Impact of Atlantic SST Anomalies on the North Atlantic Oscillation. Journal of Climate 15, 606-623.
Day, C.C. and Henderson, G.M. (2013) Controls on trace-element partitioning in cave-analogue calcite. Geochimica et Cosmochimica Acta 120, 612-627.
DeCarlo, T.M., Gaetani, G.A., Holcomb, M. and Cohen, A.L. (2015) Experimental determination of factors controlling U/Ca of aragonite precipitated from seawater: Implications for interpreting coral skeleton. Geochimica et Cosmochimica Acta 162, 151-165.
Denniston, R.F., Wyrwoll, K.-H., Polyak, V.J., Brown, J.R., Asmerom, Y., Wanamaker Jr, A.D., LaPointe, Z., Ellerbroek, R., Barthelmes, M., Cleary, D., Cugley, J., Woods, D. and Humphreys, W.F. (2013) A Stalagmite record of Holocene Indonesian–Australian summer monsoon variability from the Australian tropics. Quaternary Science Reviews 78, 155-168.
Draxler, R.R. and Rolph, G.D. (2003) HYSPLIT (HYbrid Single-Particle Lagrangian Integrated Trajectory) Model NOAA Air Resources Laboratory, Silver Spring, MD.
Dredge, J., Fairchild, I.J., Harrison, R.M., Fernandez-Cortes, A., Sanchez-Moral, S., Jurado, V., Gunn, J., Smith, A., Spötl, C., Mattey, D., Wynn, P.M. and Grassineau, N. (2013) Cave aerosols: distribution and contribution to speleothem geochemistry. Quaternary Science Reviews 63, 23-41.
Eiler, J.M. (2011) Paleoclimate reconstruction using carbonate clumped isotope thermometry. Quaternary Science Reviews 30, 3575-3588.
El-Farhan, Y.H., Denovio, N.M., Herman, J.S. and Hornberger, G.M. (2000) Mobilization and Transport of Soil Particles during Infiltration Experiments in an Agricultural Field, Shenandoah Valley, Virginia. Environmental Science and Technology 34, 3555-3559.
Esper, J., Cook, E.R. and Schweingruber, F.H. (2002) Low-Frequency Signals in Long Tree-Ring Chronologies for Reconstructing Past Temperature Variability. Science 295, 2250-2253.
Etiégni, L. and Campbell, A.G. (1991) Physical and chemical characteristics of wood ash. Bioresource Technology 37, 173-178.
Fairchild, I.J. and Baker, A. (2012) Speleothem Science: From Process to Past Environments, First Edition ed. Blackwell Publishing Ltd.
Fairchild, I.J., Baker, A., Borsato, A., Frisia, S., Hinton, R.W., McDermott, F. and Tooth, A.F. (2001) Annual to sub-annual resolution of multiple trace-element trends in speleothems. Journal of the Geological Society 158, 831-841.
Fairchild, I.J., Borsato, A., Tooth, A.F., Frisia, S., Hawkesworth, C.J., Huang, Y., McDermott, F. and Spiro, B. (2000) Controls on trace element (Sr–Mg) compositions of carbonate cave waters: implications for speleothem climatic records. Chemical Geology 166, 255-269.
Fairchild, I.J., Smith, C.L., Baker, A., Fuller, L., Spötl, C., Mattey, D., McDermott, F. and E.I.M.F (2006a) Modification and preservation of environmental signals in speleothems. Earth-Science Reviews 75, 105-153.
Fairchild, I.J., Spotl, C., Frisia, S., Borsato, A., Susini, J., Wynn, P.M. and Cauzid, J. (2010) Petrology and geochemistry of annually laminated stalagmites from an Alpine cave (Obir,

Austria): seasonal cave physiology. Geological Society, London, Special Publications 336, 295-321.
Fairchild, I.J. and Treble, P.C. (2009) Trace elements in speleothems as recorders of environmental change. Quaternary Science Reviews 28, 449-468.
Fairchild, I.J., Tuckwell, G.W., Baker, A. and Tooth, A.F. (2006b) Modelling of dripwater hydrology and hydrogeochemistry in a weakly karstified aquifer (Bath, UK): Implications for climate change studies. Journal of Hydrology 321, 213-231.
Finch, A.A., Shaw, P.A., Holmgren, K. and Lee-Thorp, J. (2003) Corroborated rainfall records from aragonitic stalagmites. Earth and Planetary Science Letters 215, 265-273.
Flor, T.H. and Moore, W.S. (1977) Radium/calcium and uranium/calcium determinations for western Atlantic reef corals, Proc 3rd Int Coral Reef Symp, pp. 555-561.
Frappier, A., Knutson, T., Liu, K.B. and Emanuel, K. (2007a) Perspective: coordinating paleoclimate research on tropical cyclones with hurricane-climate theory and modelling. Tellus A 59, 529-537.
Frappier, A., Sahagian, D., Gonzalez, L.A. and Carpenter, S.J. (2002) El Nino events recorded by stalagmite carbon isotopes. Science 298, 565-565.
Frappier, A.B. (2006) Empirical orthogonal function analysis of multivariate stalagmite trace element data: Detecting the 1982 El Chichón volcanic eruption. Archives of Climate Change in Karst, Karst Waters Institute Special Publication 10, 113-115.
Frappier, A.B. (2008) A stepwise screening system to select storm-sensitive stalagmites: Taking a targeted approach to speleothem sampling methodology. Quaternary International 187, 25-39.
Frappier, A.B. (2013) Masking of interannual climate proxy signals by residual tropical cyclone rainwater: Evidence and challenges for low-latitude speleothem paleoclimatology. Geochemistry, Geophysics, Geosystems 14, 3632-3647.
Frappier, A.B., Sahagian, D., Carpenter, S.J., González, L.A. and Frappier, B.R. (2007b) Stalagmite stable isotope record of recent tropical cyclone events. Geology 35, 111.
Friedman, G.M. (1968) Geology and geochemistry of reefs, carbonate sediments, and waters, Gulf of Aqaba (Elat), Red Sea. Journal of Sedimentary Research 38, 895-919.
Friedrich, W.L., Kromer, B., Friedrich, M., Heinemeier, J., Pfeiffer, T. and Talamo, S. (2006) Santorini Eruption Radiocarbon Dated to 1627–1600 B.C. Science 312, 548.
Frisia, S. (2015) Microstratigraphic logging of calcite fabrics in speleothems as tool for palaeoclimate studies. International Journal of Speleology 44.
Frisia, S., Borsato, A., Fairchild, I.J. and Susini, J. (2005) Variations in atmospheric sulphate recorded in stalagmites by synchrotron micro-XRF and XANES analyses. Earth and Planetary Science Letters 235, 729-740.
Frisia, S., Borsato, A. and Susini, J. (2008) Synchrotron radiation applications to past volcanism archived in speleothems: An overview. Journal of Volcanology and Geothermal Research 177, 96-100.
Frumkin, A. and Stein, M. (2004) The Sahara–East Mediterranean dust and climate connection revealed by strontium and uranium isotopes in a Jerusalem speleothem. Earth and Planetary Science Letters 217, 451-464.
Gabitov, R.I., Gaetani, G.A., Watson, E.B., Cohen, A.L. and Ehrlich, H.L. (2008) Experimental determination of growth rate effect on U6+ and Mg2+ partitioning between aragonite and fluid at elevated U6+ concentration. Geochimica et Cosmochimica Acta 72, 4058-4068.
Gabitov, R.I., Sadekov, A. and Leinweber, A. (2014) Crystal growth rate effect on Mg/Ca and Sr/Ca partitioning between calcite and fluid: An in situ approach. Chemical Geology 367, 70-82.
Gaetani, G.A. and Cohen, A.L. (2006) Element partitioning during precipitation of aragonite from seawater: A framework for understanding paleoproxies. Geochimica et Cosmochimica Acta 70, 4617-4634.

Garnett, E.R., Andrews, J.E., Preece, R.C. and Dennis, P.F. (2004) Climatic change recorded by stable isotopes and trace elements in a British Holocene tufa. Journal of Quaternary Science 19, 251-262.
Genty, D., Labuhn, I., Hoffmann, G., Danis, P.A., Mestre, O., Bourges, F., Wainer, K., Massault, M., Régnier, E., Orengo, P., Falourd, S. and Minster, B. (2014) Rainfall and cave water isotopic relationships in two South-France sites. Geochimica et Cosmochimica Acta.
Goodkin, N.F., Hughen, K.A., Doney, S.C. and Curry, W.B. (2008) Increased multidecadal variability of the North Atlantic Oscillation since 1781. Nature Geoscience 1, 844-848.
Green, H., Pickering, R., Drysdale, R., Johnson, B.C., Hellstrom, J. and Wallace, M. (2015) Evidence for global teleconnections in a late Pleistocene speleothem record of water balance and vegetation change at Sudwala Cave, South Africa. Quaternary Science Reviews 110, 114-130.
Griffiths, M.L., Drysdale, R.N., Gagan, M.K., Frisia, S., Zhao, J.-x., Ayliffe, L.K., Hantoro, W.S., Hellstrom, J.C., Fischer, M.J., Feng, Y.-X. and Suwargadi, B.W. (2010) Evidence for Holocene changes in Australian–Indonesian monsoon rainfall from stalagmite trace element and stable isotope ratios. Earth and Planetary Science Letters 292, 27-38.
Gvirtzman, G., Friedman, G.M. and Miller, D.S. (1973) Control and distribution of uranium in coral reefs during diagenesis. Journal of Sedimentary Research 43, 985-997.
Hartland, A., Fairchild, I.J., Lead, J.R., Borsato, A., Baker, A., Frisia, S. and Baalousha, M. (2012) From soil to cave: Transport of trace metals by natural organic matter in karst dripwaters. Chemical Geology 304-305, 68-82.
Hartland, A., Fairchild, I.J., Müller, W. and Dominguez-Villar, D. (2013) Preservation of NOM-metal complexes in a modern hyperalkaline stalagmite: implications for speleothem trace element geochemistry. Geochimica et Cosmochimica Acta.
Hartmann, J. and Moosdorf, N. (2012) The new global lithological map database GLiM: A representation of rock properties at the Earth surface. Geochemistry, Geophysics, Geosystems 13, n/a-n/a.
Hearty, P.J. and Vacher, H.L. (1994) Quaternary stratigraphy of Bermuda: a high-resolution pre-Sangamonian rock record. Quaternary Science Reviews 13, 685-697.
Holland, H.D., Kirsipu, T.V., Huebner, J.S. and Oxburgh, U.M. (1964) On Some Aspects of the Chemical Evolution of Cave Waters. The Journal of Geology 72, 36-67.
Hollingsworth, E. (2009) Karst Regions of the World (KROW)---Populating Global Karst Datasets and Generating Maps to Advance the Understanding of Karst Occurrence and Protection of Karst Species and Habitats Worldwide. ProQuest.
Hori, M., Ishikawa, T., Nagaishi, K., Lin, K., Wang, B.-S., You, C.-F., Shen, C.-C. and Kano, A. (2013) Prior calcite precipitation and source mixing process influence Sr/Ca, Ba/Ca and 87Sr/86Sr of a stalagmite developed in southwestern Japan during 18.0-4.5 ka. Chemical Geology.
Huang, Y. and Fairchild, I.J. (2001) Partitioning of Sr2+ and Mg2+ into calcite under karst-analogue experimental conditions. Geochimica et Cosmochimica Acta 65, 47-62.
IPCC (2013a) Climate Change 2013: The Physical Science Basis. Contribution of Working Group I to the Fifth Assessment Report of the Intergovernmental Panel on Climate Change. Cambridge University Press, Cambridge, UK.
IPCC (2013b) Summary for Policymakers, in: Stocker, T.F., Qin, D., Plattner, G.-K., Tignor, M., Allen, S.K., Boschung, J., Nauels, A., Xia, Y., Bex, V., Midgley, P.M. (Eds.), Climate Change 2013: The Physical Science Basis. Contribution of Working Group I to the Fifth Assessment Report of the Intergovernmental Panel on Climate Change. Cambridge University Press, Cambridge, UK.
Jamieson, R.A., Baldini, J.U.L., Brett, M.J., Taylor, J., Ridley, H.E., Ottley, C.J., Prufer, K.M., Wassenburg, J.A., Scholz, D. and Breitenbach, S.F.M. (2016) Intra- and inter-annual uranium concentration variability in a Belizean stalagmite controlled by prior aragonite

precipitation: A new tool for reconstructing hydro-climate using aragonitic speleothems. Geochimica et Cosmochimica Acta.
Jamieson, R.A., Baldini, J.U.L., Frappier, A.B. and Müller, W. (2015) Volcanic ash fall events identified using principal component analysis of a high-resolution speleothem trace element dataset. Earth and Planetary Science Letters 426, 36-45.
Jo, K.-n., Woo, K.S., Hong, G.H., Kim, S.H. and Suk, B.C. (2010) Rainfall and hydrological controls on speleothem geochemistry during climatic events (droughts and typhoons): An example from Seopdong Cave, Republic of Korea. Earth and Planetary Science Letters 295, 441-450.
Johnson, K.R., Hu, C., Belshaw, N.S. and Henderson, G.M. (2006) Seasonal trace-element and stable-isotope variations in a Chinese speleothem: The potential for high-resolution paleomonsoon reconstruction. Earth and Planetary Science Letters 244, 394-407.
Jouzel, J., Masson-Delmotte, V., Cattani, O., Dreyfus, G., Falourd, S., Hoffmann, G., Minster, B., Nouet, J., Barnola, J.M., Chappellaz, J., Fischer, H., Gallet, J.C., Johnsen, S., Leuenberger, M., Loulergue, L., Luethi, D., Oerter, H., Parrenin, F., Raisbeck, G., Raynaud, D., Schilt, A., Schwander, J., Selmo, E., Souchez, R., Spahni, R., Stauffer, B., Steffensen, J.P., Stenni, B., Stocker, T.F., Tison, J.L., Werner, M. and Wolff, E.W. (2007) Orbital and Millennial Antarctic Climate Variability over the Past 800,000 Years. Science 317, 793-796.
Kennett, D.J., Breitenbach, S.F., Aquino, V.V., Asmerom, Y., Awe, J., Baldini, J.U., Bartlein, P., Culleton, B.J., Ebert, C., Jazwa, C., Macri, M.J., Marwan, N., Polyak, V., Prufer, K.M., Ridley, H.E., Sodemann, H., Winterhalder, B. and Haug, G.H. (2012) Development and disintegration of Maya political systems in response to climate change. Science 338, 788-791.
Krueger, A., Krotkov, N. and Carn, S. (2008) El Chichon: The genesis of volcanic sulfur dioxide monitoring from space. Journal of Volcanology and Geothermal Research 175, 408-414.
Lachniet, M.S. (2009) Climatic and environmental controls on speleothem oxygen-isotope values. Quaternary Science Reviews 28, 412-432.
Lambert, W.J. and Aharon, P. (2011) Controls on dissolved inorganic carbon and δ13C in cave waters from DeSoto Caverns: Implications for speleothem δ13C assessments. Geochimica et Cosmochimica Acta 75, 753-768.
Lechleitner, F.A., Baldini, J.U., Breitenbach, S.F., Fohlmeister, J., McIntyre, C., Goswami, B., Jamieson, R.A., van der Voort, T.S., Prufer, K. and Marwan, N. (2016a) Hydrological and climatological controls on radiocarbon concentrations in a tropical stalagmite. Geochimica et Cosmochimica Acta 194, 233-252.
Lechleitner, F.A., Fohlmeister, J., McIntyre, C., Baldini, L.M., Jamieson, R.A., Hercman, H., Gąsiorowski, M., Pawlak, J., Stefaniak, K. and Socha, P. (2016b) A novel approach for construction of radiocarbon-based chronologies for speleothems. Quaternary Geochronology 35, 54-66.
Lorens, R.B. (1981) Sr, Cd, Mn and Co distribution coefficients in calcite as a function of calcite precipitation rate. Geochimica et Cosmochimica Acta 45, 553-561.
Luterbacher, J., Xoplaki, E., Dietrich, D., Jones, P.D., Davies, T.D., Portis, D., Gonzalez-Rouco, J.F., von Storch, H., Gyalistras, D., Casty, C. and Wanner, H. (2002) Extending North Atlantic oscillation reconstructions back to 1500. Atmospheric Science Letters 2, 114-124.
Lyons, J.J., Waite, G.P., Rose, W.I. and Chigna, G. (2009) Patterns in open vent, strombolian behavior at Fuego volcano, Guatemala, 2005–2007. Bulletin of Volcanology 72, 1-15.
Magaña, V., Amador, J.A. and Medina, S. (1999) The Midsummer Drought over Mexico and Central America. Journal of Climate 12, 1577-1588.
Mason, H.E., Frisia, S., Tang, Y., Reeder, R.J. and Phillips, B.L. (2007) Phosphorus speciation in calcite speleothems determined from solid-state NMR spectroscopy. Earth and Planetary Science Letters 254, 313-322.

Mathias, S.A., Skaggs, T.H., Quinn, S.A., Egan, S.N.C., Finch, L.E. and Oldham, C.D. (2015) A soil moisture accounting-procedure with a Richards' equation-based soil texture-dependent parameterization. Water Resources Research 51, 506-523.
MathWorks (2013) MATLAB and Statistics Toolbox Release 2013a. The MathWorks Inc., Natick, Massachusetts, United States.
Mayewski, P.A., Meeker, L.D., Whitlow, S., Twickler, M.S., Morrison, M.C., Bloomfield, P., Bond, G.C., Alley, R.B., Gow, A.J., Meese, D.A., Grootes, P.M., Ram, M., Taylor, K.C. and Wumkes, W. (1994) Changes in Atmospheric Circulation and Ocean Ice Cover over the North Atlantic During the Last 41,000 Years. Science 263, 1747-1751.
McDermott, F. (2004) Palaeo-climate reconstruction from stable isotope variations in speleothems: a review. Quaternary Science Reviews 23, 901-918.
McDermott, F., Frisia, S., Huang, Y., Longinelli, A., Spiro, B., Heaton, T.H.E., Hawkesworth, C.J., Borsato, A., Keppens, E., Fairchild, I.J., van der Borg, K., Verheyden, S. and Selmo, E. (1999) Holocene climate variability in Europe: Evidence from δ18O, textural and extension-rate variations in three speleothems. Quaternary Science Reviews 18, 1021-1038.
McDermott, F. and Hawkesworth, C. (1991) Th, Pb, and Sr isotope variations in young island arc volcanics and oceanic sediments. Earth and Planetary Science Letters 104, 1-15.
McDonald, J., Drysdale, R., Hill, D., Chisari, R. and Wong, H. (2007) The hydrochemical response of cave drip waters to sub-annual and inter-annual climate variability, Wombeyan Caves, SE Australia. Chemical Geology 244, 605-623.
McMillan, E.A., Fairchild, I.J., Frisia, S., Borsato, A. and McDermott, F. (2005) Annual trace element cycles in calcite–aragonite speleothems: evidence of drought in the western Mediterranean 1200–1100 yr BP. Journal of Quaternary Science 20, 423-433.
Medina-Elizalde, M. and Rohling, E.J. (2012) Collapse of Classic Maya civilization related to modest reduction in precipitation. Science 335, 956-959.
Meece, D.E. and Benninger, L.K. (1993) The coprecipitation of Pu and other radionuclides with CaC03. Geochimica et Cosmochimica Acta 57, 1447-1458.
Miller, T.E. (1996) Geologic and hydrologic controls on karst and cave development in Belize. Journal of Cave and Karst Studies 58, 100-120.
Mischel, S.A., Scholz, D., Spötl, C., Jochum, K.P., Schröder-Ritzrau, A. and Fiedler, S. (2016) Holocene climate variability in Central Germany and a potential link to the polar North Atlantic: A replicated record from three coeval speleothems. The Holocene.
Moseley, G.E., Edwards, R.L., Wendt, K.A., Cheng, H., Dublyansky, Y., Lu, Y., Boch, R. and Spotl, C. (2016) Reconciliation of the Devils Hole climate record with orbital forcing. Science 351, 165-168.
Mucci, A. and Morse, J.W. (1983) The incorporation of Mg2+ and Sr2+ into calcite overgrowths: influences of growth rate and solution composition. Geochimica et Cosmochimica Acta 47, 217-233.
Müller, W., Shelley, M., Miller, P. and Broude, S. (2009) Initial performance metrics of a new custom-designed ArF excimer LA-ICPMS system coupled to a two-volume laser-ablation cell. Journal of Analytical Atomic Spectrometry 24, 209.
Newhall, C.G. and Punongbayan, A.S. (1996) Fire and Mud: Eruptions and Lahars of Mount Pinatubo, Philippines. University of Washington Press, Seattle.
Newhall, C.G. and Self, S. (1982) The Volcanic Explosivity Index (VEI): An estimate of explosive magnitude for historical volcanism. Journal of Geophysical Research 87, 1231-1238.
Orland, I.J., Burstyn, Y., Bar-Matthews, M., Kozdon, R., Ayalon, A., Matthews, A. and Valley, J.W. (2014) Seasonal climate signals (1990–2008) in a modern Soreq Cave stalagmite as revealed by high-resolution geochemical analysis. Chemical Geology 363, 322-333.

Ortega, P., Lehner, F., Swingedouw, D., Masson-Delmotte, V., Raible, C.C., Casado, M. and Yiou, P. (2015) A model-tested North Atlantic Oscillation reconstruction for the past millennium. Nature 523, 71-74.
Paton, C., Hellstrom, J., Paul, B., Woodhead, J. and Hergt, J. (2011) Iolite: Freeware for the visualisation and processing of mass spectrometric data. Journal of Analytical Atomic Spectrometry 26, 2508.
Peppler, R.A., Bahrmann, C.P., Barnard, J.C., Campbell, J.R., Cheng, M.-D., Ferrare, R.A., Halthore, R.N., Heilman, L.A., Hlavka, D.L., Laulainen, N.S., Lin, C.-J., Ogren, J.A., Poellot, M.R., Remer, L.A., Sassen, K., Spinhirne, J.D., Splitt, M.E. and Turner, D.D. (2000) ARM Southern Great Plains Site Observations of the Smoke Pall Associated with the 1998 Central American Fires. Bulletin of the American Meteorological Society 81, 2563-2591.
Perrin, C., Prestimonaco, L., Servelle, G., Tilhac, R., Maury, M. and Cabrol, P. (2014) Aragonite-Calcite Speleothems: Identifying Original and Diagenetic Features. Journal of Sedimentary Research 84, 245-269.
Polag, D., Scholz, D., Mühlinghaus, C., Spötl, C., Schröder-Ritzrau, A., Segl, M. and Mangini, A. (2010) Stable isotope fractionation in speleothems: Laboratory experiments. Chemical Geology 279, 31-39.
Polzin, D., Guirola, L.G. and Hastenrath, S. (2014) Climatic variations in Central America: further exploration. International Journal of Climatology, n/a-n/a.
Pons-Branchu, E., Ayrault, S., Roy-Barman, M., Bordier, L., Borst, W., Branchu, P., Douville, E. and Dumont, E. (2015) Three centuries of heavy metal pollution in Paris (France) recorded by urban speleothems. Science of The Total Environment 518–519, 86-96.
Potsdam Institute for Climate Impact Research and Climate Analytics (2012) Turn Down the Heat: Why a 4C Warmer World Must be Avoided. International Bank for Reconstruction and Development / The World Bank, Washington.
Prins, E.M., Schmidt, C.C., Feltz, J.M., Reid, J.S., Westphal, D.L. and Richardson, K. (2003) A two-year analysis of fire activity in the western hemisphere as observed with the GOES wildfire automated biomass burning algorithm. American Meteorological Society Paper P2.28. Reprint #3298.
Proctor, C.J., Baker, A., Barnes, W.L. and Gilmour, R.A. (2000) A thousand year speleothem proxy record of North Atlantic climate from Scotland. Climate Dynamics 16, 815-820.
Railsback, L.B., Liang, F., Vidal Romaní, J.R., Grandal-d'Anglade, A., Vaqueiro Rodríguez, M., Santos Fidalgo, L., Fernández Mosquera, D., Cheng, H. and Edwards, R.L. (2011) Petrographic and isotopic evidence for Holocene long-term climate change and shorter-term environmental shifts from a stalagmite from the Serra do Courel of northwestern Spain, and implications for climatic history across Europe and the Mediterranean. Palaeogeography, Palaeoclimatology, Palaeoecology 305, 172-184.
Reed, N.M., Cairns, R.O., Hutton, R.C. and Takaku, Y. (1994) Characterization of polyatomic ion interferences in inductively coupled plasma mass spectrometry using a high resolution mass spectrometer. Journal of Analytical Atomic Spectrometry 9, 881.
Reeder, R.J., Nugent, M., Lamble, G.M., Tait, C.D. and Morris, D.E. (2000) Uranyl Incorporation into Calcite and Aragonite: XAFS and Luminescence Studies. Environmental Science & Technology 34, 638-644.
Reimer, P.J., Bard, E., Bayliss, A., Beck, J.W., Blackwell, P.G., Bronk Ramsey, C., Buck, C.E., Cheng, H., Edwards, R.L., Friedrich, M., Grootes, P.M., Guilderson, T.P., Haflidason, H., Hajdas, I., Hatté, C., Heaton, T.J., Hoffmann, D.L., Hogg, A.G., Hughen, K.A., Kaiser, K.F., Kromer, B., Manning, S.W., Niu, M., Reimer, R.W., Richards, D.A., Scott, E.M., Southon, J.R., Staff, R.A., Turney, C.S.M. and van der Plicht, J. (2013) IntCal13 and Marine13 Radiocarbon Age Calibration Curves 0–50,000 Years cal BP. Radiocarbon 55, 19.
Richards, D.A. and Andersen, M.B. (2013) Time Constraints and Tie-Points in the Quaternary Period. Elements 9, 45-51.

Ridley, H.E. (2014) Recent Central American and low latitude climate variability revealed using speleothem-based rainfall proxy records from Southern Belize, Department of Earth Sciences. Durham University, Durham.
Ridley, H.E., Asmerom, Y., Baldini, J.U.L., Breitenbach, S.F.M., Aquino, V.V., Prufer, K.M., Culleton, B.J., Polyak, V., Lechleitner, F.A., Kennett, D.J., Zhang, M.H., Marwan, N., Macpherson, C.G., Baldini, L.M., Xiao, T.Y., Peterkin, J.L., Awe, J. and Haug, G.H. (2015a) Aerosol forcing of the position of the intertropical convergence zone since AD 1550. Nature Geoscience 8, 195-200.
Ridley, H.E., Baldini, J.U.L., Prufer, K.M., Walczak, I.W. and Breitenbach, S.F.M. (2015b) High-resolution monitoring of Yok Balum Cave, Belize: An investigation of seasonal ventilation regimes and the atmospheric and drip-flow response to a local earthquake. Journal of Cave and Karst Studies 77, 183-199.
Riechelmann, S., Schröder-Ritzrau, A., Wassenburg, J.A., Schreuer, J., Richter, D.K., Riechelmann, D.F.C., Terente, M., Constantin, S., Mangini, A. and Immenhauser, A. (2014) Physicochemical characteristics of drip waters: Influence on mineralogy and crystal morphology of recent cave carbonate precipitates. Geochimica et Cosmochimica Acta.
Rolph, G.D. (2003) Real-time Environmental Applications and Display sYstem (READY) Website. NOAA Air Resources Laboratory, Silver Spring, MD. .
Rose, W.I. and Durant, A.J. (2008) El Chichón volcano, April 4, 1982: volcanic cloud history and fine ash fallout. Natural Hazards 51, 363-374.
Rutlidge, H., Baker, A., Marjo, C.E., Andersen, M.S., Graham, P.W., Cuthbert, M.O., Rau, G.C., Roshan, H., Markowska, M., Mariethoz, G. and Jex, C.N. (2014) Dripwater organic matter and trace element geochemistry in a semi-arid karst environment: Implications for speleothem paleoclimatology. Geochimica Et Cosmochimica Acta 135, 217-230.
Sackett, W. and Potratz, H. (1963) Dating of carbonate rocks by ionium-uranium ratios. Subsurface geology of Eniwetok Atoll 260, 1053-1065.
Schroeder, J.H., Miller, D.S. and Friedman, G.M. (1970) Uranium distributions in recent skeletal carbonates. Journal of Sedimentary Research 40, 672-681.
Sherwin, C.M. and Baldini, J.U.L. (2011) Cave air and hydrological controls on prior calcite precipitation and stalagmite growth rates: Implications for palaeoclimate reconstructions using speleothems. Geochimica et Cosmochimica Acta 75, 3915-3929.
Siklosy, Z., Kern, Z., Demeny, A., Pilet, S., Leel-Ossy, S., Lin, K., Shen, C.-C., Szeles, E. and Breitner, D. (2011) Speleothems and pine trees as sensitive indicators of environmental pollution – A case study of the effect of uranium-ore mining in Hungary. Applied Geochemistry 26, 666-678.
Sinclair, D.J., Banner, J.L., Taylor, F.W., Partin, J., Jenson, J., Mylroie, J., Goddard, E., Quinn, T., Jocson, J. and Miklavič, B. (2012) Magnesium and strontium systematics in tropical speleothems from the Western Pacific. Chemical Geology 294–295, 1-17.
Smith, C.L., Fairchild, I.J., Spötl, C., Frisia, S., Borsato, A., Moreton, S.G. and Wynn, P.M. (2009) Chronology building using objective identification of annual signals in trace element profiles of stalagmites. Quaternary Geochronology 4, 11-21.
Smithsonian (2014) Global Volcanism Program. Smithsonian Institution, http://volcano.si.edu/.
Spötl, C. and Mattey, D. (2006) Stable isotope microsampling of speleothems for palaeoenvironmental studies: A comparison of microdrill, micromill and laser ablation techniques. Chemical Geology 235, 48-58.
Sterrer, W. (1998) How many species are there in Bermuda? Bulletin of Marine Science 62, 809-840.
Stoll, H.M., Müller, W. and Prieto, M. (2012) I-STAL, a model for interpretation of Mg/Ca, Sr/Ca and Ba/Ca variations in speleothems and its forward and inverse application on seasonal to millennial scales. Geochemistry Geophysics Geosystems 13.

Swart, P.K. and Hubbard, J.A.E.B. (1982) Uranium in Scleractinian Coral Skeletons. Coral Reefs 1, 13-19.
Swinnerton, A.C. (1929) The Caves of Bermuda. Geological Magazine 66, 79-84.
Tan, L., Shen, C.-C., Cai, Y., Lo, L., Cheng, H. and An, Z. (2014) Trace-element variations in an annually layered stalagmite as recorders of climatic changes and anthropogenic pollution in Central China. Quaternary Research 81, 181-188.
Tan, L., Yi, L., Cai, Y., Shen, C.-C., Cheng, H. and An, Z. (2013) Quantitative temperature reconstruction based on growth rate of annually-layered stalagmite: a case study from central China. Quaternary Science Reviews 72, 137-145.
Thompson, G. and Livingston, H.D. (1970) Strontium and uranium concentrations in aragonite precipitated by some modern corals. Earth and Planetary Science Letters 8, 439-442.
Torres, O., Herman, J.R., Bhartia, P.K. and Ahmad, Z. (1995) Properties of Mount Pinatubo aerosols as derived from Nimbus 7 total ozone mapping spectrometer measurements. Journal of Geophysical Research 100, 14043-14045.
Treble, P., Shelley, J.M.G. and Chappell, J. (2003) Comparison of high resolution sub-annual records of trace elements in a modern (1911–1992) speleothem with instrumental climate data from southwest Australia. Earth and Planetary Science Letters 216, 141-153.
Treble, P.C., Fairchild, I.J., Griffiths, A., Baker, A., Meredith, K.T., Wood, A. and McGuire, E. (2015) Impacts of cave air ventilation and in-cave prior calcite precipitation on Golgotha Cave dripwater chemistry, southwest Australia. Quaternary Science Reviews 127, 61-72.
Tremaine, D.M. and Froelich, P.N. (2013) Speleothem trace element signatures: A hydrologic geochemical study of modern cave dripwaters and farmed calcite. Geochimica Et Cosmochimica Acta 121, 522-545.
Tremaine, D.M., Sinclair, D.J., Stoll, H.M., Lagerström, M., Carvajal, C.P. and Sherrell, R.M. (2016) A two-year automated dripwater chemistry study in a remote cave in the tropical south Pacific: Using [Cl−] as a conservative tracer for seasalt contribution of major cations. Geochimica et Cosmochimica Acta 184, 289-310.
Trouet, V., Esper, J., Graham, N.E., Baker, A., Scourse, J.D. and Frank, D.C. (2009) Persistent Positive North Atlantic Oscillation Mode Dominated the Medieval Climate Anomaly. Science 324, 78-80.
Uchida, S., Kurisaki, K., Ishihara, Y., Haraguchi, S., Yamanaka, T., Noto, M. and Yoshimura, K. (2013) Anthropogenic impact records of nature for past hundreds years extracted from stalagmites in caves found in the Nanatsugama Sandstone Formation, Saikai, Southwestern Japan. Chemical Geology.
Ünal-İmer, E., Shulmeister, J., Zhao, J.-X., Uysal, I.T. and Feng, Y.-X. (2016) High-resolution trace element and stable/radiogenic isotope profiles of late Pleistocene to Holocene speleothems from Dim Cave, SW Turkey. Palaeogeography, Palaeoclimatology, Palaeoecology 452, 68-79.
Vaks, A., Gutareva, O.S., Breitenbach, S.F., Avirmed, E., Mason, A.J., Thomas, A.L., Osinzev, A.V., Kononov, A.M. and Henderson, G.M. (2013) Speleothems reveal 500,000-year history of siberian permafrost. Science 340, 183-186.
Varekamp, J.C., Luhr, J.F. and Prestegaard, K.L. (1984) The 1982 eruptions of El Chichón Volcano (Chiapas, Mexico): Character of the eruptions, ash-fall deposits, and gasphase. Journal of Volcanology and Geothermal Research 23, 39-68.
Veeh, H.H. and Turekian, K.K. (1968) Cobalt, silver and uranium concentrations of reef building corals in the Pacific Ocean. Limnology and Oceanography 13, 304-308.
Verheyden, S., Keppens, E., Fairchild, I.J., McDermott, F. and Weis, D. (2000) Mg, Sr and Sr isotope geochemistry of a Belgian Holocene speleothem: implications for paleoclimate reconstructions. Chemical Geology 169, 131-144.

Vitousek, P.M. and Sanford, R.L. (1986) Nutrient Cycling in Moist Tropical Forest. Annu Rev Ecol Syst 17, 137-167.
Walczak, I. (2016) Holocene climate variability revealed using geochemistry and Computed Tomography scanning of stalagmites from the North Atlantic Basin, Department of Earth Sciences. Durham University.
Walczak, I.W., Baldini, J.U.L., Baldini, L.M., McDermott, F., Marsden, S., Standish, C.D., Richards, D.A., Andreo, B. and Slater, J. (2015) Reconstructing high-resolution climate using CT scanning of unsectioned stalagmites: A case study identifying the mid-Holocene onset of the Mediterranean climate in southern Iberia. Quaternary Science Reviews.
Wassenburg, J.A. (2013) PhD Thesis: Holocene climate evolution in NW Morocco as recorded in aragonitic speleothems: Significance of the North Atlantic Oscillation, Fakultät für Geowissenschaften. Ruhr-Universität Bochum.
Wassenburg, J.A., Immenhauser, A., Richter, D.K., Jochum, K.P., Fietzke, J., Deininger, M., Goos, M., Scholz, D. and Sabaoui, A. (2012) Climate and cave control on Pleistocene/Holocene calcite-to-aragonite transitions in speleothems from Morocco: Elemental and isotopic evidence. Geochimica et Cosmochimica Acta 92, 23-47.
Wassenburg, J.A., Immenhauser, A., Richter, D.K., Niedermayr, A., Riechelmann, S., Fietzke, J., Scholz, D., Jochum, K.P., Fohlmeister, J., Schroder-Ritzrau, A., Sabaoui, A., Riechelmann, D.F.C., Schneider, L. and Esper, J. (2013) Moroccan speleothem and tree ring records suggest a variable positive state of the North Atlantic Oscillation during the Medieval Warm Period. Earth and Planetary Science Letters 375, 291-302.
Wassenburg, J.A., Scholz, D., Jochum, K.P., Cheng, H., Oster, J., Immenhauser, A., Richter, D.K., Häger, T., Jamieson, R.A., Baldini, J.U.L., Hoffmann, D. and Breitenbach, S.F.M. (2016) Determination of aragonite trace element distribution coefficients from speleothem calcite–aragonite transitions. Geochimica et Cosmochimica Acta.
Watt, S.F.L., Pyle, D.M. and Mather, T.A. (2013) The volcanic response to deglaciation: Evidence from glaciated arcs and a reassessment of global eruption records. Earth-Science Reviews 122, 77-102.
Webb, M., Dredge, J., Barker, P.A., MÜLler, W., Jex, C., Desmarchelier, J., Hellstrom, J. and Wynn, P.M. (2014) Quaternary climatic instability in south-east Australia from a multi-proxy speleothem record. Journal of Quaternary Science 29, 589-596.
Wiesner, M.G., Wetzel, A., Catane, S.G., Listanco, E.L. and Mirabueno, H.T. (2003) Grain size, areal thickness distribution and controls on sedimentation of the 1991 Mount Pinatubo tephra layer in the South China Sea. Bulletin of Volcanology 66, 226-242.
Woodhead, J., Hellstrom, J., Pickering, R., Drysdale, R., Paul, B. and Bajo, P. (2012) U and Pb variability in older speleothems and strategies for their chronology. Quaternary Geochronology.
Woodhead, J. and Pickering, R. (2012) Beyond 500 ka: Progress and prospects in the U-Pb chronology of speleothems, and their application to studies in palaeoclimate, human evolution, biodiversity and tectonics. Chemical Geology 322–323, 290-299.
Woollings, T. and Blackburn, M. (2012) The North Atlantic Jet Stream under Climate Change and Its Relation to the NAO and EA Patterns. Journal of Climate 25, 886-902.
Wynn, P.M., Fairchild, I.J., Baker, A., Baldini, J.U.L. and McDermott, F. (2008) Isotopic archives of sulphate in speleothems. Geochimica et Cosmochimica Acta 72, 2465-2477.
Wynn, P.M., Fairchild, I.J., Frisia, S., Spötl, C., Baker, A. and Borsato, A. (2010) High-resolution sulphur isotope analysis of speleothem carbonate by secondary ionisation mass spectrometry. Chemical Geology 271, 101-107.
Wynn, P.M., Fairchild, I.J., Spötl, C., Hartland, A., Mattey, D., Fayard, B. and Cotte, M. (2014) Synchrotron X-ray distinction of seasonal hydrological and temperature patterns in speleothem carbonate. Environmental Chemistry 11, 28.

Yang, Q., Scholz, D., Jochum, K.P., Hoffmann, D.L., Stoll, B., Weis, U., Schwager, B. and Andreae, M.O. (2015) Lead isotope variability in speleothems - a promising new proxy for hydrological change? First results from a stalagmite from western Germany. Chemical Geology.
Zachos, J., Pagani, M., Sloan, L., Thomas, E. and Billups, K. (2001) Trends, rhythms, and aberrations in global climate 65 Ma to present. Science 292, 686-693.
Zhang, D., Zhang, P., Sang, W., Cheng, H., Wu, X., Yuan, Y., Bai, Y., Wang, J. and Jia, J. (2010) Implications of stalagmite density for past climate change: An example from stalagmite growth during the last deglaciation from Wanxiang Cave, western Loess Plateau. Chinese Science Bulletin 55, 3936-3943.
Zhou, J., Lundstrom, C.C., Fouke, B., Panno, S., Hackley, K. and Curry, B. (2005) Geochemistry of speleothem records from southern Illinois: Development of (234U)/(238U) as a proxy for paleoprecipitation. Chemical Geology 221, 1-20.